Information-based human motor performance models

Department of Mechanics, Mathematics and Management

MECHANICAL AND MANAGEMENT ENGINEERING
Ph.D. Program

SSD: ING-IND/17– INDUSTRIAL MECHANICAL SYSTEMS ENGINEERING

Final Dissertation

Information-based Human Motor Performance Models

by

ANDREA LUCCHESE

Supervisors:

Prof. Salvatore Digiesi

Prof. Francesco Boenzi

Coordinator of Ph.D. Program:

Prof. Giuseppe P. Demelio

Course n°35, 01/11/2019-31/10/2022

Politecnico di Bari

LIBERATORIA PER L'ARCHIVIAZIONE DELLA TESI DI DOTTORATO

Al Magnifico Rettore
del Politecnico di Bari

Il sottoscritto ANDREA LUCCHESE nato a BARI il 14/01/1993

residente a BARI in via FRANCESCO ZAMPARI 24 e-mail a.lucchese@hotmail.com

iscritto al 3° anno di Corso di Dottorato di Ricerca in INGEGNERIA MECCANICA E GESTIONALE ciclo XXXV

ed essendo stato ammesso a sostenere l'esame finale con la prevista discussione della tesi dal titolo:

INFORMATION-BASED HUMAN MOTOR PERFORMANCE MODELS

DICHIARA

1) di essere consapevole che, ai sensi del D.P.R. n. 445 del 28.12.2000, le dichiarazioni mendaci, la falsità negli atti e l'uso di atti falsi sono puniti ai sensi del codice penale e delle Leggi speciali in materia, e che nel caso ricorressero dette ipotesi, decade fin dall'inizio e senza necessità di nessuna formalità dai benefici conseguenti al provvedimento emanato sulla base di tali dichiarazioni;
2) di essere iscritto al Corso di Dottorato di ricerca in INGEGNERIA MECCANICA E GESTIONALE ciclo XXXV, corso attivato ai sensi del "*Regolamento dei Corsi di Dottorato di ricerca del Politecnico di Bari"*, emanato con D.R. n.286 del 01.07.2013;
3) di essere pienamente a conoscenza delle disposizioni contenute nel predetto Regolamento in merito alla procedura di deposito, pubblicazione e autoarchiviazione della tesi di dottorato nell'Archivio Istituzionale ad accesso aperto alla letteratura scientifica;
4) di essere consapevole che attraverso l'autoarchiviazione delle tesi nell'Archivio Istituzionale ad accesso aperto alla letteratura scientifica del Politecnico di Bari (IRIS-POLIBA), l'Ateneo archivierà e renderà consultabile in rete (nel rispetto della Policy di Ateneo di cui al D.R. 642 del 13.11.2015) il testo completo della tesi di dottorato, fatta salva la possibilità di sottoscrizione di apposite licenze per le relative condizioni di utilizzo (di cui al sito http://www.creativecommons.it/Licenze), e fatte salve, altresì, le eventuali esigenze di "embargo", legate a strette considerazioni sulla tutelabilità e sfruttamento industriale/commerciale dei contenuti della tesi, da rappresentarsi mediante compilazione e sottoscrizione del modulo in calce (Richiesta di embargo);
5) che la tesi da depositare in IRIS-POLIBA, in formato digitale (PDF/A) sarà del tutto identica a quelle **consegnate**/inviate/da inviarsi ai componenti della commissione per l'esame finale e a qualsiasi altra copia depositata presso gli Uffici del Politecnico di Bari in forma cartacea o digitale, ovvero a quella da discutere in sede di esame finale, a quella da depositare, a cura dell'Ateneo, presso le Biblioteche Nazionali Centrali di Roma e Firenze e presso tutti gli Uffici competenti per legge al momento del deposito stesso, e che di conseguenza va esclusa qualsiasi responsabilità del Politecnico di Bari per quanto riguarda eventuali errori, imprecisioni o omissioni nei contenuti della tesi;
6) che il contenuto e l'organizzazione della tesi è opera originale realizzata dal sottoscritto e non compromette in alcun modo i diritti di terzi, ivi compresi quelli relativi alla sicurezza dei dati personali; che pertanto il Politecnico di Bari ed i suoi funzionari sono in ogni caso esenti da responsabilità di qualsivoglia natura: civile, amministrativa e penale e saranno dal sottoscritto tenuti indenni da qualsiasi richiesta o rivendicazione da parte di terzi;
7) che il contenuto della tesi non infrange in alcun modo il diritto d'Autore né gli obblighi connessi alla salvaguardia di diritti morali od economici di altri autori o di altri aventi diritto, sia per testi, immagini, foto, tabelle, o altre parti di cui la tesi è composta.

Bari, 29/11/2022 Firma Andrea Lucchese

Il sottoscritto, con l'autoarchiviazione della propria tesi di dottorato nell'Archivio Istituzionale ad accesso aperto del Politecnico di Bari (POLIBA-IRIS), pur mantenendo su di essa tutti i diritti d'autore, morali ed economici, ai sensi della normativa vigente (Legge 633/1941 e ss.mm.ii.),

CONCEDE

- al Politecnico di Bari il permesso di trasferire l'opera su qualsiasi supporto e di convertirla in qualsiasi formato al fine di una corretta conservazione nel tempo. Il Politecnico di Bari garantisce che non verrà effettuata alcuna modifica al contenuto e alla struttura dell'opera.
- al Politecnico di Bari la possibilità di riprodurre l'opera in più di una copia per fini di sicurezza, back-up e conservazione.

Bari, 29/11/2022 Firma Andrea Lucchese

Department of Mechanics, Mathematics and Management

MECHANICAL AND MANAGEMENT ENGINEERING
Ph.D. Program

SSD: ING-IND/17– INDUSTRIAL MECHANICAL SYSTEMS ENGINEERING

Final Dissertation

Information-based Human Motor Performance Models

by

ANDREA LUCCHESE

Referees:

Prof. Salvatore Miranda

Prof. Luigi Ranieri

Supervisors:

Prof. Salvatore Digiesi

Prof. Francesco Boenzi

Coordinator of Ph.D Program:

Prof. Giuseppe P. Demelio

Course n°35, 01/11/2019-31/10/2022

Abstract

Despite the evolution of technologies that brought to the advent of I4.0, in current work environments, the operator still plays a crucial role in motor activities that require repetitive movements to be executed. Repetitive movements characterize a great range of motor tasks that can be performed in multiple work environments such as factories (e.g., manual assembly tasks, manual sorting), laboratories (e.g., pick and place tasks) or even outdoor (e.g., construction work manual tasks). The evaluation of motor performance by focusing on movements executed by operators or prescribed by the task has not yet considered in the current scientific literature.

The present dissertation addresses the topic of motor performance by introducing information-based models relying on the Fitts' Law Index of Difficulty (ID). The proposed models consider the entire motor behaviour (required or observed) for the correct execution of repetitive motor tasks. The topic is investigated and discussed under a new point of view, where features of the environment and individual's abilities influence the quality of the motor behaviour (demanded or executed) and affect the motor performance.

Results show the effectiveness of the models proposed, underlying the importance of the motor behaviour for the correct execution of the motor tasks. The performance is not only linked to the efficiency in achieving a task goal, but also on how physically the task goal is reached.

The proposed models have a general validity, not limited to specific applications/work environments, paving the way to a novel motor performance perspective domain independent.

Index

Abstract ... **1**
Index ... **2**
List of Figures ... **4**
List of Tables ... **8**
Introduction ... **9**
1. State of the Art on the Index of Difficulty ... **13**
1.1 The Fitts' law ... 13
1.2 The Shannon formulation ... 16
1.2.1 Effective Target Width ... 17
1.3 Variations of the Fitts' law: 2D and 3D targets ... 18
1.3.1 2D targets ... 19
1.3.2 3D targets ... 23
1.4 The continuous formulation ... 24
2. The Index of Difficulty in the 'Speed-Accuracy' trade-off model ... **28**
2.1 The 'Speed-ID-Accuracy' Model ... 28
2.2 Numerical case ... 31
2.2.1 Tunnel Traveling Task (TTT) ... 31
2.2.2 Circular Traveling Task (CTT) ... 35
2.3 Discussion ... 37
3. The Index of Difficulty as a measure of agent's motor difficulty ... **39**
3.1 The Stochastic Index of Difficulty ... 39
3.1.1 Internal and external constraints ... 39
3.1.2 Variability in Reaching Motor Tasks ... 40
3.1.3 General Model of Motor Difficulty ... 43
3.1.3.1 2D Movements ... 44
3.1.3.2 3D Movements ... 45
3.2 The influence of internal constraints ... 51
3.2.1 Evaluation of the motor difficulty for an elderly agent ... 52
3.2.2 Statistical Analysis on the Stochastic Index of Difficulty for Differently Aged Agents ... 54
3.2.3 Discussion ... 61
3.3 The influence of external constraints ... 63
3.3.1 Applying the stochastic Index of Difficulty to a manipulation task ... 63

3.3.2 Statistical Analysis 67
3.3.2.1 Stochastic Index of Difficulty 67
3.3.2.2 Stochastic Width and Velocity Profiles 70
3.3.3 Discussion 73
4. Stochastic Index of Difficulty-based affordance model 76
4.1 Background on Affordance 76
4.1.1 The industrial design perspective 79
4.1.2 The robotics perspective 80
4.2 Modeling Affordance through the Stochastic Index of Difficulty 84
4.2.1 The Stochastic Index of Difficulty-Affordance model: 2D Movements 86
4.2.1.1 The Reference Agent 86
4.2.1.2 The Observed Agent 89
4.2.1.3 The Affordance Level 97
4.2.2 Numerical Simulations 100
4.2.3 The Influence of Age 103
4.2.3.1 Kernel Density Estimation 105
4.2.3.2 Results 108
4.2.4 The affordance level as similarity between two behaviours 1111
4.2.4.1 Entropy measures as divergence between distributions 1111
4.2.4.2 Affordance level vs. JSD 1122
4.2.5 Discussion 1155
5. Applications 117
5.1 The 'Speed-ID-Accuracy' model 117
5.2 The stochastic Index of Difficulty 119
5.3 The affordance level 121
5.3.1 Manual sorting 124
5.4 Experiment apparatus 128
6. Conclusion 130
7. Bibliography 131

List of Figures

Figure 1.1 Fitts' reciprocal tapping task (MacKenzie, 1992)..... 13
Figure 1.2 Scheme of the general model of communication system (adapted from Shannon, 1948) 14
Figure 1.3 Scheme of the human motor system (Fitts, 1954); adapted and modified from (Shannon, 1948)..... 15
Figure 1.4 Effective target width W_e when the 4% of hits lie outside W (a); Effective target width W_e when the 2% of hits lie outside W (b) (MacKenzie, 1992) 18
Figure 1.5 Experiment set-up for target width W' 20
Figure 1.6 The probabilistic ID (ID_{pr}) is evaluated within the region defined by R; blue points show the spread of hits..... 22
Figure 1.7 Scheme of 3D reaching task with inclination angle θ_1 and azimuth angle θ_2..... 23
Figure 1.8 Steps to obtain the 'Tunnel Traveling' Task ID (ID_{TTT}) 25
Figure 1.9 Example of spatially constrained trajectory with variable target width $W(s)$ along the curvilinear coordinate s..... 26
Figure 2.1 'Circular Traveling' Task (CTT) experiment set-up..... 29
Figure 2.2 Semi-circular nominal trajectory with a decreasing width $W(s)$ along curvilinear coordinate s..... 30
Figure 2.3 Standard deviation at the endpoint (SD_{TTT}) evaluated through Equation 2.9 (figure 2.3a) and predicted through Equation 2.2 (figure 2.3b) vs. ID_{TTT} (Equation 1.14) and Average Speed (cm/s)..... 33
Figure 2.4 Accuracy reached at the endpoint in a Tunnel Traveling Task: $r_{SD} = SD/W$ vs. ID for different W values..... 34
Figure 3.1 $W_{obs}(s, \varphi)$ in case of 2D movements..... 44
Figure 3.2 Example of three-dimensional trial trajectories (dash-dotted lines) and their average (thick black line). The light blue ellipse shows the motor variability in the plane $P(s)$ orthogonal to t_{avg} at s. 46
Figure 3.3 Example of 'Ring and Wire' task (Zhai, Accot and Woltjer, 2004)..... 50
Figure 3.4 Human gait cycle in the sagittal plane (Pirker and Katzenschlager, 2017) 51
Figure 3.5 Ankle trajectories (coloured lines) and related average (thick black line) of a 61 years old healthy subject walking at an average speed of 1.584 m/s 52
Figure 3.6 $ID_{obs}(s^*, \varphi)$ evaluated and $W_{obs}(s, \varphi)$ with $\varphi = 0.96$ of a 61-year-old healthy subject walking at an average speed of 1.584 m/s..... 53

Figure 3.7 $ID_{obs}(s^*, \varphi)$ calculated along the x coordinate of the swing foot trajectory for "Young" (red lines, N=20) and "Old" (blue lines, N=14) agents, at "Slow" (3.7a) and "Fast" (3.7b) speed of execution 55

Figure 3.8 Average $ID_{obs}(s^*, \varphi)$ observed for "Young" (continuous lines) and "Old" (dotted lines) at "Slow" (red lines) and "Fast" (black lines) speed conditions 56

Figure 3.9 Mean values of $ID_{obs}(t_{avg}, \varphi)$ in each group at slow and fast speed conditions. Error bars show SEM (Standard Error of the Mean). Significance of differences: * = p < 0.0125; ** = p < 0.002 57

Figure 3.10 $ID_{obs}(\varphi, Speed, Age)_{|task}$ vs. age of agents for different speed conditions and probability levels φ 60

Figure 3.11 Experimental set-up and objects of the manipulation task. From left to right: plastic ellipsoid ball, full 1L water bottle, soft ellipsoid ball, half full 1L water and a tennis ball (Herbst, Zelnik-Manor and Wolf, 2020a) 64

Figure 3.12 Example of trial ttrajectories (dash-dotted lines) and their average (thick black line) during the tennis ball manipulation task 65

Figure 3.13 $ID_{obs}(s^*, \varphi)$ and $W_{obs}(s^*, \varphi)$ values averaged on 31 agents during the tennis ball manipulation task 66

Figure 3.14 Mean values and SEM (Standard Error of the Mean) of $ID_{obs}(t_{avg}, \varphi)$ of the entire manipulation task; *= statistically significant (p-value < 0.005); critical p-value = 0.05/10 = 0.005 68

Figure 3.15 Mean values and SEM (Standard Error of the Mean) of $ID_{obs}(t_{avg}, \varphi)$ of the entire manipulation task for the three different geometrical objects; *= statistically significant (p-value < 0.016); critical p-value = 0.05/3 = 0.016 69

Figure 3.16 Velocity profiles values averaged on 31 subjects during the object manipulation task 71

Figure 3.17 Mean values and SEM (Standard Error of the Mean) of velocity peaks at the reaching (3.17a) and transport (3.17b) phase for the three different geometrical objects; *= statistically significant (p-value < 0.001); critical p-value = 0.05/3 = 0.016 72

Figure 3.18 $W_{obs}(s^*, \varphi)$ values averaged on 31 subjects during the object manipulation task . 73

Figure 4.1 Biomechanical model of the critical riser height Rc=L+L1-L2,with L1=f(L) and L2=f(L); the critical ratio Rc/L= 0.88 (Warren, 1984) 77

Figure 4.2 Reference Agent's stochastic behaviour at curvilinear coordinate s 89

Figure 4.3 Observed Agent's stochastic behaviour at curvilinear coordinate s 91

Figure 4.4 Example of stochastic behaviours of two different observed agents (red and orange trends) in case of same $W_{\cap}(s)$ and $p_{\cap}(s)$, at curvilinear coordinate s. Blue trend is associated to the reference agent. 92

Figure 4.5 Graphical representation of the overlapping index $\eta_{\cap}(s)$ at curvilinear coordinate s. The red trend is associated to the observed agent, the blue trend to the reference one. 93

Figure 4.6 Evaluation of $\eta_{\cap}(s)$ by comparing various Weibull distributions (scale parameter 3, b = shape parameter) with the reference one (Gaussian distribution) 94

Figure 4.7 Values of $W_{\cap}(s)$, $p_{\cap}(s)$ and $\eta_{\cap}(s)$ by comparing the reference distribution (Gaussian) with a Weibull distribution (scale parameter 5 and shape parameter 8) shifted along T at curvilinear coordinate s 95

Figure 4.8 Values of $W_{\cap}(s)$, $p_{\cap}(s)$ and $\eta_{\cap}(s)$ by comparing the reference distribution (Gaussian) with a Weibull distribution (scale parameter 1 and shape parameter 2) shifted along T at curvilinear coordinate s 96

Figure 4.9 Graphical representation of the Affordance Level (α); in blue the Reference Behaviour (RB), in red the Observed Behaviour (OB). If the two behaviours overlaps, $\alpha \neq 0$: greater the overlapping, closer $ID_{\cap}$ to $ID_{ref,}$ higher the affordance level α 98

Figure 4.10 Schematization for the quantification of the affordance level 99

Figure 4.11 Reference trajectory (t_{ref}), average (assumed) trajectories (t_{avg_i}), and reference stochastic width ($W_{ref}(s,p)$) employed for the numerical simulations 101

Figure 4.12 The four $f_{obs}(s,T)$ employed for the numerical simulations. $T = 0$ coincides with the point $q_{ref}(s) \in t_{ref}$ at a given curvilinear coordinate s 102

Figure 4.13 Results of the numerical simulations. The affordance level α is quantified for each average trajectory t_{avg} and each $f_{obs}(s,T)$ 102

Figure 4.14 The ankle's average trajectory of each subject (t_l) and the average (t_{avg}) for each group at slow speed condition 104

Figure 4.15 The ankle's average trajectory of each subject (t_l) and the average (t_{avg}) for each group at fast speed condition 104

Figure 4.16 Example of $f_h(x)$ obtained with the use of a gaussian kernel $K_h(x - x_l)$ ((Gramacki, 2018) pag. 30)) 106

Figure 4.17 Example of the $f_h(x)$ obtained with the use of a gaussian kernel, by varying the bandwidth h ((Gramacki, 2018), pag. 30) 107

Figure 4.18 The ankle's average trajectory of each subject (t_l) and the average (t_{avg}) for 'Young' at slow speed condition; $q_l(s)$ and $q_{avg}(s)$ are shown for a given s 109

Figure 4.19 $f_{ref}(s,T)$ ('Young' agent) and $f_{obs}(s,T)$ ('Old' agent) at a given curvilinear coordinate s and 'Slow' speed condition. Points $q_l(s)$, related average for both agents, and the entity of the overlapping index $\eta_{\cap}(s)$ are also depicted. 110
Figure 4.20 Numerical results of $\alpha(s^*)\ vs. JSD$ in the univariate case, by considering Weibull distribution (scale parameter 4 and shape parameter 7) as the observed one, gaussian distribution as the reference one. 112
Figure 4.21 Example of spatial configurations achieved by the reference and observed agent 113
Figure 4.22 PDFs obtained by applying 2D KDE on the spatial configurations (points in Figure 4.21) of the reference and observed agent 114
Figure 4.23 Numerical results of $\alpha(s*)\ vs.\ JSD$ in the bivariate case 114
Figure 5.1 Example of a workstation for manual sorting 124
Figure 5.2 The three scenarios considered for the manual sorting example; R has length 8 [dm] (along x), while W has width 4 [dm] (along y). f_{ref} is gaussian along x, and constant along x (for a given y) 126

List of Tables

Table 1.1 MT=f(ID) regression Equations and ID formulations. *=three-dimensional reaching tasks..... 27
Table 2.1 Experimental data on Tunnel Traveling Task (Hourcade and Berkel, 2008)..... 31
Table 2.2 Average Speed, $W_e, ID_{TTT}, and\ SD_{TTT}$ values for the Tunnel Traveling Task (TTT) 32
Table 2.3 Regression parameters for the SD [cm] in the Tunnel Traveling Task (Average Speed [cm/s])..... 32
Table 2.4 Regression parameters for the Average Speed [cm/s] in the Tunnel Traveling Task (A [cm]; W [cm]) 33
Table 2.5 Experimental data on Circular Traveling Task (Hourcade and Berkel, 2008)..... 35
Table 2.6 Average Speed, $W_e, ID_{TTT}, and\ SD_{TTT}$ values for the Circular Traveling Task (CTT) 35
Table 2.7 Regression parameters for the SD [cm] in the Circular Traveling Task (Average Speed [cm/s])..... 36
Table 2.8 Regression parameters for the Average Speed [cm/s] in the Circular Traveling Task (A [cm]; W [cm]) 36
Table 3.1 Notation used for the PCA 47
Table 3.2 Sample size for the Mixed-Design Two-Way Repeated Measures ANOVA..... 56
Table 3.3 Age and average speed of execution of each agent at the three speed conditions (Slow, Comfortable, and Fast) (from Fukuchi, Fukuchi and Duarte, 2018). For each speed condition of the agent, the average speed is calculated across the 9 trials..... 58
Table 3.4 Regression parameters' values 60
Table 4.1 Equations and expressions for 2D KDE..... 107
Table 4.2 Results of the affordance level applied to the walking dataset..... 110
Table 4.3 Kullback-Leibler divergence..... 111
Table 5.1 Results in evaluating the Affordance level and JSD for the three scenarios of the manual sorting 127

Introduction

With the advent of Industry 4.0 (I4.0), the implementation of new digital technologies, such as Cyber-Physical Systems (CPS), Internet of Things (IoT), big data, virtual reality (VR) and augmented reality (AR), result in an important change in production, safety and maintenance systems (Lasi *et al.*, 2014; Schmidt *et al.*, 2015; Pereira and Romero, 2017). The introduction of these technologies brought improvements in processes and performance, thanks to a greater level of automation through the connection between the cyber and physical environments (Dalenogare *et al.*, 2018; Fettermann *et al.*, 2018; Xu, Xu and Li, 2018)

In manufacturing systems, the possibility of machine failures can bring to negative effects at various levels, leading to economic losses (Hooi and Leong, 2017; Habidin *et al.*, 2018). The maintenance activity has the purpose to prevent breakdowns, prevent the production of scraps and wastes, decrease the reworks through a well-programmed maintenance planning guaranteeing the correct functioning of the equipment (Kaur *et al.*, 2015), and decrease the total cost associated to the production system (Rødseth, Schjølberg and Marhaug, 2017). With the implementation of I4.0 technologies, maintenance simulations can improve schedule planning, AR can provide guidance for diagnostics and inspection (Silvestri *et al.*, 2020), IoT and cloud computing can be valuable tools to monitor efficiently the production conditions (Zheng *et al.*, 2021). With the Maintenance 4.0, new strategies and predictive maintenance policies can be adopted, bringing to economical and technical benefits (Mosyurchak *et al.*, 2017).

The I4.0 technologies can be applied in different contexts, with different purposes. In nuclear power plants (NPPs), for example, the failures that can occur in instruments or processes, such as wrong alarming or missed information, can lead to a decrease in performance, or in worst cases, to extremely harmful and dangerous consequences. These issues can be prevented by guaranteeing an efficient cyber-physical system like a decision support system able to identify abnormal operating procedures (Hsieh *et al.*, 2012), or perform a deep system analysis basing on Big Data, deep learning and autonomous algorithms (Tambouratzis *et al.*, 2019).

In case of abnormal situations in NPPs, a well-trained operator should identify in time the faults, by analyzing information and data provided by alarms, and identifying uncommon

trends in various instruments (Hogg *et al.*, 1995; Vicente *et al.*, 1996). The capacity of the operator to interpret correctly alarms and handle properly the large amounts of information, depend on the cognitive ability (Park, Kim and Jung, 2016). Therefore, the aim of the implementation of I4.0 technologies is to support the operator, by decreasing the mental burden and enhancing both the physical and cognitive capabilities of the operator, through the automation (Sun *et al.*, 2020). Properly designed Human-Machine Interaction (HMI) and alarm systems can support the operator by providing data collected from sensors with user-friendly interfaces and easy-to-use devices, helping the operator in performing tasks (Wu *et al.*, 2016; Singh and Mahmoud, 2017). Consequently, the operator still plays a critical role in the main control room of NPPs.

Therefore, despite the implementation of I4.0 technologies, the automation level has not yet reached an autonomous control, and the role of the operator is still important and necessary (Hancock *et al.*, 2013; Munir *et al.*, 2013). In this context the role of the operator is redefined as 'Operator 4.0' (Romero *et al.*, 2016). This new paradigm emphasizes the human centrality in the smart factories, where the human workforce is not replaced, but is supported during activities through a strict cooperation with machines. Under this perspective, the automation is treated as an enhancement of the operator's physical, cognitive and sensorial abilities through the integration of the human's and machine's resources in the human cyber-physical system leading to a more efficient and performant operator (Romero *et al.*, 2015). The operator 4.0 performs activities through the support of machines: operators interact with robots, advanced systems, and devices (e.g., AR, VR), exploiting benefits that these tools can provide (Zolotová *et al.*, 2020).

The cognitive skills of operators can be enhanced through advanced reality equipment, extending the operator's ability in analyzing relevant data in real-time and take the right decision promptly. The AR (Augmented Reality) technology supports the operator by overlaying in real time, relevant digital information (e.g., real-time feedback about smart manufacturing processes and machines) on the operator's field of view, with the potential result of increasing reliability and reducing human errors. The VR (Virtual Reality) technology can digitally replicate work environments, supporting the operator during the training for a new task (e.g. assembly task, maintenance procedure), optimizing the decision-making process. The implementation of AR and VR technologies can ensure greater safety by displaying warnings and make available relevant information in real

time, by reducing computational demand and enhancing operators' performance. Some of the benefits obtained through the use of these technologies are the reduction of completion times (Steel, 2019), reduction of error rates (Lai *et al.*, 2020), improvement of health and safety (Mourtzis, Xanthi and Zogopoulos, 2019), increase of motivation and flexibility of operators (Osborne and Mavers, 2019), improvement of the problem-solving and decision-making (Steel, 2019).

Other devices are employed to monitor the health status, increase the safety and the limited physical strength of operators, reduce work fatigue with the potential to increase operators' productivity. As an example, exoskeletons are powered wearable devices that provide physical protection, support and increase the strength of operators, improve the endurance time, reduce WMSDs risks and accidents due to high physical effort (Romero *et al.*, 2016). In a long-term perspective, the employment of exoskeletons can improve the social sustainability of work environments, by enabling work activities of elders; more generally advanced technologies can help elderly people to be integrated in the new manufacturing workforce (Romero *et al.*, 2016). The operator productivity, performance and job satisfaction can be boosted through the employment of industrial robots (collaborative robots) able to execute highly repetitive tasks cooperating with the smart operator. Therefore, collaborative robots can relieve operators from non-ergonomic and vulnerable tasks. Moreover, to increase the operator's safety and prevent the risk of health-related accidents at work, wearable trackers ca be used to monitor health-related metrics through health parameters such as heart rate and bloody pressure.

This briefly analysis on I4.0 provides the evidence that the operator has still a central role in current work environments, and despite the advances in the use of technological devices that support the operator's work, there is still a particular regard on manual tasks involving repetitive movements (e.g., lifting, pushing, pulling, carrying, moving, manipulating, holding or restraining objects). For these reasons the research has been focused on the theme of motor activities with the main goal of defining new models able to consider the overall motor behaviour of operators in performing repetitive motor tasks. The motivation in facing this topic lies in the lack of the current scientific literature in considering how the overall movements executed by operators influence the motor performance. To reach this goal, the theoretical basis relies on the information-based Fitts' law's Index of Difficulty measure (ID). In the text, the original ID measure has been

described and discussion about the multiple formulations proposed in the scientific literature and related applications has been provided. The analysis on the multiple ID measures brings to the conclusion that the continuous formulation of the ID can be employed as a tool to quantify the difficulty related to repetitive movements. The present dissertation shows that the motor behaviour, expressed through the quantification of movements-related difficulty, has an impact on the motor performance. In the present work, the power of the proposed information-based models will be shown and insights about their wide applicability discussed.

The main core of the dissertation is divided into six chapters, defining a path that step by step provides further in-depth analysis on the Index of Difficulty. This structure gives a valid theoretical base to develop the information-based models able to evaluate the motor performance through the quantification of movements-related difficulty in performing repetitive motor tasks. The first chapter is focused on the state of art related to the employment of the Index of Difficulty (ID) in the scientific literature. The second chapter proposes a novel model that improves the existing 'Speed-Accuracy' tradeoff model by considering the continuous formulation of the ID. The third chapter shows a novel ID formulation, able to evaluate the motor difficulty experienced by agents during the execution of a repetitive motor task. The fourth chapter is focused on employing the previously defined ID model to evaluate the agent's ability in performing a repetitive motor task through the direct quantification of the affordance. The last two chapters are aimed at describing the multiple applications of the proposed models and conclusion.

1. State of the Art on the Index of Difficulty

1.1 The Fitts' law

The Fitts' law has been theorized in 1954 (Fitts, 1954) to evaluate the information capacity of the human motor system. To reach this goal, Fitts proposed experiments where subjects performed simple rapid aimed movements. In the one called 'reciprocal tapping task', subjects were asked to tap repeatedly a target of width W, placed at distance A from the starting point, through the use of a stylus. To obtain the highest performance, the subject had to move as quickly as possible towards the target, trying to be as accurate as possible by placing the stylus inside the target's width. An error was made when the stylus was placed outside the target of width W.

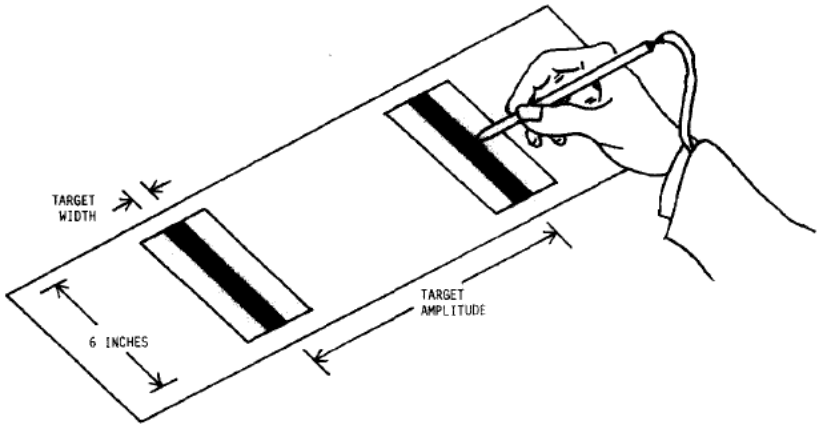

Figure 1.1 *Fitts' reciprocal tapping task (MacKenzie, 1992)*

By asking a subject to perform uniform repetitive overlearned (i.e., ballistic) movements as rapidly as possible, while holding constant the task conditions, the subject's performance is only limited by the capacity of the motor system in producing the same motor response while several alternatives are available. Fitts defined the information capacity of a motor system as the ability to execute repeatedly the same movement from various alternatives, in a specific time window. Greater the number of alternatives, greater the amount of information to be processed by the human motor system in the limited time. The information capacity threshold is due to the intrinsic variability of the motor response, expressing the effort in executing the same movement during repetitive trials. In this context the intrinsic variability refers to the 'noise' of the human motor system, responsible for the inability to produce exactly the same movement. Fitts evaluated the information capacity of the human motor system by analogy with the capacity to transmit

information in a communication channel, stated in the theorem n° 17 of Shannon (Shannon, 1948).

In communication theory, when a signal must be transmitted through a channel, the resulting received signal will be distorted due to an intrinsic interference, referred to the 'normal noise': it expresses a random interference (random motions of electrons inside the conductor due to the heating of system components such as bandwidth, transmitter, type of cable, distance, etc.) that degrades the system performance (i.e., capacity to transmit information).

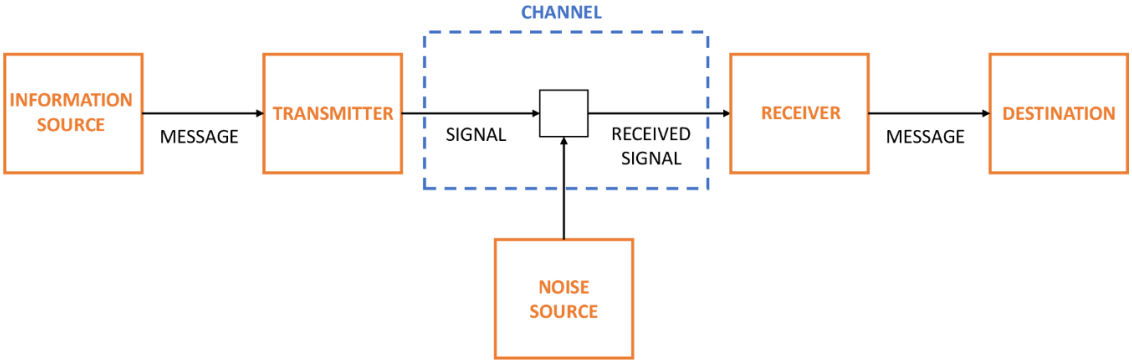

Figure 1.2 *Scheme of the general model of communication system (adapted from Shannon, 1948)*

The entity of the noise follows a normal distribution, due to the stochasticity of the phenomenon. The theorem n° 17 of Shannon (Shannon, 1948), states that the channel capacity can be evaluated as the difference between the entropy of the received signal and the entropy of the normal noise, bringing to:

$$\boldsymbol{C = B \cdot log_2\left(\frac{P}{N} + 1\right)} \tag{1.1}$$

C is the information capacity of the communication channel (bit/s), B is its bandwidth (1/s), S is the signal power to be transmitted, perturbed by the normal noise of power N. The entity of N limits the information capacity of the channel. The logarithmic term expresses the amount of information (bit) that can be transmitted through the communication channel: lower the entity of N, higher the channel capacity.

With reference to the 'reciprocal tapping task' experiment of Fitts, the log term of Equation (1.1), properly modified, can express the amount of motor information that the subject has to process. The amplitude of movement A is the motor information that must be transmitted through the human channel and then processed (i.e., execution of movement), while the target of width W can refer to allowable noise, i.e., the maximum tolerance allowed at the target.

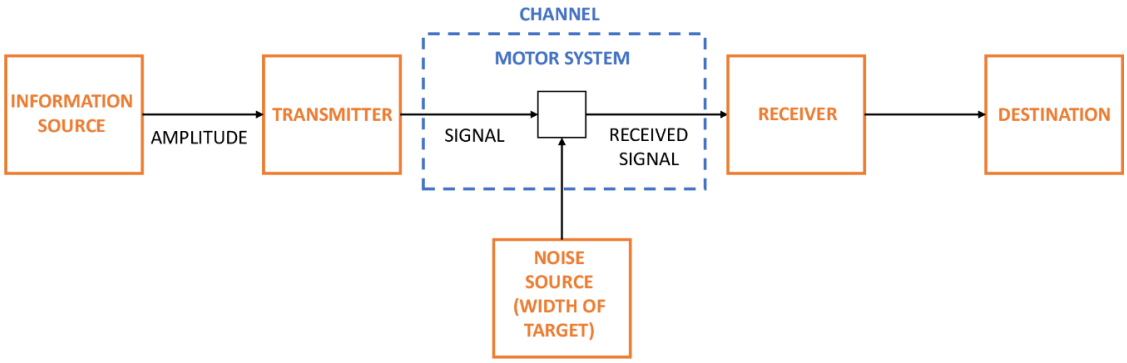

Figure 1.3 *Scheme of the human motor system (Fitts, 1954); adapted and modified from (Shannon, 1948)*

By decreasing the entity of W, the task becomes more difficult since the subject makes a greater effort to replicate the same movement while trying to not exceed the target thresholds. The minimum amount of motor information required by the task, characterized by a specific target tolerance (W) and amplitude (A), is evaluated through the Index of Difficulty (ID):

$$\boldsymbol{ID = log_2\left(\frac{2A}{W}\right)} \tag{1.2}$$

Therefore, a certain reaching motor task defined by A and W, corresponds to a specific ID, expressing the amount of information (in bit unit) that should be transmitted through the human channel and then processed by the human motor system to execute properly the pre-defined movements. In analogy with the log term of Equation 1.1, Fitts associated the signal power (S) to the amplitude of movement (A) to travel, while the noise (N) is associated to the target width (W). By considering the time needed by the subject to execute movements (Movement Time (MT), expressed in seconds), the information capacity of the human motor system is evaluated as:

$$\boldsymbol{IP = \frac{ID}{MT}} \tag{1.3}$$

IP is defined as Index of Performance (bit/s). Therefore, by maintaining constant A and W (constant ID), greater the movement time, and lower the amount of motor information that the subject can process per unit time (bit/s). In the opposite case, by maintaining the task features constant, lower the movement time, higher the ability of the human motor system to replicate the same movement. The IP is the rate (bit/s) at which the subject is able to generate the minimum amount of motor information demanded by the task.

Starting from the reasoning that subjects take more time to execute more difficult tasks (higher ID by increasing A and/or decreasing W), Fitts defined the linear relationship MT=f(ID) by regressing the MT with the ID, obtaining the Fitts' law:

$$\boldsymbol{MT = a + b \cdot ID} \tag{1.4}$$

Where a and b are two empirical determined constants. Results of the Fitts' experience brought to considerations that the performance capacity of the human motor system is almost constant when considering certain ranges of task conditions (variations of A and W), since the MT is proportional to ID (Equation 1.4), and therefore IP constant (Equation 1.3). Nevertheless, Fitts stated that both the IP and MT=f(ID) can behave differently when considering other task conditions, or when different movement limbs and muscle groups are involved during the task execution. For these reasons, in the last decades, a particular attention has been paid on the Fitts' law to verify the effectiveness in predicting the movement time starting from the ID, by considering new task conditions (A, W) mainly in the field of kinematics and human factors. In the last decades, the increasing interest in predicting the human performance through technological devices, laid the foundation for analysing the Fitts' law in new task environments, such as in case of HCI (Human-Computer Interaction). The great power of the Fitts' law has been further verified in case of subjects performing movement by holding devices (e.g., computer mouse, trackball, joystick) and interacting with machine interfaces (e.g, computer screen): the MT has been satisfactorily predicted by the ID also considering these types of tasks. Due to the importance of results obtained by employing the Fitts' law in HCI environments, the following paragraph is focused on describing briefly the first ID formulation (called 'Shannon formulation') that enabled the extension of the Fitts' law in new environments and research fields (MacKenzie, 1992).

1.2 The Shannon formulation

MacKenzie (MacKenzie, 1992) proposed a variation of the ID formulation in Equation 1.2, after observing some critical points. Firstly, scatter plots of (MT, ID) reveal a deviation from the linear regression (Equation 1.4), showing an upward curvature for low values of ID (ID < 3 bit). Furthermore, despite the ratio A/W has been multiplied by 2 to ensure the positive values of ID for the task conditions considered in the Fitts' experiments, in case of A<W, a negative ID value is obtained (see Equation 1.2).

Moreover, the ID proposed by Fitts, does not reflect the structure of the log term of Equation 1.1. Due to these reasons, MacKenzie proposed the following ID formulation, mostly known as 'Shannon formulation':

$$\boldsymbol{ID = log_2\left(\frac{A}{W} + 1\right)} \tag{1.5}$$

The first observation that can be made is about the perfect analogy with the log term of Equation 1.1 since the signal of power P to be transmitted through the communication channel is substituted by the amplitude of movement A, expressing the motor information to be transmitted through the human channel, while the normal noise of power N, is substituted by the target width W, expressing the maximum allowable tolerance (~noise) at the reaching target. In this case, even in the scenario A<W, the ID cannot be negative; furthermore, by substituting the ID of Equation 1.4 with the one of Equation 1.5, MacKenzie found better regression results, since the (A/W+1) in the log term, respects the upward curvature of scatter plots (MT, ID) for low values of ID.

1.2.1 Effective Target Width

The Index of Difficulty can be interpreted as the maximum uncertainty that can be tolerated for a properly movement execution (W), specified by a given amplitude of movement A. Nevertheless, in performing the reaching task of given amplitude of movement A, subjects can execute movements characterized by a lower variability at the target, than the one tolerated by the task (W): in this case the subject is able to generate more information, than the one demanded by the task. To reflect the actual motor responses of subjects, whose endpoint variability may be different from the pre-defined target width, MacKenzie proposed a normalization of W. This adjustment, called 'Effective Target Width', W_e, is derived in analogy with the 'normal noise' of the communication channel, mentioning that the dispersion of hits at the target, expressing the intrinsic variability of the motor response, is associated to the motor noise. As for the noise associated to the communication channel, the dispersion of hits at the target can be represented by a normal distribution. The entropy of a normal distribution is evaluated as $\log_2(\sqrt{2\pi e}\sigma)$ by applying the entropy of a continuous distribution to the normal probability density function (Shannon, 1948); σ is the standard deviation associated to the normal noise. By considering $\sigma = 1,$ and by splitting $\sqrt{2\pi e} \approx 4.133$ in a pair of z-scores, it is found that W is bounded by $-2.066 < z < +2.066$. This means that the

target width W = W_e when the 96% of hits, normal distributed, fall within the target. In other scenarios, W_e > W, when less than the 96% of hits fall within the target, while W_e < W, when more than the 96% of hits lie within the target. Knowing the error rates, W_e is evaluated as:

$$W_e = \frac{2.066 \cdot W}{z_e} \tag{1.6}$$

z_e = 2.066 if 96% of hits fall inside W, and therefore W= W_e; z_e is evaluated from the z-score tables. As an example in Figure 1.4, if 2% of hits fall outside W, the corresponding z_e is equal to 2.326 (98%), and therefore W_e = 2.066·W/2.326 < W.

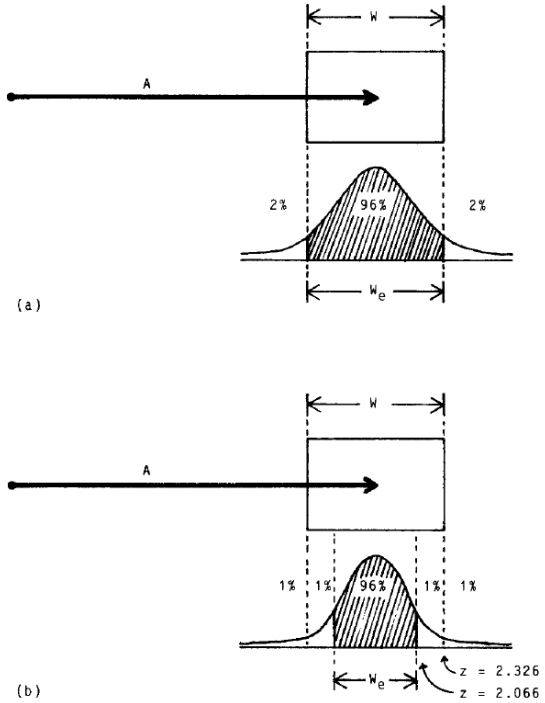

Figure 1.4 *Effective target width W_e when the 4% of hits lie outside W (a); Effective target width W_e when the 2% of hits lie outside W (b) (MacKenzie, 1992)*

Therefore, the reduced variability at the target, decreases the W_e and increases the ID; in particular if W ≠ W_e, the ID (Equation 1.5) is modified by substituting W_e with W, bringing to higher (W_e < W), or lower (W_e > W) amount of information that the human motor system is able to process with respect to the amount of information demanded by the task.

1.3 Variations of the Fitts' law: 2D and 3D targets

Despite the Fitts' law has been theorized for simple rapid aimed movements with the goal of evaluating the information capacity of the human motor system, it has been mainly

employed as a tool to predict the execution time (MT) of subjects performing different motor activities involving hand movements (Hoffmann, 1991), dart throwing (Kerr and Langolf, 1977), linear and rotary movements (Sheridan and Ferrell, 1963), discrete "one-shot" unidirectional movements (Fitts and Peterson, 1964). Thanks to information-theoretical foundation of the ID, its employment has been extended in multiple research fields (ergonomics, human factors), with a widespread application in the HCI community, where the use of technological devices was involved (e.g., mouse, trackball, joystick, haptic devices, 3D glasses (AR/VR)). In the latter case, the ID was evaluated from the movement amplitude (A), and from the target's shape and entity (2D, 3D), visible on computer screens, tablets, touchpads or in VR/AR. This shows the great strength of the Fitts' law in being applied in any environment and of the ID in being employed in applications different from its original conceptualization.

1.3.1 2D targets

The extension of the ID to motor tasks regarding two-dimensional targets has been widely studied due to the greater number of applications where the 2D reaching target is involved, both in HCI (pointing tasks on display through the use of technological interactive devices such as mouse or eye-gaze input system) and physical environments (reaching a 2D physical target). MacKenzie was the very first author who studied the topic of 2D targets, and focused on how to take into account the target characterized by both a width (W) and a height (H) in the ID (MacKenzie and Buxton, 1992). Various models were analyzed, by considering instead of the target width W in Equation 1.5, other contributions, such as the smaller between W and H (min (W, H)), the width of the target evaluated along the approach axis (W') considering the approach angle (θ) (Figure 1.5), or the sum of W and H (W+H).

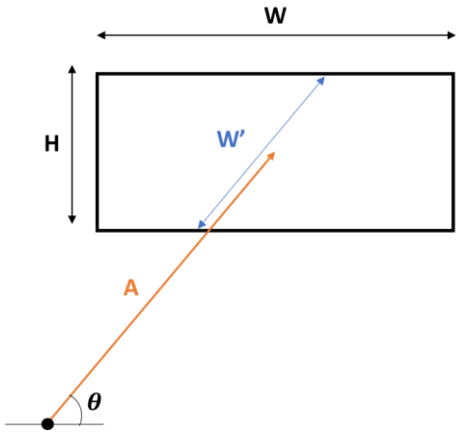

Figure 1.5 *Experiment set-up for target width W'*

MacKenzie found that by the regression analysis of the MT with the various ID formulations, the ID model that allowed to obtain best results was:

$$\boldsymbol{ID = log_2\left(\frac{A}{min\,(W,H)} + 1\right)} \tag{1.7}$$

Although this model is valuable, since it guarantees the bit unit of the ID while considering a bi-dimensional target, it takes into account only one of the two dimensions characteristics of the target. For this reason, Accot and Zhai (Accot and Zhai, 2003) focused on considering both the contributions of the target's height (H) and width (W) in a new ID formulation. Nevertheless, problems emerged since there was the need to consider both dimensions of the target, while maintaining the dimensionless ratio between the numerator and denominator of the logarithm. In order to satisfy this constraint, Accot and Zhai defined the desirable properties of the new ID formulation:

- When multiplying A, W, H by the same constant, the MT should not change (scale independency).
- If W or H tends to infinity, the other dimension contributes to the target size, and the ID regresses towards Equation 1.5.
- The smaller between W and H should have the greater impact on ID.
- Both W and H should be considered in the same ID model.

To define the new ID model with these properties, Accot and Zhai evaluated the entity of the target as the weighted l_p-norm of a vector X whose components are $\frac{A}{W}$ and $\frac{A}{H}$:

$$\|X\|_{p,w} = \sqrt[p]{w_1 \left|\frac{A}{W}\right|^p + w_2 \left|\frac{A}{H}\right|^p} \tag{1.8}$$

By regressing MT with the ID, best results were obtained by considering a Euclidean norm (p=2), where the weight w_1 is equal to one, while w_2 is given by the empirical coefficient η. Therefore, by substituting the A/W ratio in Equation 1.5 with the Euclidean norm representative of the contributions of W and H, the following ID model has been obtained:

$$ID = log_2\left(\sqrt{\left(\frac{A}{W}\right)^2 + \eta\left(\frac{A}{H}\right)^2} + 1\right) \tag{1.9}$$

Although Equation 1.9 satisfies the desired properties, takes into account both W and H, and guarantees the bit unit of the ID, it does not consider the approach angle θ (as defined in Figure 1.5). Zhang et al. (Zhang, Zha and Feng, 2012) improved the Accot and Zhai's ID model by expressing the contribution due to the movement direction in empirical coefficients. Zhang et al. found that the angle between the movement direction and the horizontal axis (θ) has a simultaneous effect on both the width (W) and height (H) of the target. As in (Accot and Zhai, 2003), the entity of the target is defined as a Euclidean norm (p=2), whose components $\frac{A}{W}$ and $\frac{A}{H}$ are weighted by $cos(\theta)$ and $sin(\theta)$ respectively: in this case the effect of approach angle θ is directly considered in the ID. The ID model that allowed to obtain the best MT=f(ID) regression results was:

$$ID = log_2\left(\sqrt{\omega\left(\frac{A}{W}\right)^2 + \eta\left(\frac{A}{H}\right)^2} + 1\right) \tag{1.10}$$

Where $\omega = c_1 + c_0 \cdot \cos^2\theta,\ \ \eta = c_2 + c_0 \cdot \sin^2\theta$ with constraint $\omega + \eta = 1$. $c_2,\ c_1, c_0$ are empirical coefficients.

The Fitts' law has been applied also in reaching tasks requiring solely eye-gaze movements, without the use of any body part. The aim of (Murata and Fukunaga, 2018) was to investigate the effect of target shape and movement direction on the reaching time, and to incorporate those factors in the ID model. Experiments involved the use of an eye-tracker system capable of capturing eye-gaze movements of subjects Murata et al. obtained the best MT=f(ID) regression results with the following ID model:

$$\boldsymbol{ID = log_2\left(\alpha\beta\left(\frac{A}{W}\right) + 1\right)} \tag{1.11}$$

Where $\frac{A}{W}$ is weighted by two coefficients: the first $\left(\alpha = \sqrt{W/H}\right)$ considers the contribution due to the target shape (where H is the target's height); the second ($\beta = f(\theta)$) considers the contribution due to the approach angle (θ).

A particular attention should be paid to the model proposed by Grossman et al. (Grossman and Balakrishnan, 2005). In this case, the ID model (called ID_{pr}) is evaluated as function of the probability of reaching inside a target of any given region (R) (Figure 1.6). From the observation of the spread of hits (S) at the target, assumed to follow a bivariate normal distribution, the probability of reaching inside the region is quantified. The probability of hitting a 2D target is directly considered to quantify the ID, i.e., $ID_{pr} = f(P_{R,S}(hit))$. The probability of hitting the target is function of R, since a smaller target will be harder to hit, with more hits lying outside the target, bringing to lower $P_{R,S}(hit)$; conversely, a larger region R will be easier to hit, with more hits lying inside the target, bringing to higher $P_{R,S}(hit)$. $ID_{pr} = f(P_{R,S}(hit))$ is expressed by the following:

$$\boldsymbol{ID_{pr} = f\left(\iint_R \frac{1}{cA\sqrt{2\pi}} e^{-\left(\frac{X'^2}{2cA^2}\right)} \cdot \frac{1}{dA\sqrt{2\pi}} e^{-\left(\frac{Y'^2}{2dA^2}\right)} dX'dY'\right)} \tag{1.12}$$

A is the amplitude of movement, R is region defined by the target, c and d are empirical coefficients.

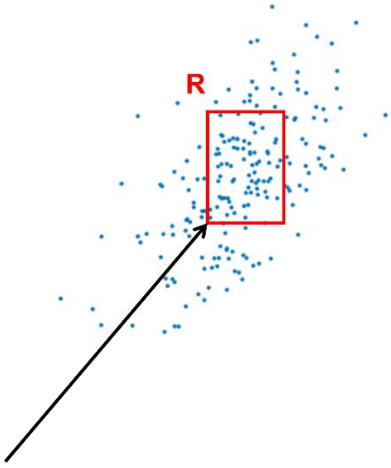

Figure 1.6 *The probabilistic ID (ID_{pr}) is evaluated within the region defined by R; blue points show the spread of hits*

While the previous ID models have been applied to two-dimensional reaching tasks, considering 1D, or 2D targets, other authors focused on the extension of the ID model as

well as of the Fitts' law in applications that require a three-dimensional reaching task, considering 2D targets. In these works, subjects were asked to reach a 2D target whose depth is neglected, placed in a physical three-dimensional environment: 2D targets were not placed horizontally, or shown on a desktop, but placed in the 3D space, forcing subjects to execute three-dimensional movements (left/right, forward/backward, up/down).

In case of (Murata and Iwase, 2001), subjects were asked to reach a vertical board, where various circular 2D targets were placed in different positions. A sensor was used as a pointer, attached to the right index of the participant. To improve regression results of MT=f(ID), in the regression model it has been added the azimuth angle θ_2 (equal to the approach angle in (Zhang, Zha and Feng, 2012)). Other authors considered both θ_2 and inclination angle θ_1 (Cha and Myung, 2010) (Figure 1.7).

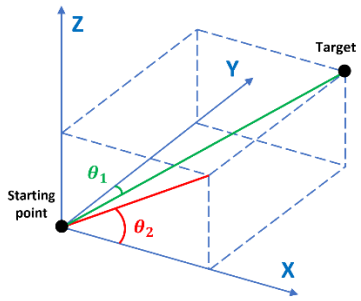

Figure 1.7 *Scheme of 3D reaching task with inclination angle θ_1 and azimuth angle θ_2*

1.3.2 3D targets

Despite multiple works focused on extending the ID model in reaching tasks characterized by 1D or 2D targets, very few authors deepened the case of three-dimensional reaching task characterized by a 3D target; this phenomenon is mainly due to the application of the proposed ID formulations, strictly related to the use of computers, touchpad, tablets etc…, as well as due to problems related to the visualization of 3D targets through technological devices. In (Grossman and Balakrishnan, 2004) experiments were characterized by the use of a 3D display (volumetric display) allowing to observe a 3D volumetric target; subjects were asked to reach repetitively the target, as for the classical Fitts' 'tapping task', but experiments involved the execution of three-dimensional movements, and a 3D target. The ID model able to predict better the MT was modified by considering the Euclidean norm of a vector whose components are A/W,

A/H and A/D with D target's depth; to consider the approach angle in reaching the 3D target, each component is weighted by a value, function of the angle θ. The ID model is shown in the following:

$$\boldsymbol{ID = log_2\left(\sqrt{f_W(\theta)\left(\frac{A}{W}\right)^2 + f_H(\theta)\left(\frac{A}{H}\right)^2 + f_D(\theta)\left(\frac{A}{D}\right)^2} + 1\right)} \quad (1.13)$$

Where D is the target's depth, while $f_W(\theta), f_H(\theta), f_D(\theta)$ empirical coefficients.

In (Machuca and Stuerzlinger, 2019), instead, the 3D target was visualized through the use of 3D glasses. Subjects performed the three-dimensional reaching task, by reaching the 3D target through the use of a wand.

Differently from the previous case, the regression analysis between MT and ID was optimized by adding a term called CTD (change in target depth) rather than modifying the ID model employed (Equation 1.5).

1.4 The continuous formulation

All the ID formulations analyzed previously preserve the original structure of Fitts' experiments: the target width W, and the movement amplitude A. The contribution due to the target is evaluated differently basing on the type of target considered (1D, 2D, 3D), while A is always the minimum distance between the starting point and the target point. This structure allows to evaluate the difficulty associated to a simple reaching task, where features considered are only A and the width. Nevertheless, if an agent is asked to execute a reaching task by following a particular trajectory, spatially constrained along the entire path, the related difficulty is expected to increase. This phenomenon can be attributable to the fact that subjects' movements are not constrained only at the target, but along the entire path: movements' accuracy is required from the starting to the target point. This topic has been discussed by (Accot and Zhai, 1997) that focused on experiments involving trajectory-based interactions such as navigating through nested-menus on computer interfaces.

To obtain an ID formulation able to quantify the difficulty in following a general trajectory fully constrained, Accot and Zhai considered initially a simple 'goal passing' task, where the target width is perpendicular to the movement amplitude, placed at distance A from the starting point (Figure 1.8, (a)). By considering 2 identical targets, each one placed at A/2, the total ID will be the sum two contributions, each one defined

as $log_2\left(\frac{A}{2W}+1\right)$. Only by adding a further target placed at A/2 from the starting point, the total difficulty increases, and becomes: $ID_2 = 2log_2\left(\frac{A}{2W}+1\right)$ (Figure 1.8, (b)). Consequently, by considering N identical targets, $ID_N = Nlog_2\left(\frac{A}{NW}+1\right)$ (Figure 1.8, (c)). This last result is in line with previous observations, since being the subjects' movements more constrained (compared to case (a) or (b)), the consequent difficulty increases. As described in (Accot and Zhai, 1997), by considering the number of identical targets N that tends to infinite, the task becomes a 'Tunnel Traveling' Task where movements are fully constrained along A ((Figure 1.8, (d)).), and therefore:

$$\boldsymbol{ID_{TTT} = \frac{A}{W} \cdot \frac{1}{ln\,(2)}} \tag{1.14}$$

The logarithmic expression disappears, and, except for the constant $\frac{1}{\ln(2)}$, the difficulty related to the 'Tunnel Traveling' is function only of the movement amplitude A and the path's width W.

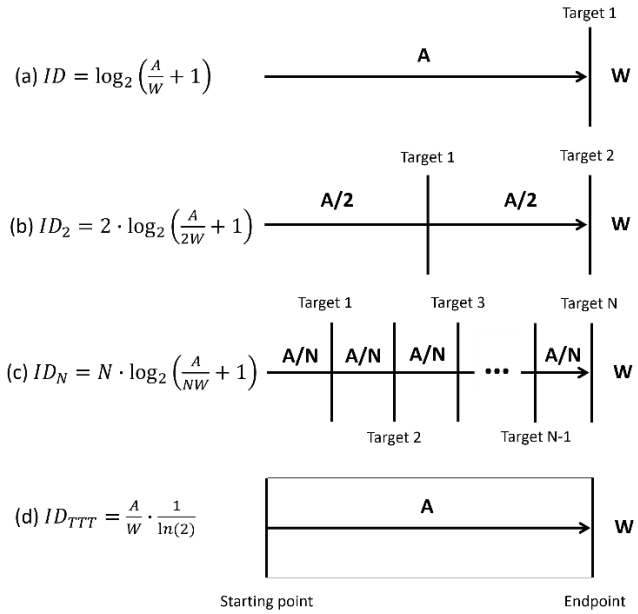

Figure 1.8 *Steps to obtain the 'Tunnel Traveling' Task ID (ID_{TTT})*

Therefore, if the movement amplitude A is substituted by a general trajectory spatially constrained along the entire path, the relative difficulty is:

$$\boldsymbol{ID_t = \int_t \frac{ds}{W(s)}} \tag{1.15}$$

Where t is a general trajectory, while $W(s)$ is the target width perpendicular to t at curvilinear coordinate s (Figure 1.9).

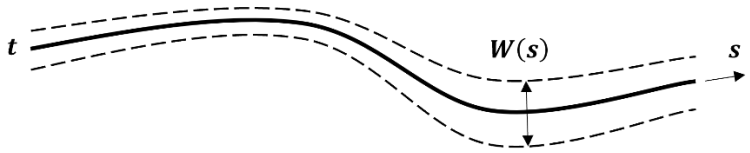

Figure 1.9 *Example of spatially constrained trajectory with variable target width $W(s)$ along the curvilinear coordinate s*

The main features that distinguish the task depicted in Figure 1.9 with the classical Fitts' 'tapping task' (Figure 1.1) is that the trajectory to follow is predefined, the target width is placed along the path and not only at the endpoint, and finally that $W(s)$ is perpendicular to t at curvilinear coordinate s, and not in the same axis of motion. This feature is attributable to the fact that when subjects are asked to follow a trajectory constrained between two boundaries (that could be variable along s) the greatest constraint that limit the movements to be performed is located perpendicular to the direction of motion: an example could be drawing between two boundaries (e.g., by assuming t in Figure 1.9 as the curve to draw). A summary table of the various ID formulations analysed is depicted in Table 1.1.

In the following section, the continuous formulation of the ID is applied in experiments involving 'steering tasks'. Subjects were asked to place an interactive pen on a tablet and move it along a 'Tunnel Traveling' or 'Circular Traveling' Task by following the spatial constraints that define the allowable region where the pencil can be moved. Results obtained show an improvement of the 'Speed-Accuracy' trade-off model, by adding the contribution due to the task difficulty (continuous formulation).

Table 1.1 *MT=f(ID) regression Equations and ID formulations. *=three-dimensional reaching tasks.*

Author	Target	MT=f(ID)	Features
(Fitts, 1954)	1D	$MT = a + b \cdot log_2\left(\frac{2A}{W}\right)$	A: movement amplitude W: target width
(MacKenzie, 1992)	1D	$MT = a + b \cdot log_2\left(\frac{A}{W} + 1\right)$	W: target width or effective target width W_e
(Accot and Zhai, 1997)	1D	$MT = a + b \cdot \int_t \frac{ds}{W(s)}$	s: curvilinear coordinate W(s): target perpendicular to trajectory at s
(MacKenzie and Buxton, 1992)	2D	$MT = a + b \cdot log_2\left(\frac{A}{min\,(W,H)} + 1\right)$	H: target height
(Accot and Zhai, 2003)	2D	$MT = a + b \cdot log_2\left(\sqrt{\left(\frac{A}{W}\right)^2 + \eta\left(\frac{A}{H}\right)^2} + 1\right)$	η: empirical coefficient
(Zhang, Zha and Feng, 2012)	2D	$MT = a + b \cdot log_2\left(\sqrt{\omega\left(\frac{A}{W}\right)^2 + \eta\left(\frac{A}{H}\right)^2} + 1\right)$	$\omega + \eta = 1$ $\omega = c_1 + c_0 \cdot \cos^2\theta$ $\eta = c_2 + c_0 \cdot \sin^2\theta$ $c_2,\ c_1, c_0$ empirical coefficients θ: approach angle
(Murata and Fukunaga, 2018)	2D	$MT = a + b \cdot log_2\left(\alpha\beta\left(\frac{A}{W}\right) + 1\right)$	$\alpha = \sqrt{W/H}$ (H: target height) $\beta = f(\theta)$
(Grossman and Balakrishnan, 2005)	2D	$MT = a + b \cdot ID_{pr}$ $ID_{pr} = f\left(\iint_R \frac{1}{cA\sqrt{2\pi}} e^{-\left(\frac{X'^2}{2cA^2}\right)} \cdot \frac{1}{dA\sqrt{2\pi}} e^{-\left(\frac{Y'^2}{2dA^2}\right)} dX'dY'\right)$	R: region defined by the target c, d: empirical coefficients
(Murata and Iwase, 2001)*	2D	$MT = a + b \cdot log_2\left(\frac{A}{W} + 1\right) + c \cdot sin\theta$	
(Cha and Myung, 2010)*	2D	$MT = a + c \cdot \theta_1 + d \cdot cos\theta_2 + log_2\left(\frac{A}{W} + 1\right)$	θ_1: approach angle θ_2: azimuth angle
(Grossman and Balakrishnan, 2004)*	3D	$MT = a + b \cdot ID$ $ID = log_2\left(\sqrt{f_W(\theta)\left(\frac{A}{W}\right)^2 + f_H(\theta)\left(\frac{A}{H}\right)^2 + f_D(\theta)\left(\frac{A}{D}\right)^2} + 1\right)$	D: target depth θ: approach angle $f_W(\theta), f_H(\theta), f_D(\theta)$ em pirical coefficients
(Machuca and Stuerzlinger, 2019)*	3D	$MT = a + b \cdot log_2\left(\frac{A}{W} + 1\right) + c \cdot CTD$	CTD: change in target depth [cm]

2. The Index of Difficulty in the 'Speed-Accuracy' trade-off model

In rapid aimed movements, there is a trade-off between the accuracy of movements, and the speed of movements' execution. This phenomenon has been firstly observed by Woodworth in 1899 (Woodworth, 1899); in one experiment, subjects that were asked to move a pencil between target points, experienced a loss of accuracy when the speed of movement was increased. This trade-off phenomenon has been observed by many authors, such as Schmidt et al. (Schmidt and et al, 1979), who found a linear relationship between the standard deviation of configurations reached at the target (spread of hits), and the speed of execution, evaluated as the ratio between the distance to travel, and the time of execution. The linear 'Speed-Accuracy' trade-off, is expressed in the following (Schmidt and et al, 1979):

$$\boldsymbol{SD = a + b \cdot \frac{A}{MT}} \tag{2.1}$$

These results have been observed not only by considering a punctiform target (Woodworth, 1899; Zelaznik *et al.*, 1988), but also considering a target that defines the allowable region to reach (Crossman and Goodeve, 1983; Meyer *et al.*, 1988; Zelaznik *et al.*, 1988). Nevertheless, in Equation 2.1, no explicit information about the difficulty related to the execution of a fully spatially constrained reaching task is provided. Since the endpoint variability may be affected by the spatial limits imposed by the task, as well as the nominal trajectory to execute, in the following is proposed a new model that takes into account the influence of the continuous formulation of the ID (Equation 1.15) on the standard deviation of the endpoint position.

2.1 The 'Speed-ID-Accuracy' Model

Equation 2.1 states that higher the velocity in executing a movement amplitude A, higher is the uncertainty of meeting the target, defined by a certain width W. As in Fitts' 'tapping task' experiment, the 'Speed-Accuracy' trade-off takes into account only the distance to cover through movements, without considering what happens or features/constraints demanded by the task between the starting and endpoint (target). In (Digiesi, Lucchese

and Mummolo, 2020), it has been proposed to extend the 'Speed-Accuracy' trade-off model by considering the standard deviation of the endpoint position function of both speed of execution, and the continuous formulation of the ID. Basing on data available in literature (Hourcade and Berkel, 2008), where subjects were asked to place an interactive pen on a tablet and move it along a spatially fully constrained trajectory, the SD=f(speed, ID_t) relationship that allowed to obtain the best regression result was:

$$\boldsymbol{SD = a + b \cdot v^{\beta} + c \cdot \int_t \frac{ds}{W(s)}} \tag{2.2}$$

a, b, c, and β are empirical coefficients.

In (Hourcade and Berkel, 2008) two types of experiments have been considered: the first involves the execution of a 'Tunnel Traveling' Task (TTT) (Figure 1.8, (d)); the second involves the execution of a 'Circular Traveling' Task (CTT) as the one depicted in Figure 2.1.

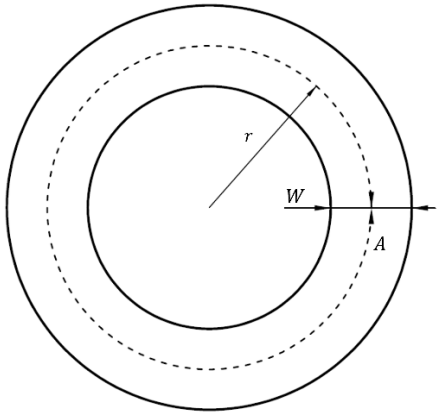

Figure 2.1 *'Circular Traveling' Task (CTT) experiment set-up*

In this case the nominal trajectory is a circumference (dashed black line in Figure 2.1), therefore the movement amplitude $A = 2\pi r$, with r the radius of the nominal trajectory. As for the TTT, W is constant along the nominal trajectory.

The difficulty related to the TTT case (ID_{TTT}) is equal to $\frac{A}{W} \cdot \frac{1}{\ln(2)}$ (Figure 1.8, (d)); the difficulty related to the CTT can be obtained as a specific case of a more general scenario where the nominal trajectory is equal to a circumference's arc, and the target width W is decreasing along the curvilinear coordinate s. In Figure 2.2 an example of a semi-circular nominal trajectory.

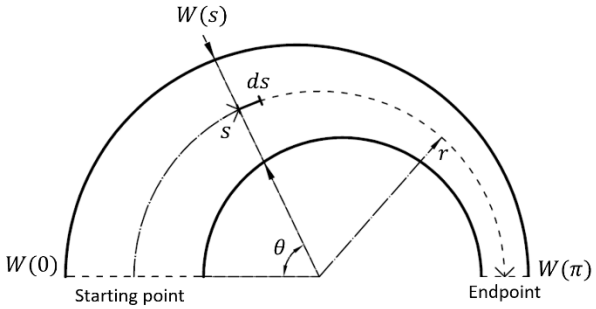

Figure 2.2 *Semi-circular nominal trajectory with a decreasing width $W(s)$ along curvilinear coordinate s*

The decreasing entity of $W(s)$ can be expressed analytically by the following formulation:

$$\boldsymbol{W(s) = W(0) - k \cdot s} \tag{2.3}$$

Where:

- $s = r \cdot \theta$ is function of the polar angle θ
- $W(0)$ is the initial target width ($\theta = 0$)
- k is a constant tuning the reduction of the target width with the polar angle, θ

Being $ds = rd\theta$, the formulation that expresses the difficulty in executing a circumference's arc is:

$$\boldsymbol{ID_t = \int_t \frac{ds}{W(s)} = \int_0^{\theta_f} \frac{r}{W(0) - k \cdot r \cdot \theta} d\theta} \tag{2.4}$$

By solving Equation (2.4)

$$\boldsymbol{ID_{arc} = \frac{1}{k} \cdot ln\left(\frac{W(0)}{W(0) - k \cdot r \cdot \theta_f}\right)} \tag{2.5}$$

By assuming a given reduction factor ($f_{rid} > 1$), it can be defined the relation between the initial target width ($W(0)$) and the final target width ($W(r \cdot \theta_f)$) as:

$$\boldsymbol{W(r \cdot \theta_f) = \frac{W(0)}{f_{rid}}} \tag{2.6}$$

Therefore, by considering the last value of the curvilinear coordinate $s = r \cdot \theta_f$ in Equation 2.3, and by expressing $W(r \cdot \theta_f)$ through Equation 2.6, k is defined as:

$$\boldsymbol{k = \frac{W(0)}{r \cdot \theta_f}\left(1 - \frac{1}{f_{rid}}\right)} \tag{2.7}$$

The difficulty related to the CTT is a particular case where $f_{rid} = 1$, and $\theta_f = 2\pi$.

ID_{CTT} is equal to:

$$\boldsymbol{ID_{CTT} = \frac{2\pi r}{W}} \tag{2.8}$$

In the following, the numerical case, as well as results obtained are shown.

2.2 Numerical case

Starting from experimental data available in the scientific literature (Hourcade and Berkel, 2008), the 'Speed-ID-Accuracy' model has been applied to both Tunnel Traveling Task (TTT) and Circular Traveling Task (CTT): 60 subjects were asked to place an interactive pen on a tablet and move it along a spatially fully constrained trajectory of different shape (straight line or circumference).

2.2.1 Tunnel Traveling Task (TTT)

The TTT row data available in (Hourcade and Berkel, 2008) are summarized in Table 2.1.

Table 2.1 *Experimental data on Tunnel Traveling Task (Hourcade and Berkel, 2008)*

A (cm)	**W (cm)**	**MT (s)**	**Probability Success (%)**
1.152	0.384	0.290	97.6
1.536	0.384	0.379	96.9
1.920	0.384	0.459	94.5
1.728	0.576	0.353	98.7
2.304	0.576	0.444	98.0
2.880	0.576	0.549	97.3
2.304	0.768	0.399	99.1
3.072	0.768	0.515	98.0
3.840	0.768	0.640	97.2

As depicted in Figure 1.4, when considering the case of reaching a target characterized by a given width, the dispersion of hits can be considered normally distributed, in analogy with the 'normal noise' of the communication channel. The Effective Target Width W_e is representative of this behaviour and can be employed to evaluate indirectly the dispersion of hits. From the Probability Success, the corresponding z-score (z_e) can be evaluated from the z distribution tables. By knowing the target width at the endpoint (W) and z_e, W_e can be quantified through Equation 1.6. The standard deviation (SD) of hits can be easily evaluated as:

$$\boldsymbol{SD = \frac{W_e}{2 * z_e}} \tag{2.9}$$

The employment of both Equations 1.6 and 2.9 is a powerful tool that allows to calculate the standard deviation of hits at the target even in the case when each hits position is not recorded, under the only assumption of a normal distribution. Results in the case of TTT are depicted in Table 2.2.

Table 2.2 *Average Speed, W_e, ID_{TTT}, and SD_{TTT} values for the Tunnel Traveling Task (TTT)*

Average Speed (A/MT) (cm/s)	**Probability Success (%)**	$\boldsymbol{z_e}$ **(z-tables)**	$\boldsymbol{W_e}$ **(cm) (eq. 1.6)**	$\boldsymbol{ID_{TTT}}$ **(eq. 1.14)**	$\boldsymbol{SD_{TTT}}$ **(cm) (eq. 2.9)**
3.972	97.6	2.26	0.351	4.328	0.078
4.053	96.9	2.17	0.366	5.771	0.084
4.183	94.5	1.93	0.411	7.213	0.106
4.895	98.7	2.51	0.474	4.328	0.094
5.189	98.0	2.33	0.511	5.771	0.110
5.246	97.3	2.23	0.534	7.213	0.120
5.774	99.1	2.65	0.599	4.328	0.113
5.965	98.0	2.33	0.681	5.771	0.146
6.000	97.2	2.20	0.721	7.213	0.164

By regressing SD_{TTT} values on the average speed and ID_{TTT} values, the parameters of the 'Speed-ID-Accuracy' model (Equation 2.2) have been obtained (Table 2.3).

Table 2.3 *Regression parameters for the SD [cm] in the Tunnel Traveling Task (Average Speed [cm/s])*

Coefficient	**a**	**b**	**c**	**β**	R^2 = 91.78%
Value	-0.0806	0.0274	0.0096	1	p-value = 0.001

SD_{TTT} values evaluated through Equation 2.9, are plotted in Figure 2.3a against the Average Speed observed in experiments (Hourcade and Berkel, 2008) for different ID_{TTT} values evaluated by Equation 1.14; similarly, dependency of SD_{TTT} on both Average Speed observed and ID_{TTT} values predicted by the model (Equation 2.2), is plotted in Figure 2.3b. It is worth nothing the significant dependency of SD_{TTT} on ID_{TTT}. Such a finding is due to the extension of the classical 'Speed-Accuracy' model by the proposed model. By neglecting the influence of ID_{TTT} on SD_{TTT}, the regression analysis on experimental data by Equation 2.1 (classical linear 'Speed-Accuracy' trade-off model) provides a less accurate goodness of fit, being R^2 = 73.46% and p-value = 0.003.

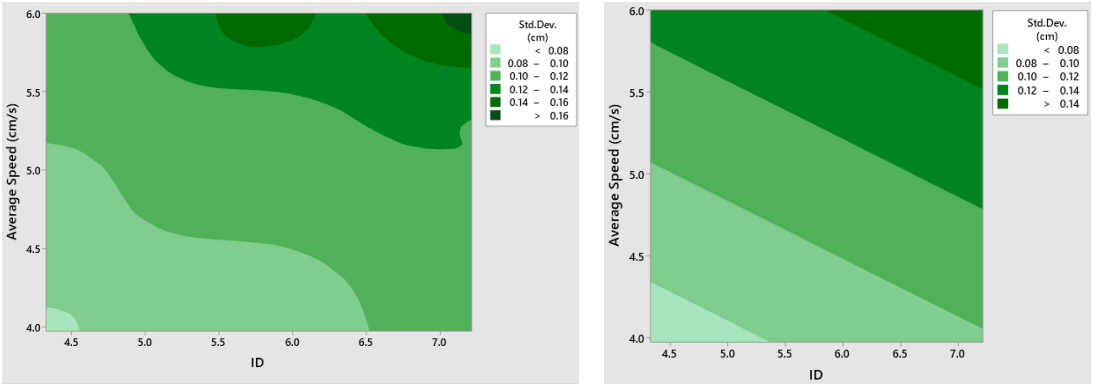

2.3a *2.3b*

Figure 2.3 *Standard deviation at the endpoint (SD_{TTT}) evaluated through Equation 2.9 (figure 2.3a) and predicted through Equation 2.2 (figure 2.3b) vs. ID_{TTT} (Equation 1.14) and Average Speed (cm/s)*

In order to analyse if the Average Speed can be predicted by geometrical features of the task, it has been investigated the power of the information inherent in A and W (data in Table 2.1) to predict the Average Speed (data in Table 2.2), through a regression analysis. The regression model that allowed to predict optimally the Average Speed of execution is:

$$\boldsymbol{v = a' + b' \cdot A + c' \cdot W} \tag{2.10}$$

Regression results are depicted in Table 2.4.

Table 2.4 *Regression parameters for the Average Speed [cm/s] in the Tunnel Traveling Task (A [cm]; W [cm])*

Coefficient	**a'**	**b'**	**c'**	R^2 = 98.97%
Value	2.265	0.213	3.948	p-value < 0.001

Therefore, by considering different values of A (from 20 to 45 cm), and W (3,6, 10 cm), and by predicting the Average Speed through Equation 2.10, 'Speed-ID-Accuracy' model can be extended considering greater ID_{TTT}. Results are in Figure 2.4. Here, the accuracy of individuals is measured in relative terms, i.e. by the ratio (r_{SD}) between the standard deviation of the endpoint (SD) and the target width (W): a higher r_{SD} value represents low relative accuracy of an individual in acquiring a given target.

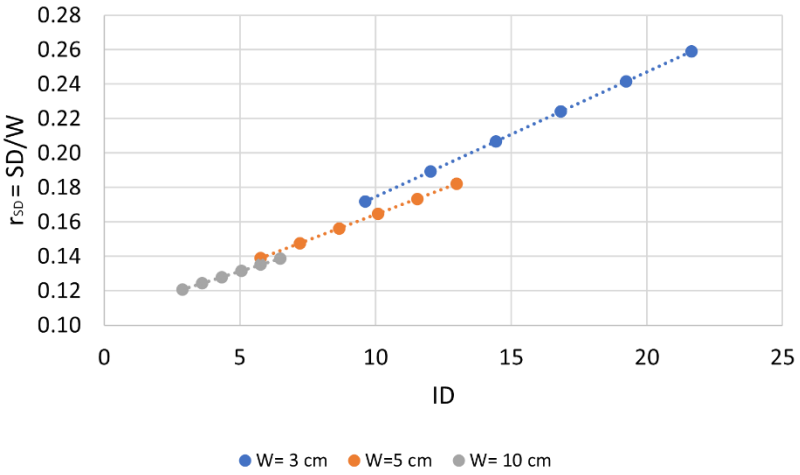

Figure 2.4 *Accuracy reached at the endpoint in a Tunnel Traveling Task: ($r_{SD} = SD/W$) vs. ID for different W values*

The ratio r_{SD} linearly increases with *ID* for a given *W*: less accuracy performance is consequence of higher trajectory lengths as *ID* increases with *A*. Moreover, r_{SD} decreases for higher *W* values at a given *ID*: higher accuracy can be obtained in meeting larger targets' width following a trajectory of a given length. Furthermore, r_{SD} shows a higher sensitivity to *ID* for lower *W* values and same *A* range, as it can be observed in Figure 2.4. In the following, Equation 2.2 has been applied in case of Circular Traveling Task (CTT).

2.2.2 Circular Traveling Task (CTT)

The CTT row data available in (Hourcade and Berkel, 2008) are summarized in Table 2.5.

Table 2.5 *Experimental data on Circular Traveling Task (Hourcade and Berkel, 2008)*

A=2πr (cm)	**W (cm)**	**MT (s)**	**Probability Success (%)**
2.304	0.384	1.324	90.6
3.072	0.384	1.519	89.6
3.840	0.384	1.772	88.0
4.608	0.384	2.151	84.8
3.456	0.576	1.230	97.7
4.608	0.576	1.471	97.9
5.760	0.576	1.770	94.2
6.912	0.576	2.076	91.7
4.608	0.768	1.279	97.7
6.144	0.768	1.513	95.5
7.680	0.768	1.864	93.0
9.216	0.768	2.235	88.6

As in the previously TTT, by considering the normal distribution of the dispersion of hits at the endpoint, Equations 1.6 and 2.9 can be employed to evaluate the z-score (z_e) and the standard deviation (SD), respectively.

Table 2.6 *Average Speed, W_e, ID_{CTT}, and SD_{CTT} values for the Circular Traveling Task (CTT)*

Average Speed (A/MT) (cm/s)	**Probability Success (%)**	**z_e (z-tables)**	**W_e (cm) (eq. 1.6)**	**ID_{CTT} (eq. 1.14)**	**SD_{CTT} (cm) (eq. 2.9)**
1.740	90.6	1.675	0.474	6.000	0.141
2.022	89.6	1.625	0.488	8.000	0.150
2.167	88	1.555	0.510	10.000	0.164
2.142	84.8	1.43	0.555	12.000	0.194
2.810	97.7	2.29	0.520	6.000	0.113
3.133	97.9	2.29	0.520	8.000	0.113
3.254	94.2	1.9	0.626	10.000	0.165
3.329	91.7	1.74	0.684	12.000	0.197
3.603	97.7	2.29	0.693	6.000	0.151
4.061	95.5	2.215	0.716	8.000	0.162
4.120	93	1.81	0.877	10.000	0.242
4.123	88.6	1.58	1.004	12.000	0.318

By adopting the same approach followed for the Tunnel Traveling Task, the regression

parameters of the 'Speed-ID-Accuracy' model (Equation 2.2) are depicted in the following:

Table 2.7 *Regression parameters for the SD [cm] in the Circular Traveling Task (Average Speed [cm/s])*

Coefficient	**a**	**b**	**c**	**β**	R^2 = 80.66 %
Value	0.010	$1.0 \cdot 10^{-5}$	0.0154	2.673	p-value = 0.001

By applying the classical 'Speed-Accuracy' model (Equation 2.1) to the same data set in (Hourcade and Berkel, 2008), the goodness of regression significantly declines, being R^2 = 19.85 and p-value = 0.147. As one can see, the usefulness of the proposed 'Speed-ID-Accuracy' model is even more evident when subjects execute more geometrically complex and demanding tasks, since the different results (R^2 and p-values) in applying both Equations 2.1 and 2.2 are more relevant in the CTT case. In fact, the classical 'Speed-Accuracy' model gives still significant results when considering the TTT (R^2 = 73.46% and p-value = 0.003), compared to the CTT (R^2 = 19.85 and p-value = 0.147), although for both scenarios the 'Speed-ID-Accuracy' model provides the best results enabling to predict more accurately the SD at the endpoint.

As done in the TTT case, it has been investigated the power of geometrical information in predicting the Average Speed of execution. A linear regression model (as Equation 2.10), allowed to obtain the best regression results, whose values are depicted in Table 1.9.

Table 2.8 *Regression parameters for the Average Speed [cm/s] in the Circular Traveling Task (A [cm]; W [cm])*

Coefficient	**a'**	**b'**	**c'**	R^2 = 98.04%
Value	0.104	0.128	3.951	p-value < 0.001

It is important to notice that the geometric features of the task enable to predict almost optimally the Average Speed of execution related to a given task (TTT, or CTT in this context). These results further support the relevance of geometric features in evaluating the Index of Difficulty related to the task (ID_t) as well as in predicting the Average Speed of execution.

Regression parameters of the 'Speed-ID-Accuracy' model provide specific information about the components that most influence the SD at the endpoint. By comparing coefficients between Table 2.3 (TTT case), and Table 2.7 (CTT case), it can be observed that the weight of the Average Speed in the evaluation of SD is greater in TTT (b=0.0274, β=1) rather than in the CTT (b=0.00001, β=2.673); the opposite case is observed by

focusing on the ID_t, whose weight is an order of magnitude greater in the CTT case (c=0.0154) compared to the TTT case (c=0.0096). These results bring to the conclusion that the behaviour of the subject in acquiring a target, depends on the length of the path, on the spatial constraints, and speed of execution; the entity of these three features (the first two summarized in ID_t) depends on the complexity of the trajectory to follow (i.e. linear, circular or other shapes), and affect differently the SD at the endpoint.

2.3 Discussion

The need of quantifying the accuracy of subjects in executing reaching motor tasks characterized by different geometric features is a problem of relevant importance in different work activities. Geometric features of the task can be summarized in a measure that allows to express the difficulty of the task (i.e., ID_t). Differently from the scientific literature, it has been shown that the ID_t is not only useful to predict the time that a subject needs to execute the task (temporal information, such as the MT), but can be employed as a valuable tool to enhance the prediction in quantifying spatial information, such as the SD in acquiring a given target. The proposed 'Speed-ID-Accuracy' model extends the 'Speed-Accuracy' trade-off model towards two directions: firstly, it considers a general geometry of the trajectory which is constrained along the entire path (ID_t); furthermore, the accuracy of subjects in reaching the target is considered as dependent not only on the average speed of execution, but also on the task difficulty calculated for the assigned geometry of the task. It has been observed through experimental data that the classical 'Speed-Accuracy' model tends to fail in predicting the SD when no information about the task difficulty is provided.

The model can be usefully applied in real cases to assess whether the accuracy required in accomplishing a reaching motor task of a given complexity (ID_t), can be ensured with a given speed of execution. An operator able to guarantee the required movement accuracy by executing the task with a higher speed means that he/she needs less time to complete the activity; therefore, this behaviour is preferrable to slower operators, since it ensures to save time. Conversely, the model can be applied also to assess the speed limit in executing a task of a given complexity under accuracy constraints.

A first step to investigate the potential of the ID as tool to predict the accuracy in reaching a target has been performed. Nevertheless, the ID is not yet considered as a measure able

to evaluate the difficulty experienced by the agent. In fact, in its current form, the ID_t does not take into account the trajectory executed, as well as the stochasticity of movements performed. ID_t is a deterministic measure evaluated basing on predefined geometric features of the task and does not summarize features of movements executed. ID_t is a deterministic measure, unable to discriminate between different motor behaviours of agents. For these reasons, the research proceeded toward this direction, by investigating the potential of the ID as a measure of the agent's motor difficulty.

3. The Index of Difficulty as a measure of agent's motor difficulty

As discussed in the introductory chapter, in current work environments the role of the operator is still essential in motor activities that require the execution of repetitive motor tasks (e.g., lifting, carrying, manipulating, holding or restraining objects). In this context, there is still the necessity to evaluate the movements-related difficulty of an agent (e.g., operator) in performing repetitive motor tasks. Therefore, in the following, it is described a new ID model (called ID_{obs}) able to evaluate the motor difficulty related to a given agent, by considering its motor behaviour and stochasticity of movements performed.

3.1 The Stochastic Index of Difficulty

3.1.1 Internal and external constraints

The wide scientific literature on the various ID models (see Table 1.1) and experimental testing (MacKenzie and Oniszczak, 1998; Guiard, Beaudouin-Lafon and Mottet, 1999; Mackenzie and Jusoh, 2000; Hornof, 2001; Oh and Stuerzlinger, 2002; Poupyrev, Okabe and Maruyama, 2004), are aimed at quantifying the 'geometrical' task difficulty: tasks with smaller targets and longer paths are more difficult. Nevertheless, these models do not directly measure the agent-specific motor behaviour during the execution of a given repetitive reaching motor task, representative of the agent-environment interaction. Variability of movements, length of trajectories executed, subject-specific strength, skills, and required environment-related features are all factors that contribute to the motor difficulty experienced by a moving agent as he/she repeatedly interacts with the environment (e.g., target-reaching movement, locomotion, etc.).

Environment-related features can be summarized in 'external constraints', since they define characteristics of the motor task 'external' to the agent. On the contrary, factors such as age, sex, experience, number of degrees of freedom available to control the motor system, strength and other physical features can be attributable to the 'internal constraints' of the agent. Both internal and external constraints influence movements of agents since changes of these constraints bring to different motor behaviours.

The novel concept of motor difficulty experienced by an agent performing repetitive

motor tasks represents how much the flexibility of movements is limited by both the agent and the environment features. In general, flexibility is limited by the presence of several constraints that can be relative to the specific agent (internal constraints) or to the task/environment (external constraints) (Smeets, 1994). When an agent's movement is more (or less) limited due to internal/external constraints, the difficulty experienced in the task execution should be higher (or lower). The stochastic behavior of agents performing any repetitive motor tasks, as enabled by the redundant motor system, implicitly and simultaneously reflects the characteristics of the agent (e.g., motor redundancy, strength, skill) and the type of interaction (e.g., task and environmental features).

No single performance measure exists that captures the experienced motor difficulty, while taking into account the above-mentioned factors. This concept of motor difficulty can be expressed by the stochastic motor behavior of an agent that arises during a desired interaction with the environment, quantified by the novel stochastic Index of Difficulty (ID_{obs}): it will be affected by internal (Lucchese *et al.*, 2021), and external constraints (Lucchese, Digiesi and Mummolo, 2022). Due to the importance of motor variability and its link with flexibility during the execution of repetitive motor tasks, a related discussion must be carried out before describing the novel model of motor difficulty.

3.1.2 Variability in Reaching Motor Tasks

During the repetitive execution of a reaching motor task, the motor system of an agent follows one of the infinite paths (trajectories) that allows the end-effector (e.g. hand, wrist etc…) to reach the target. When an agent performs multiple trials for the same reaching motor task, trajectories of the agent's end-effector will vary stochastically.

A task executed with low motor difficulty represents a type of agent-environment interaction that allows greater flexibility in the choice of equivalent motor solutions; in this case, the stochastic behavior on the end-effector is characterized by greater natural variability, calculated relative to an average trajectory throughout the entire path. Vice versa, a greater motor difficulty is associated to limited flexibility in the task execution, quantified by the small variability of the end-effector trajectories throughout the movement.

Limited flexibility (and great difficulty) could be due to external constraints that restrain end-effector movements, hence requiring great accuracy in the control of its position. On

the other hand, the source of limited flexibility (and great difficulty) could come from internal constraints that make the agent overly rigid and less adaptable to potential perturbations. Lastly, a reduced flexibility could be the result of a particular agent-environment coupling that exhibits a more rigid (hence, difficult) behaviour as compared to one that is assumed to be optimal with respect to some criterion (e.g., resilience, speed, success rate).

It is well known that motor variability is a phenomenon that stems from multiple origins and arises during the execution of repetitive movements. Nevertheless, in the scientific literature there is still a debate about its nature and role. For example, different theoretical perspectives, such as reinforcement learning vs. some motor control theories, give to motor variability two opposite roles (Singh *et al.*, 2016): in the former, the presence of motor variability is seen as a useful feature in the learning process (Herzfeld and Shadmehr, 2014; Wu *et al.*, 2014; Cashaback, McGregor and Gribble, 2015); in the latter, variability is seen as a disturbance. (Singh *et al.*, 2016) attempted to unify these two perspectives giving an explanation of the co-existence of the two aspects ("positive" and "negative") of motor variability in repeated movements, through the uncontrolled manifold theory (Scholz and Schöner, 1999; Latash, Scholz and Schöner, 2002, 2007). (Singh *et al.*, 2016) showed that there are two components of motor variability: one component, which arises from redundancy, does not affect the task-relevant dimension, increases exploration, and facilitates the learning; the other component is a task-relevant variability that should be minimized. The task-relevant dimension relates to the task's phase where accuracy of movements is required. Results obtained from (Singh *et al.*, 2016) are in line with the optimal feedback control theory (Todorov and Jordan, 2002; Liu and Todorov, 2007). Todorov et al. observed that during the execution of a repetitive reaching motor task, the subject reached the target by executing different paths thanks to the motor redundancy.

The concept of motor redundancy has been introduced by Bernstein (Bernstein, 1967) through the 'degrees-of-freedom' problem: the number of degrees of freedom of the human motor system is greater than the ones needed. Since humans have more degrees of freedom than needed, this motor redundancy allows a more flexible motor behaviour resulting in reaching the same target by executing different trajectories. During an activity involving the hitting of an anvil through a hammer, the task can be performed by executing different repetitive trajectories: the motor variability stemming from the

execution of repetitive movements enables a more flexible behaviour, afforded by the motor redundancy (Müller and Sternad, 2009). In (Robertson and Miall, 1997) is observed that when all the possible arm configurations are allowed, a greater flexibility and a greater motor variability are obtained during the execution of reaching movements; lower variability is obtained, instead, while making the arm non-redundant by restraining the allowable movements (by forbidding wrist movements).

With this perspective, the motor redundancy allows a flexible motor command by enabling multiple joint configurations for any specific hand position (Robertson and Miall, 1997). Other authors came to the same conclusions, like (Gielen, van Bolhuis and Theeuwen, 1995) who stated that redundancy allow great flexibility in the choice of the motor response since the large number of degrees of freedom makes that a particular position may corresponds to a large number of joint configurations. When focusing on the walking task, (Dingwell, John and Cusumano, 2010) showed that during walking on a treadmill, humans exploit redundancy by adjusting stepping movements while maintaining performance: this perspective gives a positive meaning to variability, strictly related to redundancy. The motor redundancy, allows to perform complex tasks repeatedly while allowing motor variability, that is, potentially beneficial (Dingwell, John and Cusumano, 2010). As observed by (Todorov and Jordan, 2002; Liu and Todorov, 2007), during the execution of a repetitive reaching motor task, when the subject can reach the target by executing different paths, thanks to the motor redundancy, a higher motor variability is observed in task-irrelevant dimensions (task's phase where accuracy of movements is not required).

Our model and perspective are in line with these views in which redundancy plays a role in enabling motor variability in redundant motor systems. A typical example of redundant motor system is one with a great number of joints, so that the multiple joints configurations result in a more flexible end-effector movement. A greater flexibility of the agent's motor system means a greater number of configurations reachable, and therefore a motor task can be successfully executed in multiple ways. In this context, therefore, flexibility has a positive connotation, since it is opposed to the case of overly-rigid systems that are less adaptable to perturbations (Stergiou, Harbourne and Cavanaugh, 2006), and can be achieved by channeling the natural movement variability (i.e., variability observed within the same movement, without any externally imposed perturbations) (Ranganathan, Lee and Newell, 2020): flexibility is the ability to achieve

the same task outcome using different movement solutions.

Constraints limit the configurations achievable by the agent and make the motor system less flexible. Constraints can be associated to the agent or can be task-related (Smeets, 1994). As previously discussed, the first ones characterize the agent (internal constraints), the second ones characterize the task and the environment (external constraints). Both types of constraints affect the movement execution, limiting the exploitation of motor redundancy and the equivalent motor solutions that an agent can assume. Under this perspective, the exploitation of motor redundancy allows a higher flexibility in the choice of the motor response, affected by both internal and external constraints.

3.1.3 General Model of Motor Difficulty

In order to quantify the motor difficulty of an agent in executing a reaching motor task repeatedly executed by considering the entire movements executed (not only at the target), and the motor variability, the stochastic Index of Difficulty (ID_{obs}) can be quantified through Equation 1.15; nevertheless, being ID_{obs} a measure evaluated after the movements' observation, components of Equation 1.15 (nominal trajectory t and $W(s)$) must be adapted and re-interpreted.

Firstly, since during the execution of a repetitive reaching motor task, movements performed change at each trial, the average behaviour of the agent can be expressed by its average trajectory (t_{avg}). Consequently, when an agent performs multiple trials for the same motor task, trajectories of the agent's end-effector will vary stochastically, and the natural variability associated to movements can be expressed by $W(s)$. In fact, in Equation 1.15, $W(s)$ represents the maximum allowable pre-defined tolerance of movements, i.e. the maximum allowable variability that can be tolerated, or spatial constraints that define the allowed region of motion. In this case, instead, $W(s)$ expresses the natural motor variability, evaluated a posteriori to quantify the observed flexibility of agents.

Consequently, the nominal trajectory (t) is substituted by the average trajectory (t_{avg}), and the target width $W(s)$ is substituted by $W_{obs}(s, \varphi)$, the 'stochastic' width that stores information about the motor variability. Since $W_{obs}(s, \varphi)$ expresses the spread of movements at each curvilinear coordinate s, its entity depends on the probability level φ considered. Consequently, Equation 1.15 becomes:

$$\boldsymbol{ID_{obs}(t_{avg}, \varphi) = \int_{t_{avg}} \frac{ds}{W_{obs}(s, \varphi)}} \tag{3.1}$$

$ID_{obs}(t_{avg}, \varphi)$ has been named as 'stochastic' Index of Difficulty, since the agent's motor difficulty depends on the average trajectory executed, as well as on the probability level φ considered for the stochastic width $W_{obs}(s, \varphi)$. The agent's motor difficulty can be evaluated also until a specific point of t_{avg}. In this case let's define s^* a given value of the curvilinear coordinate s, with $s^* \in [0; t_{avg}]$. Therefore, Equation 3.1 is defined as:

$$\boldsymbol{ID_{obs}(s^*, \varphi) = \int_{0}^{s^*} \frac{ds}{W_{obs}(s, \varphi)}} \tag{3.2}$$

As in Equation 1.15, $W_{obs}(s, \varphi)$ is perpendicular to t_{avg} at a given curvilinear coordinate s. In the following, the method to evaluate $W_{obs}(s, \varphi)$ is firstly described in case of reaching motor tasks involving 2D movements, and then is extended to the case of 3D movements.

3.1.3.1 2D Movements

Let's consider an agent performing n trials of the same reaching motor task involving 2D movements. For each trial, a t_k trajectory is observed ($k = 1, \dots, n$), and the average trajectory is given by t_{avg} (Figure 3.1); $q_{avg}(s)$ is the point $\in t_{avg}$ at curvilinear coordinate s. $q_k(s)$ is the configuration $\in$ to the k^{th} trial trajectory at curvilinear coordinate s, given by the intersection between the axis orthogonal to t_{avg} at the curvilinear coordinate s (T) and the k^{th} trial trajectory.

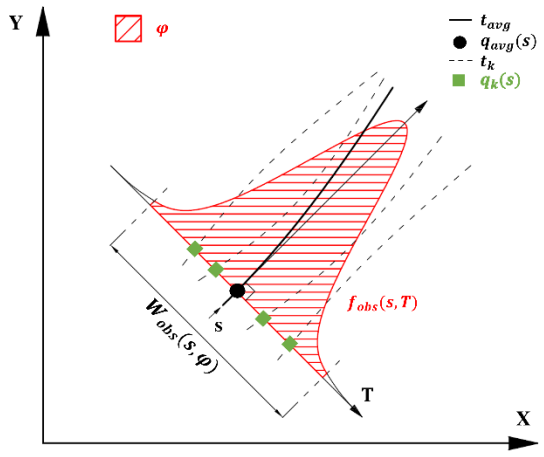

Figure 3.1 *$W_{obs}(s, \varphi)$ in case of 2D movements*

Since the theorization of the Fitts' law (Fitts, 1954) it was observed that in reaching motor

tasks, repetitive agent's movements follow a normal distribution (Ghahramani and Wolpert, 1997; Messier and Kalaska, 1997; Van Beers, Haggard and Wolpert, 2004; Guigon, Baraduc and Desmurget, 2008). Therefore, basing on these results, it can be assumed that the spread of the n configurations follow a normal distribution. $f_{obs}(s,T)$ expresses the probability distribution function obtained from the spread of configurations observed on T at curvilinear coordinate s; in this case $f_{obs}(s,T)$ is the PDF of a normal distribution, and the entity of $W_{obs}(s,\varphi)$ can be evaluated as:

$$\boldsymbol{W_{obs}(s,\varphi) = 2 \cdot z(\varphi) \cdot \sigma(q_k(s))} \tag{3.3}$$

Where z is the z-score of the standardized normal distribution, that depends on the probability level φ (z = 1 for φ = 0.6827; z = 2 for φ = 0.9545; z = 2.066 for φ = 0.9600; z = 3 for φ = 0.9973), while $\sigma(q_k(s))$ is the standard deviation of the configurations evaluated on $T(s)$. Since both $q_k(s)$ and $q_{avg}(s)$ can be expressed in an (x,y) coordinate system with $q_k(s) = (x_k(s), y_k(s))$, and $q_{avg}(s) = \left(x_{avg}(s), y_{avg}(s)\right)$, $\sigma(q_k(s))$ can be evaluated as:

$$\boldsymbol{\sigma(q_k(s)) = \sqrt{\frac{1}{n-1} \cdot \sum_{k=1}^{n} \left(\left(x_k(s) - x_{avg}(s)\right)^2 + \left(y_k(s) - y_{avg}(s)\right)^2 \right)}} \tag{3.4}$$

Since $\sigma(q_k(s))$ expresses the spatial dispersion of configurations with respect to $q_{avg}(s)$, it has the unit of measurement of a distance.

In paragraph 3.2, both formulations 3.1 and 3.2, with $W_{obs}(s,\varphi)$ expressed by Equation 3.2, will be applied in a 2D reaching motor task (walking task), showing that the agent's motor difficulty is affected by internal constraints. In the following paragraph, the method to evaluate $W_{obs}(s,\varphi)$ in case of 3D movements, is described.

3.1.3.2 3D Movements

The method to evaluate $W_{obs}(s,\varphi)$ is slightly different when considering a reaching motor task involving 3D movements. In this case, by considering the plane orthogonal to the 3D average trajectory at curvilinear coordinate s, the spread of configurations lies in a two-dimensional plane $P(s)$ (Figure 3.2).

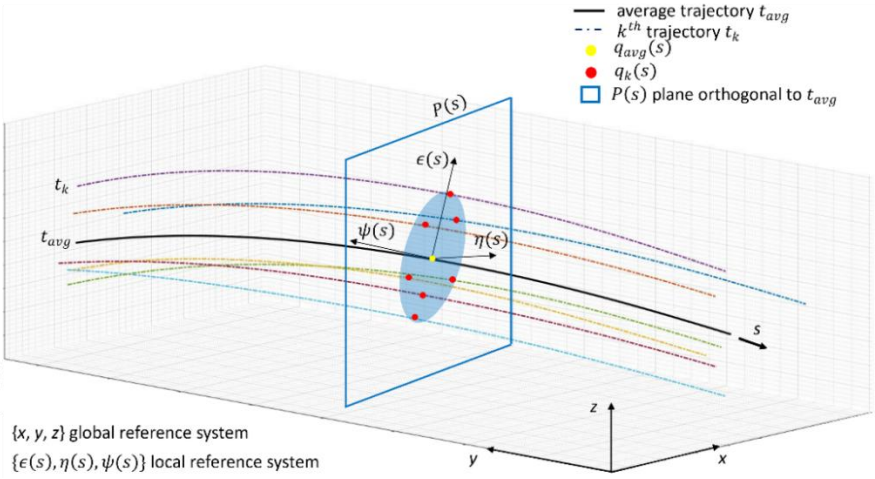

Figure 3.2 *Example of three-dimensional trial trajectories (dash-dotted lines) and their average (thick black line). The light blue ellipse shows the motor variability in the plane $P(s)$ orthogonal to t_{avg} at s.*

As analysed in the paragraph describing variations of the Fitts' law (paragraph 1.3), a relevant problem emerges when considering a 2D targets, since it must be ensured the dimensionless ratio between the travelling distance and the dimension of the target: some authors considered the contribution of both the height and width of the target in a Euclidean norm (Accot and Zhai, 2003; Zhang, Zha and Feng, 2012), rather than the minimum between the two (MacKenzie and Buxton, 1992) (see Table 1.1 for other examples). Moving this problem in case of 3D observed movements, the entity of the stochastic width $W_{obs}(s, \varphi)$ must store the information about the two-dimensional motor variability while maintaining the dimensionless ratio with the average trajectory t_{avg}. To calculate the entity of $W_{obs}(s, \varphi)$, firstly the Principal Component Analysis (PCA) technique is applied to evaluate the distribution of the n points $q_k(s)$ at curvilinear coordinate s, secondly an analytical method must be defined to store information about the two-dimensional motor variability, in the one-dimensional stochastic width $W_{obs}(s, \varphi)$. As observed in field studies (Messier and Kalaska, 1997; Van Beers, Haggard and Wolpert, 2004; Hansen, Elliott and Khan, 2008), the variability of the configurations ($q_k(s)$) follow a bivariate normal distribution, and their spatial distribution is expressed by an elliptical shape (called standard deviation ellipse); the elliptical shape of the spatial distribution of the n configurations $q_k(s)$ is evaluated by applying the Principal Component Analysis (PCA) technique (Daffertshofer *et al.*, 2004; Müller and Sternad, 2009; Elliott *et al.*, 2010; Preatoni *et al.*, 2013). For a better clarity, the notation of all the variables and parameters used in applying the PCA, has been summarized in the following table.

Table 3.1 *Notation used for the PCA*

Name	Definition
PCA	Principal Component Analysis
$\{x, y, z\}$	Global reference system
n	Number of observed trajectories (i.e., trials) executed
k	Index for the k^{th} observed trajectory; $1 < k < n$
t_k	k^{th} oabserved trajectory
t_{avg}	Average trajectory
s	Curvilinear coordinate of t_{avg}
φ	Probability level
$ID_{obs}(t_{avg}, \varphi)$	Stochastic Index of Difficulty associated to the entire average trajectory t_{avg} with probability level φ
$ID_{obs}(s^*, \varphi)$	Stochastic Index of Difficulty at the curvilinear coordinate $s = s^*$ ($s^* \in [0; t_{avg}]$) with probability level φ
$W_{obs}(s, \varphi)$	Stochastic width, representative of the variability of observed trajectories at the curvilinear coordinate s and probability level φ
$P(s)$	Plane orthogonal to t_{avg}, at coordinate s
$q_k(s)$	Intersection point between t_k and $P(s)$
$q_{avg}(s)$	Point $\in t_{avg}$ at curvilinear coordinate s
$\{\epsilon(s), \eta(s), \psi(s)\}$	Local reference system laying on $P(s)$ with origin at $q_{avg}(s)$
$f = 3$	Number of coordinates of the reference systems
i	Index for the i^{th} coordinate of a reference system; $1 < i < f$
$X_{n\times f}(s)$	Data matrix containing the global coordinates of $q_k(s)$
$X'_{n\times f}(s)$	Data matrix containing the local coordinates of $q_k(s)$
$\Sigma_{f\times f}(s)$	Covariance matrix of $X_{n\times f}(s)$
$\Sigma'_{f\times f}(s)$	Covariance matrix of $X'_{n\times f}(s)$
$\sigma_\epsilon(s)$	Standard deviation of all $q_k(s)$ points, $1 < k < n$, along the local ϵ-coordinate
$\sigma_\eta(s)$	Standard deviation of all $q_k(s)$ points, $1 < k < n$, along the local η-coordinate
$\lambda_\epsilon(s)$	First eigenvalue of $\Sigma'_{f\times f}(s)$
$\lambda_\eta(s)$	Second eigenvalue of $\Sigma'_{f\times f}(s)$
c^2	Constant statistical distance squared for the standard deviation ellipse
MD^2	Squared Mahalanobis distance
T^2	Hotelling's T-squared distance
$\chi^2_{\nu_1,\varphi}$	Chi-squared distribution with ν_1 degrees of freedom, at a given probability level
$F_{\nu_1,\nu_2,\varphi}$	F-distribution with ν_1 degrees of freedom of the numerator and ν_2 degrees of freedom of the denominator

The PCA is a multivariate statistical analysis technique commonly employed to reduce the dimensionality of an experimental problem characterized by a great number of f interrelated variables (f-dimensions) by firstly identifying new f variables that are uncorrelated and independent (Principal Components (PCs)): the f^{th} PC is orthogonal to the $f - 1$ PCs, defining a new coordinate system where data are not correlated (null covariance) (Jolliffe, 2002; Johnson and Wichern, 2015). The n global coordinates of $q_k(s)$, and the f coordinates of the global reference system are considered in the original data matrix $X_{\mathrm{n}\times f}(s)$.

By evaluating the covariance matrix of $X_{\mathrm{n}\times f}(s)$ ($\Sigma_{f\times f}(s)$), and applying the eigenvalue-

eigenvector problem to $\Sigma_{f\times f}(s)$, the PCs are obtained: each PC is defined by the i^{th} eigenvalue λ_i (maximum variance of the i^{th} PCs), and the i^{th} eigenvector (direction of maximum variance of the i^{th} PCs), $\forall\ 1 < i < f$. By applying the PCA at each curvilinear coordinate s, a local reference system, expressed by uncorrelated independent variables $\epsilon(s)$, $\eta(s)$, $\psi(s)$, is identified (Figure 3.2). By rewriting the data matrix in the local reference system ${X'}_{\mathrm{n}\times f}(s)$, the resulting ${\Sigma'}_{f\times f}$ has a null covariance since $\epsilon(s)$, $\eta(s)$, $\psi(s)$ are uncorrelated. These variables represent directions of maximum variance, and the square root of eigenvalues expresses the standard deviations along those directions. The first PC is $\epsilon(s)$ ($\sigma_\epsilon = \sqrt{\lambda_\epsilon}$), the second PC is $\eta(s)$ ($\sigma_\eta = \sqrt{\lambda_\eta}$), with $\lambda_\eta < \lambda_\epsilon$; since all the n points $q_k(s)$ lay in the plane $P(s)$ orthogonal to t_{avg} at s, the eigenvalue and standard deviation of the third PC ($\psi(s)$), is null ($\sigma_\psi = \sqrt{\lambda_\psi} = 0$) (Figure 3.2). Under the assumption that at each value of the curvilinear coordinate s, the n points $q_k(s)$ are normally distributed along directions defined by ϵ and η, the sum of the squared normalized ϵ and η ($z_\epsilon^2(s) = \left(\frac{\epsilon(s)}{\sigma_\epsilon(s)}\right)^2$ and $z_\eta^2(s) = \left(\frac{\eta(s)}{\sigma_\eta(s)}\right)^2$), are equal to a constant squared distance c^2:

$$\boldsymbol{z_\epsilon^2(s) + z_\eta^2(s) = \left(\frac{\epsilon(s)}{\sigma_\epsilon(s)}\right)^2 + \left(\frac{\eta(s)}{\sigma_\eta(s)}\right)^2 = c^2} \tag{3.5}$$

By rewriting the formulation as the following:

$$\boldsymbol{\left(\frac{\epsilon(s)}{\sqrt{c^2}\cdot\ \sigma_\epsilon(s)}\right)^2 + \left(\frac{\eta(s)}{\sqrt{c^2}\cdot\ \sigma_\eta(s)}\right)^2 = 1} \tag{3.6}$$

Where:

- $\epsilon(s)$ is the new variable defined by the first eigenvector.
- $\eta(s)$ is the new variable defined by the second eigenvector.
- $\sigma_\epsilon^2(s) = \lambda_\epsilon(s)$ is the first eigenvalue of the covariance matrix.
- $\sigma_\eta^2(s) = \lambda_\eta(s) < \lambda_\epsilon(s)$ is the second eigenvalue of the covariance matrix.

Formulation 3.5 expresses geometrically the equation of an ellipse whose semi-axes are $\sqrt{c^2}\cdot\sigma_\epsilon(s)$ and $\sqrt{c^2}\cdot\sigma_\eta(s)$. The area contoured by the ellipse's Equation represents the variability; since variability varies basing on the confidence region considered, the ellipse must be consequently adapted. This information in inherent in c^2: by choosing a specific

value of c^2 the semi-axes can be properly modified to consider an ellipse that expresses the variability for a given confidence region (i.e., probability level). Depending on the number of samples considered to evaluate the motor variability, c^2 is calculated differently (Jolliffe, 2002; Johnson and Wichern, 2015). If the entire population is known, c^2 is expressed by the squared Mahalanobis distance (MD^2) and evaluated through the critical values of the Chi-squared distribution with $\nu_1 = f$ degrees of freedom ($\chi^2_{\nu_1,\varphi}$). The critical values of a $\chi^2_{\nu_1,\varphi}$ distribution can be read from the Chi-squared distribution tables, by knowing the number of degrees of freedom ν_1, and the probability level φ. ν_1 is equal to the dimensionality of the motor variability: in the current case $\nu_1 = 2$. If the entire population is not known, and a limited number of trials are executed, c^2 is expressed by the Hotelling's T-squared distance (T^2), and evaluated as the following:

$$\boldsymbol{T^2 = \frac{(n-1)\cdot f}{(n-f)} \cdot F_{\nu_1,\nu_2,\varphi}} \tag{3.7}$$

Where $F_{\nu_1,\nu_2,\varphi}$ is the F-distribution with ν_1 degrees of freedom of the numerator ($\nu_1 = 2$ in the current case), ν_2 degrees of freedom of the denominator (equal to $n - \nu_1$ in the current case), and φ as probability level. The $F_{\nu_1,\nu_2,\varphi}$ critical values can be obtained from the F-distribution tables.

By considering the interval $\theta \in [0, 2\pi]$, parametrization of Equation 3.6 leads to:

$$\begin{cases} \boldsymbol{\epsilon(\theta, s, \varphi) = c(\varphi)\cdot \sigma_\epsilon(s)\cdot cos(\theta)} \\ \boldsymbol{\eta(\theta, s, \varphi) = c(\varphi)\cdot \sigma_\eta(s)\cdot sin(\theta)} \end{cases} \tag{3.8}$$

At curvilinear coordinate s, the distance between the center of the ellipse $q_{avg}(s)$ and a point on the ellipse, i.e. the variable radius of the ellipse in the interval $\theta \in [0, 2\pi]$ at a probability level φ, can be obtained as:

$$\boldsymbol{r(\theta, s, \varphi) = \sqrt{(c(\varphi)\cdot \sigma_\epsilon(s)\cdot cos(\theta))^2 + \left(c(\varphi)\cdot \sigma_\eta(s)\cdot sin(\theta)\right)^2}} \tag{3.9}$$

Whose integral mean value is:

$$\boldsymbol{r_{mean}(s, \varphi) = \frac{1}{2\pi}\int_0^{2\pi} r(\theta, s, \varphi)\, d\theta} \tag{3.10}$$

$r_{mean}(s, \varphi)$ is the semi-width of $W_{obs}(s, \varphi)$. Therefore:

$$\boldsymbol{W_{obs}(s, \varphi) = 2\cdot r_{mean}(s, \varphi)} \tag{3.11}$$

Through the integral mean value, $W_{obs}(s, \varphi)$ is one-dimensional; by considering Equation 3.11 in both formulations 3.1 and 3.2, the stochastic Index of Difficulty is still

dimensionless as previous ID formulations. The information of the two-dimensional variability of the n configurations $q_k(s)$ is stored in the one-dimensional stochastic width $W_{obs}(s, \varphi)$. By evaluating the integral mean value of the variable radius of the ellipse, is equal to convert the elliptical area representing the spatial distribution of the n configurations $q_k(s)$ into a circular area, whose diameter is equal to $W_{obs}(s, \varphi)$. In fact, as stated in (Zhai, Accot and Woltjer, 2004), when the target is circular, its characteristic size is constant, and equal to the diameter (example of the 'Ring and Wire' task, Figure 3.3).

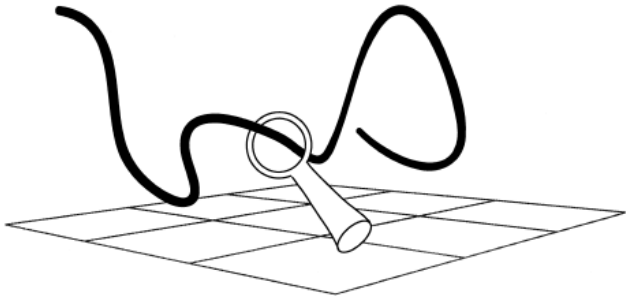

Figure 3.3 *Example of 'Ring and Wire' task* (Zhai, Accot and Woltjer, 2004)

Even if Figure 3.3 refers to the original continuous formulation of the ID (ID_t, Equation 1.15), where the nominal trajectory and the target are defined a priori, it is easy to notice that in case of circular target, the value that characterizes the maximum allowable variability that can be tolerated is the target's diameter since there is no difference between the target's height and width.

Aside from the two cases, $W_{obs}(s, \varphi)$ expresses the motor variability of agents while executing reaching motor tasks, as the result of the kinematic observation of repetitive movements.

3.2 The influence of internal constraints

In this paragraph, the stochastic Index of Difficulty is applied in a 2D reaching motor task (walking task), showing that the agent's motor difficulty is affected by internal constraints (Lucchese *et al.*, 2021). In this case $W_{obs}(s,\varphi) = 2 \cdot z(\varphi) \cdot \sigma(q_k(s))$ (Equation 3.3), is considered in the evaluation of $ID_{obs}(s^*,\varphi)$ (Equation 3.2). The stochastic Index of Difficulty is valid for any reaching motor task observed at a generic end-effector (e.g., foot, hand) of an agent. Walking is an everyday motor task, consisting of repetitive movements of the feet, represented by the gait cycle (Figure 3.4).

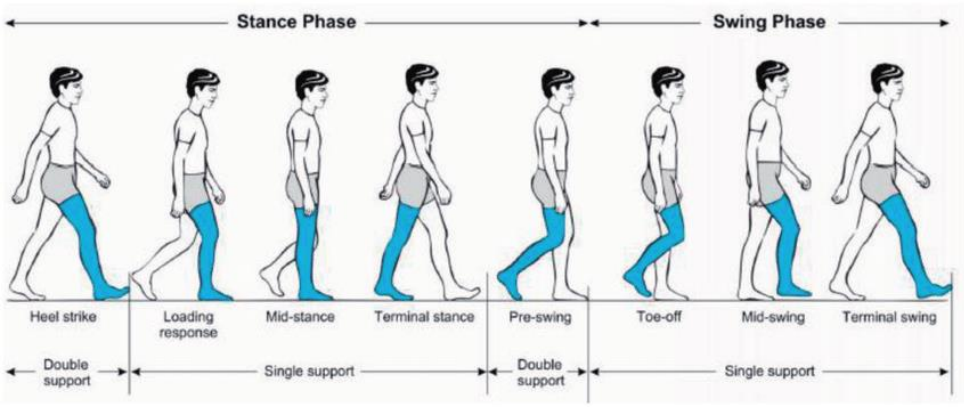

Figure 3.4 *Human gait cycle in the sagittal plane* (Pirker and Katzenschlager, 2017)

When the walking task is performed in an environment where boundary conditions are constant, and do not change during the execution of the task (no obstacles or unpredictable events that may affect movements, the surface is flat etc…) movements are performed automatically, without any reasoning about where to place the end-effector (foot), like on the treadmill. The task is composed by rhythmic stride movements that are performed repeatedly, and therefore motor variability can be detected. In the following, healthy subjects differently aged are observed during the execution of a walking task, with different speed conditions. The ankle of the swing foot is considered as the agent's end-effector that during each stride of the gait cycle follows a repetitive trajectory, traveling a distance equal to the stride length along the direction of forward progression (Mummolo, Mangialardi and Kim, 2013). The experimental dataset, publicly available in (Fukuchi, Fukuchi and Duarte, 2018), consists of the subjects' kinematics captured during multiple overground walking trials at three speed levels: slow, comfortable, and fast.

3.2.1 Evaluation of the motor difficulty for an elderly agent

The proposed stochastic Index of Difficulty has been firstly tested on one human subject (male, 61 years old) walking at an average speed of 1.584 m/s. Trajectories of the swing foot's ankle are recorded over 11 walking trials (Fukuchi, Fukuchi and Duarte, 2018) and projected onto the anatomical sagittal plane (*x*,*y*) (as in Figure 3.4), where the *x* coordinate indicates the direction of forward gait progression and the *y* coordinate indicates the direction normal to the ground. Trajectories executed by the ankle during the second stride of each k^{th} walking trial ($k = 1, \dots, 11$) are sampled and averaged for the analysis of agent's motor difficulty (Figure 3.5). The stride movement is modelled as a generalized reaching motor task starting from the instant of "flat foot" (i.e., the foot is in full contact with the ground, right before the swing phase) and terminating at the instant of "heel strike" (i.e., when the same foot makes the new contact with the ground, terminating the swing phase). For each stride trajectory, the condition of 'flat' foot has been detected in order to align all the strides on the instant of 'flat' foot and consider that position as the starting point of the ankle's movement (Figure 3.5).

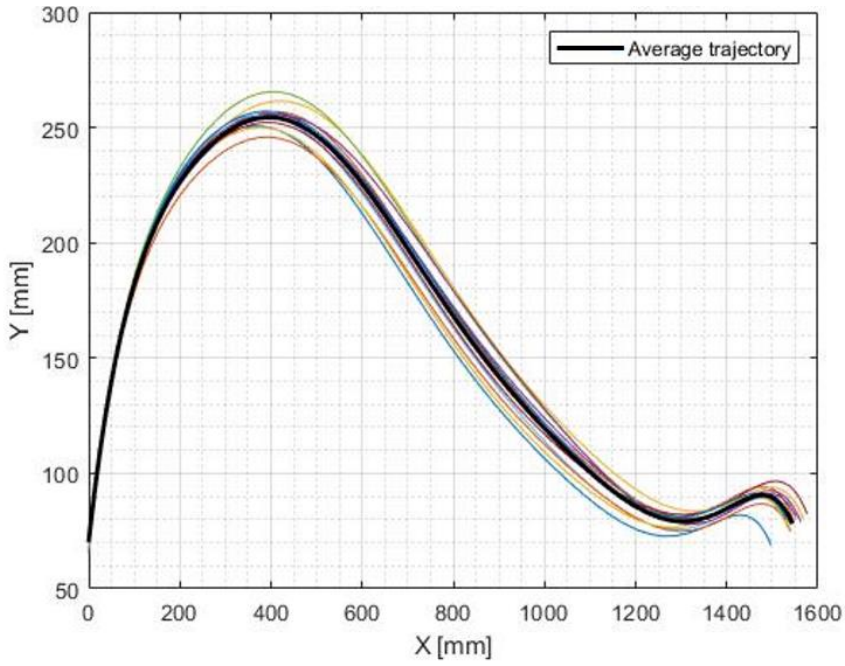

Figure 3.5 *Ankle trajectories (coloured lines) and related average (thick black line) of a 61 years old healthy subject walking at an average speed of 1.584 m/s*

The agent's motor difficulty of a of a 61-year-old healthy subject walking at an average speed of 1.584 m/s is evaluated through $ID_{obs}(s^*, \varphi)$ by considering $\varphi = 0.95$. By expressing the relationship $s = f(x)$ it is possible to show the trend of $ID_{obs}(s^*, \varphi)$ and

$W_{obs}(s,\varphi)$ along the x coordinate (Figure 3.6). $ID_{obs}(s^*,\varphi)$ is a cumulative stochastic measure that takes into account the average trajectory and all the $W_{obs}(s,\varphi)$ considering $s^* \in [0; t_{avg}]$; $W_{obs}(s,\varphi)$, instead, is evaluated locally by applying Equation 3.3.

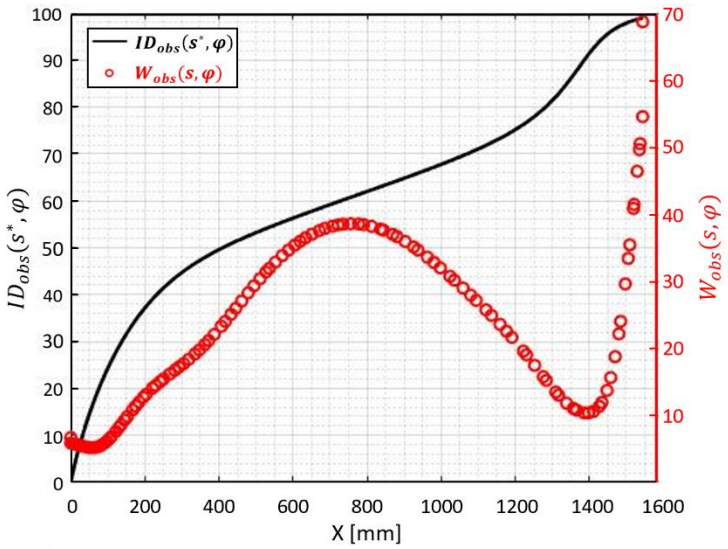

Figure 3.6 *$ID_{obs}(s^*,\varphi)$ evaluated and $W_{obs}(s,\varphi)$ with $\varphi = 0.96$ of a 61-year-old healthy subject walking at an average speed of 1.584 m/s*

By analysing the trend of $ID_{obs}(s^*,\varphi)$, three phases of the stride are identified. In the first phase ($0 < x < 400$ [mm]), the end-effector (swing foot) is lifted from the ground and executes a trajectory with high motor difficulty: it can be observed that 50% of the total agent's (subject's) motor difficulty is allocated in the first quarter of the trajectory, from flat foot to the point of maximum swing foot height (Figure 3.6). Towards the end of this phase, the end-effector agent's motor difficulty decreases, as shown by the decreasing derivative of $ID_{obs}(s^*,\varphi)$, and its flexibility increases, as shown by increasing values of $W_{obs}(s,\varphi)$.

In the second phase ($400 < x < 1200$ [mm]), 25% of the total agent's motor difficulty is realized during the central portion of the trajectory, in which the swing foot is moving from a point of maximum to minimum height, while traveling about 50% of the total stride length. In this phase, the rate of increase of $ID_{obs}(s^*,\varphi)$ is approximately constant, with $W_{obs}(s,\varphi)$ first increasing, reaching a maximum at about half of the stride, and then decreasing. In this phase, the agent's flexibility is on average constant, and higher than the previous phase, demonstrating that in this second phase, the agent is able to explore more the spatial domain through its end-effector, exploiting its redundant motor system. Higher values of $W_{obs}(s,\varphi)$ define higher possibilities to perform the same task by

executing different trajectories, more spread in the axis orthogonal to the average trajectory (see T Figure 3.1).

Finally, in the last quarter of the stride (1200 < x < 1600 [mm]), i.e., the last 25% of travelled distance, the agent is employing 25% of its total motor difficulty. The $ID_{obs}(s^*, \varphi)$ shows first a high rate of increase, due to the rapid decrease of trajectories variability ($W_{obs}(s, \varphi)$) while the foot prepares for the upcoming contact with the ground; then, as the end-effector approaches the trajectory endpoint (x $\sim$ 1600 [mm]), the $ID_{obs}(s^*, \varphi)$ derivative decreases due to a higher variability of trajectories.

Evaluating the ratio between the percent increase of the $ID_{obs}(s^*, \varphi)$ and the percent increase of distance travelled in each of the three phases of the task (2, 0.5, and 1, respectively), it can be noted that the stride movement of the given agent is characterized by consecutive phases at high, low, and intermediate level of motor difficulty, respectively.

Preliminary results presented above are the proof-of-concept demonstration of the stochastic model proposed for motor difficulty and its ability to describe the level of flexibility of a given agent during different phases of the task. This application represents an example of how the model can be used for benchmarking important subject-specific motor performances during a generalized reaching motor task. In following paragraph, it is investigated the ability of $ID_{obs}(s^*, \varphi)$ to capture different motor difficulties of agents characterized by different internal constraints.

3.2.2 Statistical Analysis on the Stochastic Index of Difficulty for Differently Aged Agents

The ankle's walking trajectories of 34 agents have been analysed at three different speed conditions: slow, comfortable and fast. Agents are grouped into "Young" (21-37 years old, N = 20) and "Old" (50-73 years old, N = 14) age groups. Each agent performs an average of nine walking trials per speed level. The second stride of each trial is sampled to avoid non-steady gait effects and averaged for each subject over the nine walking trials, and for each speed condition. The stochastic Index of Difficulty $ID_{obs}(s^*, \varphi)$ has been evaluated for the considered reaching motor task, demonstrating that the proposed model has the capability of capturing statistical differences in comparing different populations (different internal constraints), while maintaining the boundary conditions of the environment constant (constant internal constraints)

The $ID_{obs}(s^*, \varphi)$ profiles (as the thick black line in Figure 3.6) for each agent are shown for the "Young" and "Old" groups at "Slow" and "Fast" speed of execution (Figure 3.7) with probability level $\varphi = 0.95$.

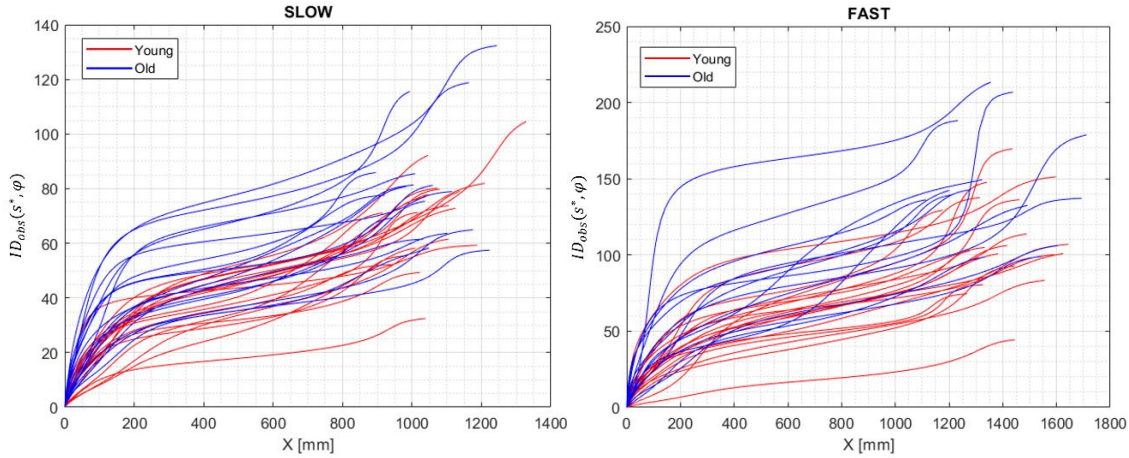

3.7a *3.7b*

Figure 3.7 *$ID_{obs}(s^*, \varphi)$ calculated along the x coordinate of the swing foot trajectory for "Young" (red lines, N=20) and "Old" (blue lines, N=14) agents, at "Slow" (3.7a) and "Fast" (3.7b) speed of execution*

In both speed conditions, the elderly population shows a steeper increase of the $ID_{obs}(s^*, \varphi)$ during the first part of the trajectory (0 < x < 200 [mm]), compared to the young population. This is a consequence of lower values of $W_{obs}(s, \varphi)$ for old agents, who show a small adaptation capability and flexibility during the pre-swing phase of the trajectory, bringing to higher values of motor difficulty at a given coordinate x.

Similarly, by considering the overall path executed, the agent's motor difficulty during the entire motor task $ID_{obs}(t_{avg}, \varphi)$ (Equation 3.1) for old agents are, on average, greater than young agents; consequently, the conclusion about the lower level of flexibility of the motor system for old agents observed during the first phase of the trajectory, holds also by considering the entire movements executed. This conclusion has been further supported by results of the statistical analysis (described later).

The average $ID_{obs}(s^*, \varphi)$ profiles have been calculated for the categories "Young" and "Old", at "Slow" and "Fast" speed of execution (Figure 3.8). It can be observed that a higher speed of execution leads to higher $ID_{obs}(s^*, \varphi)$ values for both the young and old population. Higher speed of execution also leads to greater stride length.

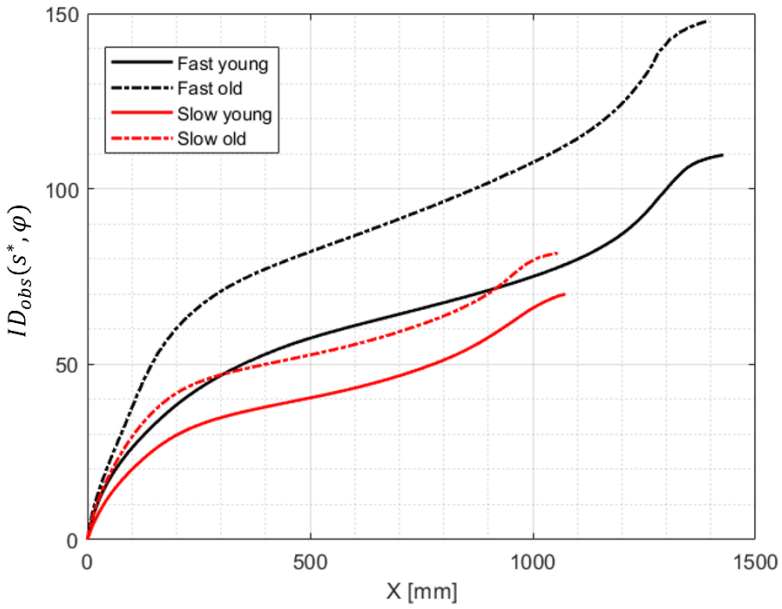

Figure 3.8 *Average $ID_{obs}(s^*, \varphi)$ observed for "Young" (continuous lines) and "Old" (dotted lines) at "Slow" (red lines) and "Fast" (black lines) speed conditions*

A Mixed-Design Two-Way Repeated Measures ANOVA is conducted to assess the effects of age and speed on the overall agent's motor difficulty $ID_{obs}(t_{avg}, \varphi)$. This case refers to a Mixed-Design Two-Way since there is one 'within-subjects' factor and one 'between-subjects' factor. The 'within-subjects' factor refers to the speed of execution and has two levels, since every agent performed the walking task with both 'Slow' and 'Fast' speed of execution; the 'between-subjects' factor refers to the age of the agent and has two levels ('Young' and 'Old'). Each agent performed the task multiple times for each speed condition. In the following the table that summarizes the sample size considered for the statistical analysis.

Table 3.2 *Sample size for the Mixed-Design Two-Way Repeated Measures ANOVA*

	Slow	**Fast**
Young	N=20	N=20
Old	N=14	N=14

Prior to the ANOVA, both between-subjects and within-subjects assumptions are checked. All agents are independent from each other. The Shapiro-Wilk test is used to determine whether each subset of data (according to the categorization from Table 3.2) is approximately normal; older agents within the slow condition did not meet this assumption ($p = 0.018$). Aside from this subset, the remainder of the dataset are approximately normally distributed. The ANOVA is typically robust to violations of

normality, therefore the analysis was pursued even though one subset of the data did not meet the assumption. The variances are tested using the Levene's test, where it is confirmed that the variances among both age groups for each speed condition are approximately similar (Slow vs. Age: p = 0.789 > 0.05; Fast vs. Age: p = 0.701 > 0.05). The within-subjects assumptions are also met: each agent participated in both the slow and fast speed conditions, the total number of agents (N = 34) is large enough to assume normality, and sphericity can be assumed since there are only two conditions. The Mixed-Design Two-Way Repeated Measures ANOVA reveals a significant within-subjects effect of speed ($F(1,32) = 73.71$, $p < 0.001$) and between-subjects effect of age ($F(1,32) = 14.70$, $p < 0.001$) on $ID_{obs}(t_{avg}, \varphi)$. An interaction between both factors ($F(1,32) = 4.38$, $p < 0.05$) is also observed. To further examine the significance, four post-hoc tests are conducted, where two independent-samples t-tests are used to determine the between-subjects significance of age and two paired-samples t-tests are used to determine the within-subjects significance of speed conditions (Figure 3.9). Post-hoc independent-samples t-tests, using Bonferroni correction ($\alpha = 0.05/4 = 0.0125$), confirmed that the $ID_{obs}(t_{avg}, \varphi)$ of the two age groups did differ during the slow condition ($t(32) = 2.65$, $p = 0.01248$) and during the fast condition ($t(32) = 3.47$, $p < 0.002$), with higher $ID_{obs}(t_{avg}, \varphi)$ values for older agents. Post-hoc paired t-tests, using Bonferroni correction ($\alpha = 0.05/4 = 0.0125$), confirmed that the $ID_{obs}(t_{avg}, \varphi)$ of each age group did differ significantly (young: $t(19) = -4.94$, $p < 0.001$; old: $t(13) = -7.23$, $p < 0.001$) across the two within-subjects conditions (Slow vs. Fast).

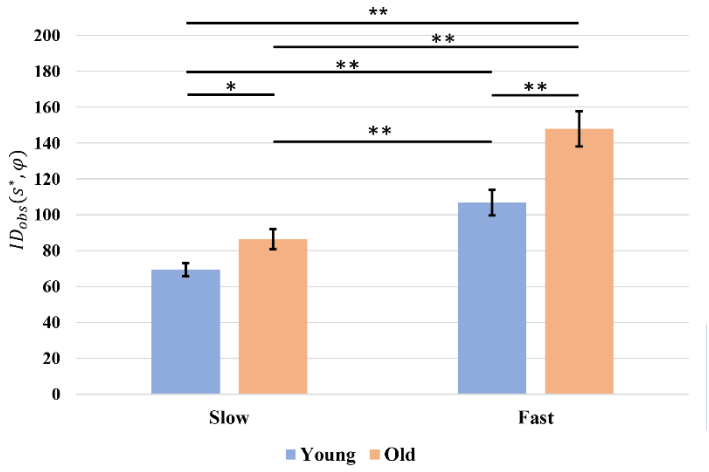

Figure 3.9 *Mean values of $ID_{obs}(t_{avg}, \varphi)$ in each group at slow and fast speed conditions. Error bars show SEM (Standard Error of the Mean). Significance of differences: * = $p < 0.0125$; ** = $p < 0.002$*

In Table 3.3, the age and average speed of execution of each agent during the three speed conditions, obtained from the publicly available dataset (Fukuchi, Fukuchi and Duarte, 2018) are shown.

Table 3.3 *Age and average speed of execution of each agent at the three speed conditions (Slow, Comfortable, and Fast)* (from Fukuchi, Fukuchi and Duarte, 2018). *For each speed condition of the agent, the average speed is calculated across the 9 trials*

			Speed (m/s)		
Group	**Age**	**Subject**	**Slow**	**Comfortable**	**Fast**
Young	25	1	0.824	1.245	1.544
	22	2	0.879	1.207	1.446
	33	3	0.659	0.929	1.233
	24	4	0.880	1.233	1.585
	25	5	0.890	1.276	1.474
	25	6	0.824	1.113	1.514
	31	7	0.912	1.206	1.759
	32	8	0.902	1.289	1.553
	24	9	0.715	1.066	1.353
	36	10	0.964	1.275	1.759
	24	11	0.732	1.082	1.343
	23	12	1.056	1.404	1.821
	31	13	0.724	1.141	1.414
	28	14	0.956	1.295	1.600
	28	15	0.851	1.262	1.588
	29	16	0.791	1.128	1.530
	21	17	0.910	1.203	1.638
	25	18	1.085	1.366	1.615
	28	19	1.024	1.264	1.598
	37	20	0.716	0.996	1.214
Old	57	21	0.911	1.296	1.570
	63	22	0.844	1.143	1.584
	71	23	0.943	1.284	1.517
	58	24	0.724	1.082	1.277
	68	25	1.029	1.234	1.542
	59	26	0.978	1.317	1.517
	50	27	0.868	1.146	1.406
	63	28	0.726	1.154	1.302
	62	29	0.737	0.997	1.286
	63	30	1.040	1.269	1.569
	55	31	0.751	0.994	1.343
	61	32	0.904	1.266	1.498
	63	33	0.839	1.159	1.498
	73	34	0.760	1.011	1.376

From statistical results obtained, it can be concluded that the agent's motor difficulty is influenced by the internal constraints of the agent, such as age and speed of execution, as in the current case. To formalize the relationship between $ID_{obs}(t_{avg}, \varphi)$, age and speed of execution, it has been investigated the opportunity to predict the agent's motor difficulty by considering constraints as independent variables, through the following regression model:

$$\boldsymbol{ID_{obs}(\varphi, Speed, Age)_{|task} = a_{\varphi} \cdot Speed^{\alpha} + b_{\varphi} \cdot Age^{\beta}} \quad (3.12)$$

Of course, the regression model is valid for a specific reaching motor task, identified by t_{avg}. Therefore, Equation 3.12 is valid only in case of a walking task when boundary environmental conditions do not affect the execution of the task (and are maintained constant). In general, different regression models can be obtained for different motor tasks. In Equation 3.12, the entity of the agent's motor difficulty depends not only on the Age and speed of execution, but also on the probability level considered (included in $W_{obs}(s, \varphi)$); therefore, to be capable to compare and detect differences between various agents, the probability level φ must be fixed. By clarifying terms in Equation 3.12:

- *"Age"* = age of the agent
- *"Speed"* = average speed of the agent in performing a trajectory at a given speed condition
- $a_{\varphi} = a_{\varphi_1} \cdot \frac{z(\varphi_1)}{z(\varphi)}$
- $b_{\varphi} = b_{\varphi_1} \cdot \frac{z(\varphi_1)}{z(\varphi)}$

Where:

- $z(\varphi)$ *is* the generic z-score of a unit normal distribution corresponding to a generic probability level φ
- $z(\varphi_1)$ is the reference z-score of a unit normal distribution corresponding to a reference probability value of φ_1: we set $\varphi_1 = 0.6827$ ($z(\varphi_1) = 1$)
- $(a_{\varphi}, b_{\varphi})$ are the regression parameters obtained for a probability level φ, depending on the reference regression parameters $(a_{\varphi_1}, b_{\varphi_1})$
- (α, β) are the regression parameters which proved, in the dataset considered, not varying with probability φ values

To obtain the reference regression parameters $(a_{\varphi_1}, b_{\varphi_1})$ it must be considered initially $\varphi_1 = \varphi$, therefore $z(\varphi_1) = z(\varphi)$, getting $b_\varphi = b_{\varphi_1}$ and $a_\varphi = a_{\varphi_1}$. The ratio between the z-scores is a useful expedient allowing to automatically calculate the agent's motor difficulty when considering a probability level different from φ_1, instead of re-analysing data and re-calculating all the $W_{obs}(s, \varphi)$. Values of the regression parameters, by considering $\varphi_1 = \varphi$, are depicted in Table 3.4.

Table 3.4 *Regression parameters' values*

φ	$z(\varphi)$	a_φ	b_φ	α	β	R^2	p-value
0.68	1	88.60	11.85	1.3898	0.5364	93.35%	< 0.001

In Figure 3.10 it is plotted the trend of $ID_{obs}(\varphi, Speed, Age)_{|task}$ of the walking task by considering different probability levels φ, speed of execution and age of agents.

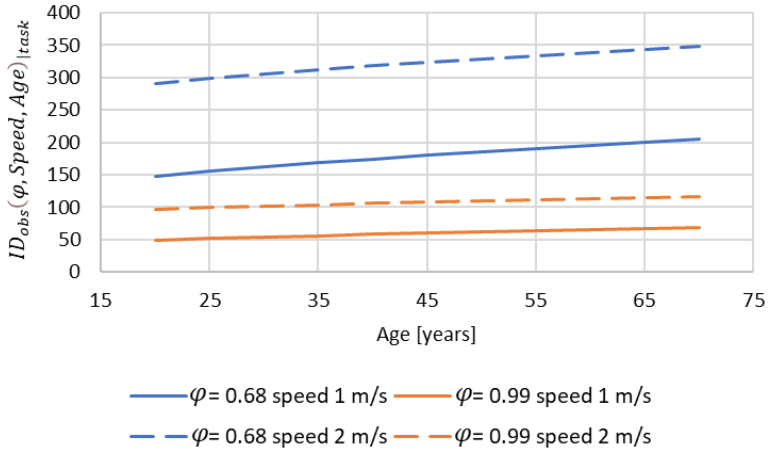

Figure 3.10 $ID_{obs}(\varphi, Speed, Age)_{|task}$ *vs. age of agents for different speed conditions and probability levels* φ

As previously noted, for a given probability level φ, the agent's motor difficulty increases with the age and speed. In Figure 3.10, it can be observed that higher ID_{obs} values are obtained for higher speed (at a given probability value), indicating that the agent has less capability to exploit the motor redundancy and explore the space of motion while executing the walking task: the set of possible trajectories is smaller in case of higher speed, since the agent's motor system is more constrained during movements.

Results obtained in this context proved the effectiveness of the regression model in capturing the ID_{obs} major dependency on age and average speed, as already observed in the previous statistical analysis. Although the model and results are strictly referable to the dataset adopted, the approach proposed is of general validity and could be applied to

different motor tasks, as will be discussed in paragraph 3.3.

3.2.3 Discussion

This study deals with the evaluation of the agent's motor difficulty through a stochastic Index of Difficulty (ID_{obs}) that takes into account movements performed by agents, as well as motor variability. Differently from the previous continuous formulation of the Index of Difficulty (ID_t, (Accot and Zhai, 1997)), this measure considers the motor behaviour of the agent and the related difficulty, rather than the difficulty associated to the task (defined a priori). In fact, ID_t was originally defined as being dependent on only the geometry of a spatially constrained trajectory; on the contrary, stochasticity of movements has to be considered for taking into account of the natural variability of agents in executing repetitive movements while performing a reaching motor task in a given environment.

The issue of motor difficulty is of great scientific and industrial interest as it pertains the ability of an agent to accomplish different trajectories considering both environmental conditions and task features (external constraints), and features that characterize the ability of the agent in accomplishing the motor task (internal constraints).

The model proposed has been applied to an available dataset of differently aged agents executing a walking task at three different speed conditions in a given environment (constant environmental conditions). One of the main novelties of the proposed stochastic Index of Difficulty relies on a new understanding of the role and effects of motor variability, which can be considered as a measure of redundancy exploitation and can be an indicator of optimal motor control (see paragraph 3.1.3).

A statistical analysis (Mixed-Design Two-Way Repeated Measures ANOVA and post hoc tests) provided significant differences in the average ID_{obs} for "Young" vs. "Old" agents, and, for each age class, for "Slow" vs. "Fast" average speed of execution. A regression model confirms the significant dependency of the ID_{obs} on age and speed execution.

The dependency of the agent's motor difficulty on the age is of a great industrial interest due to the increasing importance related to the ageing phenomenon. In fact, it has been estimated that in developed countries half of the workers will be aged over 50 by 2050 (UNFPA, 2012). Humans are inevitably subjected to the ageing, phenomenon that brings

to decrease the ability of workers involved in both motor and cognitive tasks.

By focusing on motor tasks, physical abilities gradually decline from 30 to 40-50, and accelerate from 50 on (Millanvoye, 1998). Even without a physical disability related to illnesses or diseases, older workers show an important decrease in the joints' range of motion, defined as the maximum excursion that a body segment can make before the constraints imposed by bones, ligaments, tendons, or muscles restrain the movement. With the advance of age, movements achievable could be restricted due to the decreased length of muscles and a decreased amount of cartilage (Nonaka *et al.*, 2002). Changes in joint structures, and muscles composition of older adults, bring to a reduced flexibility and range of joint movements (Spirduso, 1995; Bloem *et al.*, 2002), observed body parts such as hip, knee and ankle (Gehlsen and Whaley, 1990; Ronsky, Nigg and Fisher, 1995). These observations further support conclusions provided by the statistical results, since it has been observed that, for each speed condition, older agents execute the walking task with a greater motor difficulty, mainly due to the limited flexibility of the motor system and the limited motor variability, information expressed through the stochastic width $W(s, \varphi)$. In fact, the limited motor flexibility affects the execution of daily tasks (Spirduso, 1995; Nonaka *et al.*, 2002) as well as reaching motor tasks involving repetitive movements. Repetitive movements may bring also to changes in both lower and upper extremities mobility, affecting movements such as gait cycle (walking task) and grip strength (manipulation task) (Cooper, 2016; Walker-Bone *et al.*, 2016).

Nevertheless, the aging phenomenon affects not only motor, but also cognitive capacities of agents. Changes in physical movements related to motor activities such as walking and manipulation tasks, have been shown to predict also cognitive decline (Clouston *et al.*, 2013). The cognitive decline in older workers is not a negligible event, since it may increase safety risks associated to falls and slips (Schwatka, Butler and Rosecrance, 2012; Zhang, Lockhart and Soangra, 2014) in motor tasks that demand cognitive resources, such as in walking and balance tasks (Hsu *et al.*, 2012). Furthermore, it is observed that older agents are more vulnerable, and subjected to an overall frailty (e.g., decrease in muscle mass, feel more weakened and fatigued) (Fried *et al.*, 2001; Morley *et al.*, 2013) that leads to cognitive impairments (Gale, Cooper and Sayer, 2015). The effect of the reduction of both motor and physical abilities becomes to be important in workers aged between 45-64 (Peruzzini and Pellicciari, 2017); work-limited disabilities have been estimated to be 3.4% in workers aged 18-28, 13.6% in workers greater than 60 (*National Research*

Council, Health and safety needs of older workers, 2004). The theme of the motor-cognitive decline due to the aging phenomenon is surely a topic of great interest in current industrial context arousing the attractiveness of the scientific community. Although results obtained by applying the ID_{obs} on a walking task are referrable to the dataset considered, the approach proposed is of general applicability and surely in future works can be investigated the effect of the motor-cognitive decline due to the ageing phenomenon on the agent's motor difficulty. Nevertheless, before taking this step forward, the proposed model should be validated by considering the effects of different external constraints, i.e., quantify the variation of motor behaviours when the task- and environment-related features (external constraints) are altered for a given agent. For this reason, the following paragraph will be focused on applying the proposed ID_{obs} model to a reaching motor task involving the manipulation of different objects, requiring three-dimensional movements to be performed by agents.

3.3 The influence of external constraints

The previous paragraph focused on investigating the motor difficulty of differently aged agents performing movements in a two-dimensional plane (sagittal plane) with constant external constraints. This section is focused on investigating the effect of different external constraints on agents belonging to the same population (young healthy adults), i.e., with constant internal constraints, while performing a reaching motor task involving three-dimensional movements. A manipulation task (reaching-to-grasp-and-release task) of objects with different features has been considered. Objects' features refer to the external constraints, since influence movements to be performed, being 'external' to the agent. Results show that the agent's motor difficulty is affected by the different objects' features (Lucchese, Digiesi and Mummolo, 2022).

3.3.1 Applying the stochastic Index of Difficulty to a manipulation task

A publicly available dataset regarding a three-dimensional manipulation task of different objects (Herbst, Zelnik-Manor and Wolf, 2020b) is used to test the effectiveness of the stochastic Index of Difficulty in capturing the effect of different external constraints

(objects' features) on the agent's motor difficulty. Data analysis is carried out using MATLAB® software (version R2021a). Data refer to 31 healthy individuals; each of them sits in front of a table to perform a reaching task with the dominant hand. Each individual approaches the grasping position placed 300 mm from the edge of the table on the same side of the dominant hand; here, the agent grasps an object and moves it to the release position 500 mm symmetrically on the other side of the table, release the object and, finally, replace the dominant hand at the starting point. For the experiment, five different objects have been considered: a tennis ball (105 mm diameter), two one-litre water bottles (80 mm diameter), one full and the other half-full, two ellipsoid shaped balls (62 mm maximum diameter), one soft and the other of stiff plastic. The experimental set-up is shown in Figure 3.11. Reflective markers have been placed on the agent's end-effector to obtain, through a motion capture system, kinematics parameters of the movement. In this context the hand's palm is considered for the agent's end-effector. Further information on the dataset are available in (Herbst, Zelnik-Manor and Wolf, 2020a).

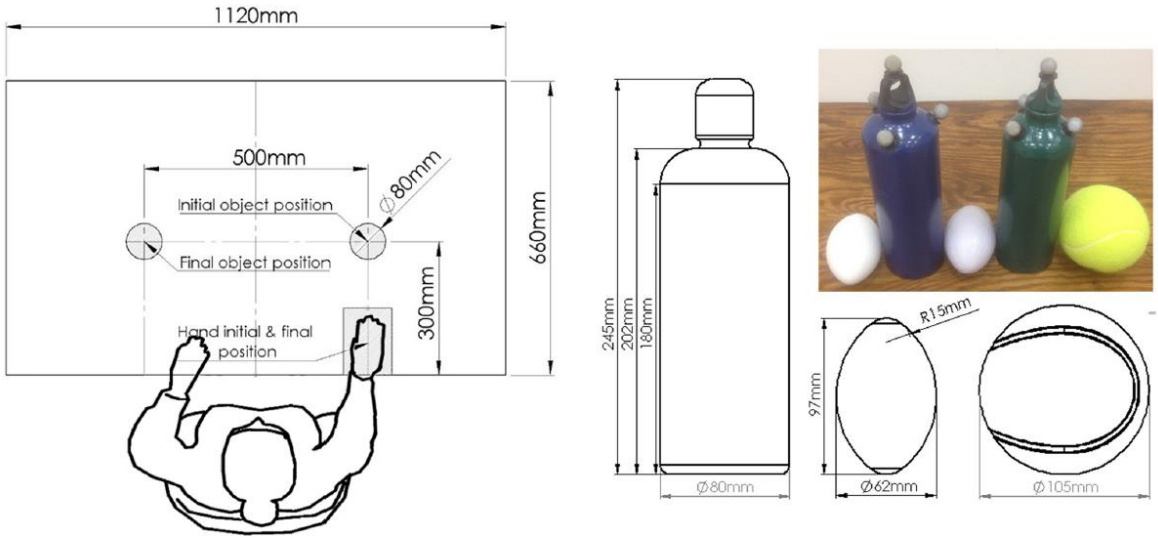

Figure 3.11 *Experimental set-up and objects of the manipulation task. From left to right: plastic ellipsoid ball, full 1L water bottle, soft ellipsoid ball, half full 1L water and a tennis ball (Herbst, Zelnik-Manor and Wolf, 2020a)*

In this context, external constraints refer to the different objects to be manipulated, and to positions where the agent's end-effector movements are required to be accurate (initial and final object positions). Nevertheless, since across trials the initial and final object positions are fixed and do not change (Figure 3.11), the influence of the different external constraints on the agent's motor difficulty refer only to the different objects manipulated. The agent's end-effector average trajectory is evaluated on 7 trial trajectories performed

during the motor task, for each of the five objects. Figure 3.12 shows an example of the trial trajectories (dash-dotted lines) and their average (thick black line) of an agent's end-effector during the grasp and release of the tennis ball.

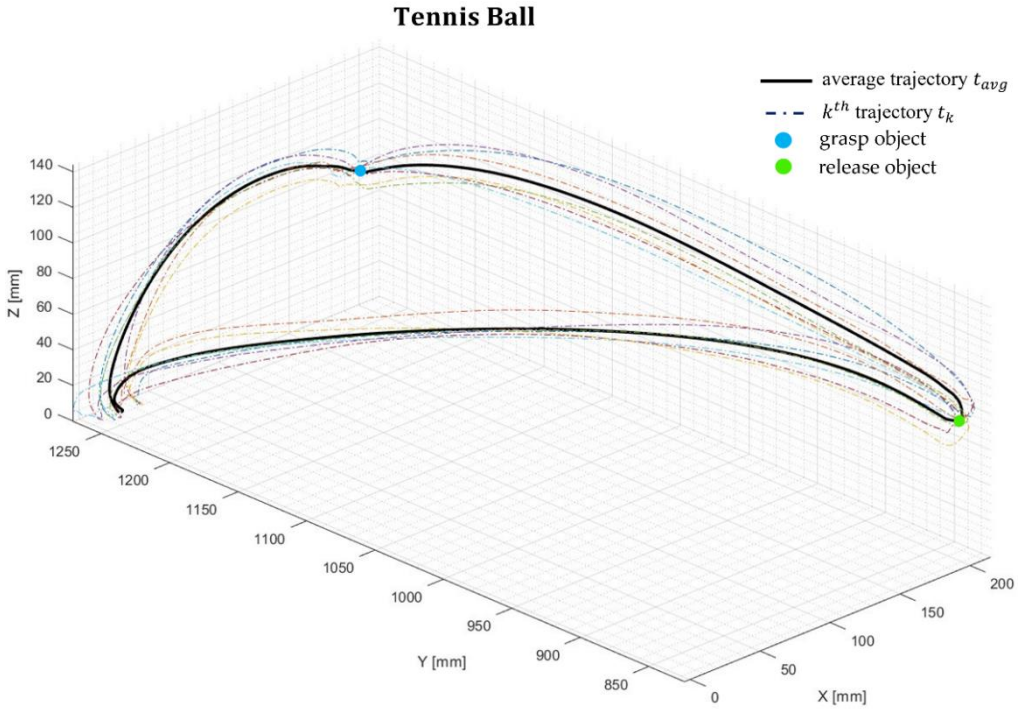

Figure 3.12 *Example of trial ttrajectories (dash-dotted lines) and their average (thick black line) during the tennis ball manipulation task*

Since the manipulation task involves three-dimensional movements, the stochastic width $W_{obs}(s^*, \varphi)$ has been evaluated by considering the methodology described in paragraph 3.1.2. To takes into account the probability level φ, the stochastic width must be scaled by a statistical distance (as described in paragraph 3.1.2). Since the sample size to evaluate $W_{obs}(s^*, \varphi)$ is limited (7 trials for each agent at a given condition [i.e., object to manipulate]), the stochastic width is scaled by the Hotelling's T-squared distance (Equation 3.7), instead of considering the Mahalanobis distance ($\sim$ sample size > 100). By considering the trial trajectories observed during the grasp and release of the tennis ball, the stochastic width $W_{obs}(s^*, \varphi)$ (Equation 3.11) and the stochastic Index of Difficulty $ID_{obs}(s^*, \varphi)$ (Equation 3.2) values averaged on 31 agents are calculated, with probability value $\varphi = 0.95$. Results are in Figure 3.13.

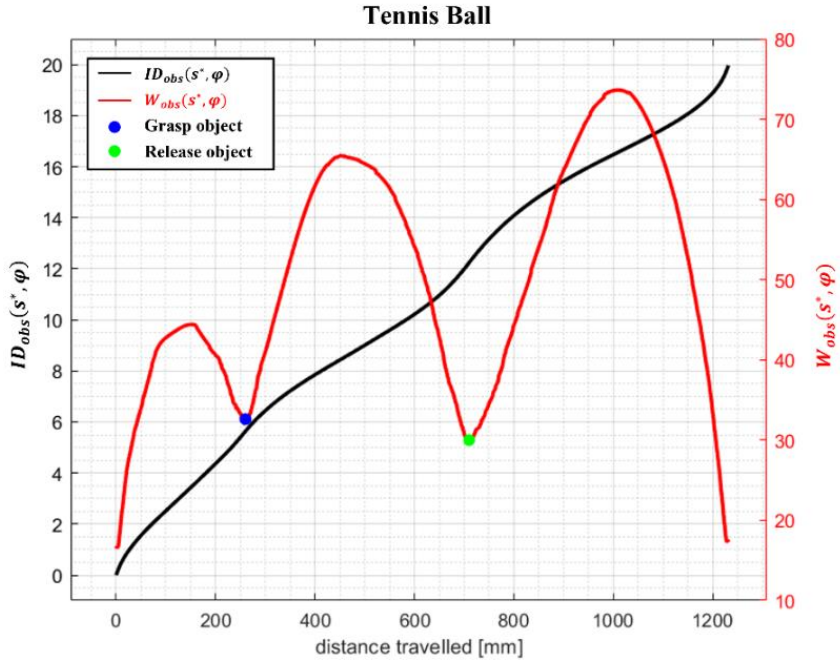

Figure 3.13 *$ID_{obs}(s^*, \varphi)$ and $W_{obs}(s^*, \varphi)$ values averaged on 31 agents during the tennis ball manipulation task*

The trend of $W_{obs}(s^*, \varphi)$ highlights three phases, each of them characterized by a travelling action (gross movement) and a positioning action (fine movement). The first phase (grasp phase) consists of moving the end-effector (hand's palm) from the starting point to reach the grasping position; the second phase (release phase) consists of moving the object from the grasping position and releasing it at the releasing position; finally, the third phase (return phase) consists of moving the empty hand from the releasing point to the starting point where the cycle ends (final placing). For each phase, the trend of $W_{obs}(s^*, \varphi)$ is bell-shaped, with lowest values at points where a greater precision of the end-effector movements is required (positioning action). These results are in line with (Todorov and Jordan, 2002) since $W_{obs}(s^*, \varphi)$ values are higher at the task-irrelevant dimensions (travelling action of each phase), and reach the lowest values at task-relevant dimensions (positioning action of each phase) where accuracy is required. The exploitation of motor redundancy is greater in the task-irrelevant dimensions since a greater motor variability is observed, witnessed by the higher extent of $W_{obs}(s^*, \varphi)$ values. At points where accuracy is required, the environment forces the agents to reach a specific target. In short, each phase is characterized by a travelling action where the agent's end effector is free to explore the space with greater spatial configurations, followed by the positioning action where accuracy is required, resulting in minima values of $W_{obs}(s^*, \varphi)$. At points where accuracy is required, the lowest values

of $W_{obs}(s^*, \varphi)$ cause steeper slopes of the $ID_{obs}(s^*, \varphi)$ trend resulting in a greater increase of the motor difficulty. In the next section, results of the statistical analysis on $ID_{obs}(s^*, \varphi)$ values are provided and discussed.

3.3.2 Statistical Analysis

Different analyses have been performed to test the following two main hypothesis:

1) The manipulation of different objects represents a change in the external constraints, affecting the agent-environment interaction, and influencing the motor difficulty experienced by the subjects during the entire manipulation task. To test the hypothesis, a one-way repeated measures ANOVA on $ID_{obs}(t_{avg}, \varphi)$ values of the 31 subjects has been performed for each condition (i.e., each object). Results show that there is a significative change in the subjects' motor difficulty when manipulating different objects.
2) In (Herbst, Zelnik-Manor and Wolf, 2020a) it has been observed that objects with different geometry affect the subjects' motor behaviour during the object manipulation. In order to test this hypothesis, a one-way repeated measures ANOVA on $ID_{obs}(t_{avg}, \varphi)$ values of the 31 subjects for the three geometrical different objects (tennis ball, bottle, ellipsoid ball), has been performed. Results show that differences in the motor behaviour, expressed by $ID_{obs}(t_{avg}, \varphi)$, are not associated to the different geometry, but to the different grasp type.

3.3.2.1 Stochastic Index of Difficulty

To verify whether the five different objects determine a relevant difference on $ID_{obs}(t_{avg}, \varphi)$, a statistical analysis has been performed using IBM SPSS Statistics® software (version 26). Assumption prior to the one-way repeated measures ANOVA for the $ID_{obs}(t_{avg}, \varphi)$ values of the 31 subjects (normality through Shapiro-Wilk test, sphericity through Mauchly's test) have been confirmed for all the five objects. ANOVA results show statistically significant differences by comparing the $ID_{obs}(t_{avg}, \varphi)$ values of different objects ($F(4,120) = 4.361, p < 0.003$). By applying the post hoc test with Bonferroni correction, the statistically significant difference of $ID_{obs}(t_{avg}, \varphi)$ is evident in case of ellipsoid balls (soft and plastic) vs. bottles (half and full) ($p < 0.005$). Results

are in Figure 3.14.

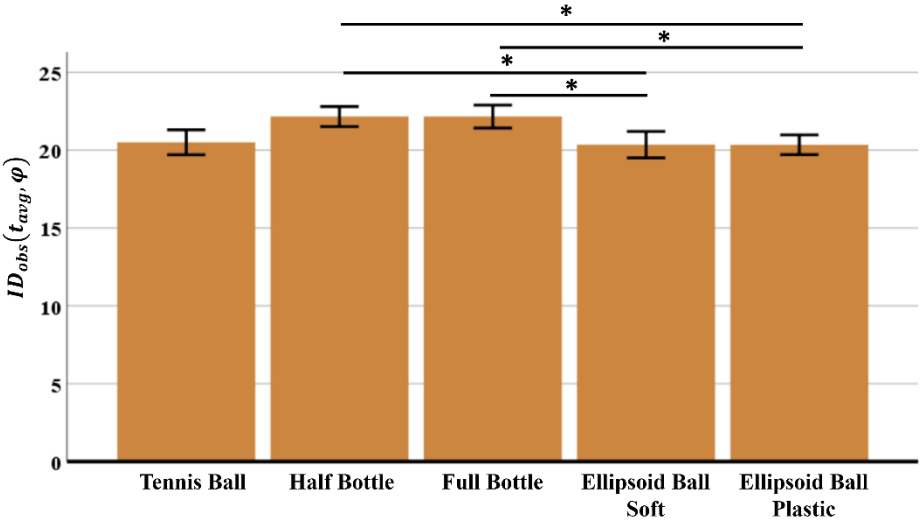

Figure 3.14 *Mean values and SEM (Standard Error of the Mean) of $ID_{obs}(t_{avg}, \varphi)$ of the entire manipulation task; *= statistically significant (p-value < 0.005); critical p-value = 0.05/10 = 0.005*

These results verify the first hypothesis: the proposed stochastic Index of Difficulty is sensitive to capture the different motor difficulty experienced by the population while executing a motor task (object manipulation) whith different external conditions (objects). In particular, subjects experience a greater motor difficulty when manipulating the bottles (half and full), compared to the ellipsoid balls (soft and plastic). Since results do not provide relevant differences between the two bottles (half full vs. full), and between the two ellipsoid balls (soft vs. plastic), it can be concluded that the different mass alone as well as, the different stiffness of objets do not influence the population's motor difficulty; the same conclusion holds in (Herbst, Zelnik-Manor and Wolf, 2020a) where it has been observed that the alteration of the mechanical properties (weight variations in the bottles, stiffness and friction in the ellipsoid ball), does not affect the motor behaviour. Therefore, the mass end stiffness can be removed from the features that affect the subjects' motor difficulty.

A further investigation can be carried out focusing only on objects characterized by different geometry. The following analysis is aimed at verifying if the different geometry is the main object's feature that affects the subjects' motor difficulty. Assumption prior to the one-way repeated measures ANOVA for the $ID_{obs}(t_{avg}, \varphi)$ values of the 31 subjects (normality through Shapiro-Wilk test, sphericity through Mauchly's test) have been confirmed for all the geometrically different objects. ANOVA results show statistically significant differences by comparing the $ID_{obs}(t_{avg}, \varphi)$ values of different

objects ($F(2,60) = 4.010, p < 0.02$). By applying the post hoc test with Bonferroni correction ($\alpha = 0.05/3 = 0.016$), the statistically significant difference of $ID_{obs}(t_{avg}, \varphi)$ is evident in case of ellipsoid/tennis ball vs. bottle ($p < 0.001$). Results are in Figure 3.15.

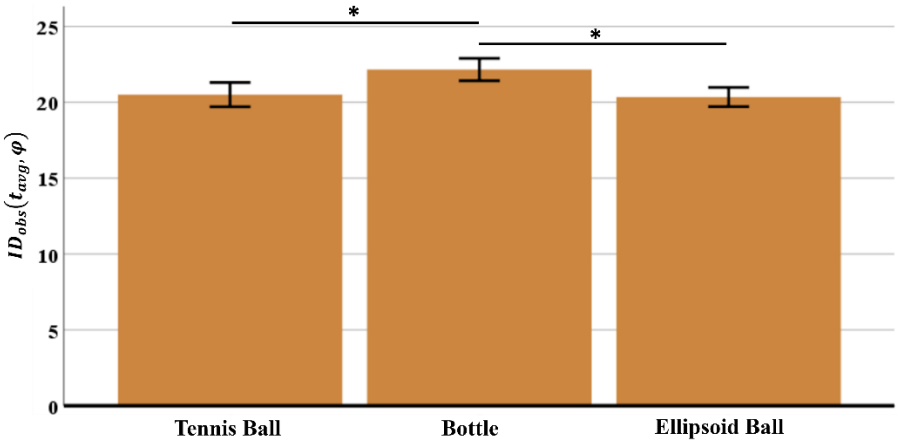

Figure 3.15 *Mean values and SEM (Standard Error of the Mean) of $ID_{obs}(t_{avg}, \varphi)$ of the entire manipulation task for the three different geometrical objects; *= statistically significant (p-value < 0.016); critical p-value = 0.05/3 = 0.016*

These results do not support the hypothesis that the geometry is the main feature that affects the subjects' motor difficulty. Nevertheless, statistical differences can be associated with the grasp type of the objects: the tennis ball (spherical) and ellipsoid ball (ellipsoid) are gripped with the same type of grip ('power sphere' grip), while the bottle (cylinder) is gripped with the 'large diameter' grip (Feix, Bullock and Dollar, 2014; Feix *et al.*, 2016). By observing Figure 3.15, no relevant differences are observed by comparing objects with the "power sphere" grip (tennis ball vs. ellipsoid ball); on the contrary, relevant differences are observed when comparing objects with different type of grips, i.e. tennis/ellipsoid ball ("power sphere" grip) vs. bottle ("large diameter" grip) (Feix, Bullock and Dollar, 2014; Feix *et al.*, 2016). When differentiating the objects basing on the grasp type, both the geometry and the volume are considered (Feix, Bullock and Dollar, 2014; Feix *et al.*, 2016). These two features influence the level of accuracy in grasping the object (precision/intermediate/power), the number of fingers involved, and the positioning of the thumb (adducted/abducted). Therefore, the influence of both the geometry and volume of objects, summarized in the grasp type, have an impact on the subjects' motor difficulty, and not only the object's geometry.

In this section, it has been shown that the manipulation of different objects affects the

stochastic Index of Difficulty, and in particular, agents experience a different motor difficulty when manipulating objects with different grasp types. In the next section a further analysis has been performed to investigate how objects characterized by a given grasp type, affect the speed of execution and the stochastic width.

3.3.2.2 Stochastic Width and Velocity Profiles

The velocity profiles related to the manipulation of the five objects are bell-shaped (Fig 3.16). Features of the velocity profiles are in line with the scientific literature since highest values are reached approximately halfway the path travelled (Morasso, 1981; Jeannerod, 1984), with greater peaks for greater distances travelled (Atkeson and Hollerbach, 1985; Gordon, Ghilardi and Ghez, 1994).

By focusing on the reaching and transport phases, it can be observed that the bell-shaped velocity profiles of the ellipsoid balls (soft and plastic) are greater than both the tennis ball and bottles (full and half); differences, are accentuated halfway the path of each phase, where the peak velocity is reached. These differences are not substantial during the return phase, since subjects do not handle any object.

Furthermore, in both the reaching and transport phases, it can be observed that the velocity profiles of the two bottles (half full and full) and of the two ellipsoid balls (soft and plastic) are almost overlapping, confirming that neither the mass nor the stiffness influence the speed of execution (as well as difficulty, as observed before).

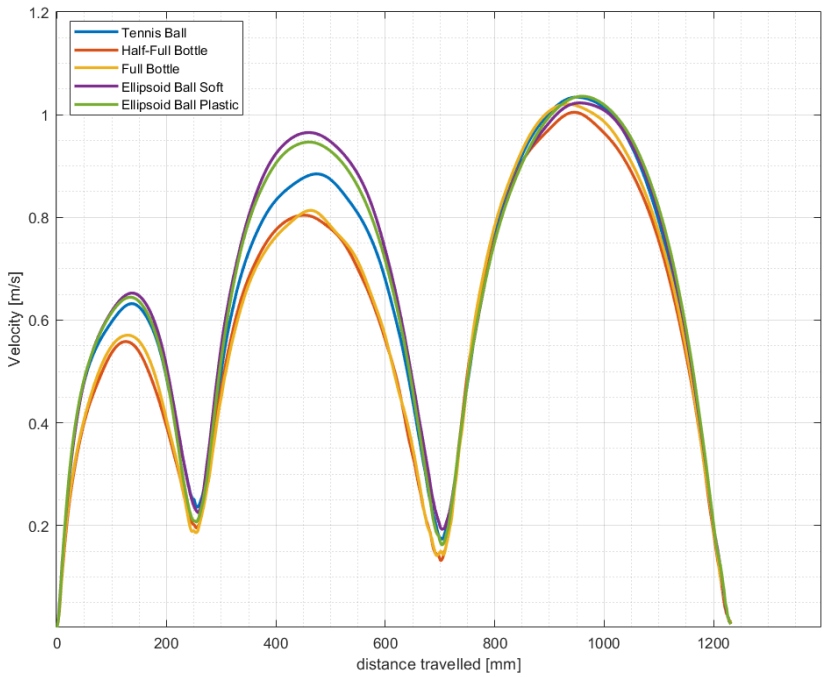

Figure 3.16 *Velocity profiles values averaged on 31 subjects during the object manipulation task*

A statistical analysis between the velocity peaks of the three different geometrical objects has been performed. The goals is to understand if the geometry alone or the grasp type have a significant effect on the velocity profiles. A one-way repeated-measures ANOVA has been conducted to evaluate if there is a statistically significant difference between the velocity peaks of the three different geometrical objects for the reaching and transport phases. After checking the assumptions prior to ANOVA (normality through Shapiro-Wilk test, sphericity through Mauchly's test), results show statistically significant differences in the reaching $(F(2,60) = 39.234, p < 0.0001)$ and transport phase $(F(2,60) = 45.219, p < 0.0001)$. By applying the post hoc test with Bonferroni correction, the statistically significant difference of velocity peaks is evident in case of the ellipsoid/tennis ball vs. bottle ($p < 0.001$) in both the reaching and transport phases.

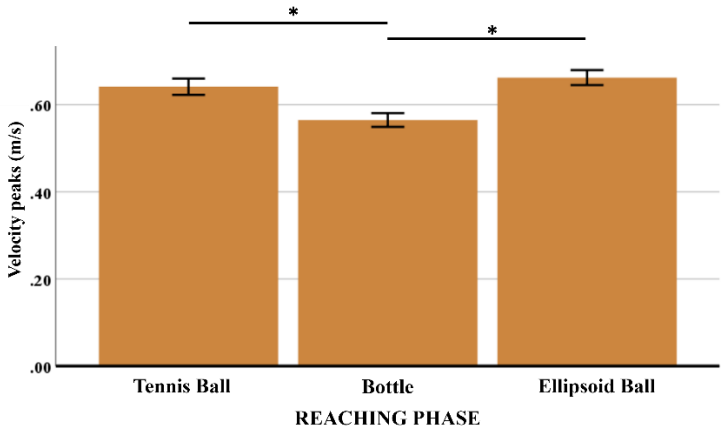

7a

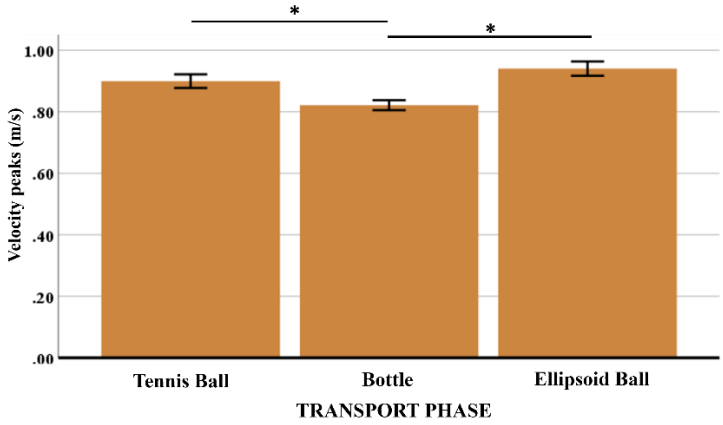

7b

Figure 3.17 *Mean values and SEM (Standard Error of the Mean) of velocity peaks at the reaching (3.17a) and transport (3.17b) phase for the three different geometrical objects; *= statistically significant (p-value < 0.001); critical p-value = 0.05/3 = 0.016*

These results confirm that velocity peaks (and velocity profiles) of movements executed to reach, grasp, move and release an object are affected by the object-related grasp type. Again, the geometry of the object is not the only feature that influence movements performed, but also the volume. These two features together characterize the object's grasp type (Feix, Bullock and Dollar, 2014; Feix *et al.*, 2016). Moreover, by comparing Figure 3.17 with Figure 3.15, it can be observed that in presence of a greater motor difficulty ($ID_{obs}(t_{avg}, \varphi)$), velocity peaks (and profiles) are lower. This phenomenon is caused by the external constraints: higher motor difficulty implies that the agent's motor system is more constrained and is not able to be flexible in velocity (maximum speed), and configurations reachable (exploitation of motor redundancy). This phenomenon may be caused by the position of reaching targets that limit the maximum speed of execution to guarantee the task performance where accuracy is required. In fact, by focusing on the stochastic width, it can be observed in each phase that $W_{obs}(s^*, \varphi)$ values (averaged on

31 subjects) are distributed with bell-shaped profile, with smaller values where accuracy on the end-effector's position is required (Figure 3.18).

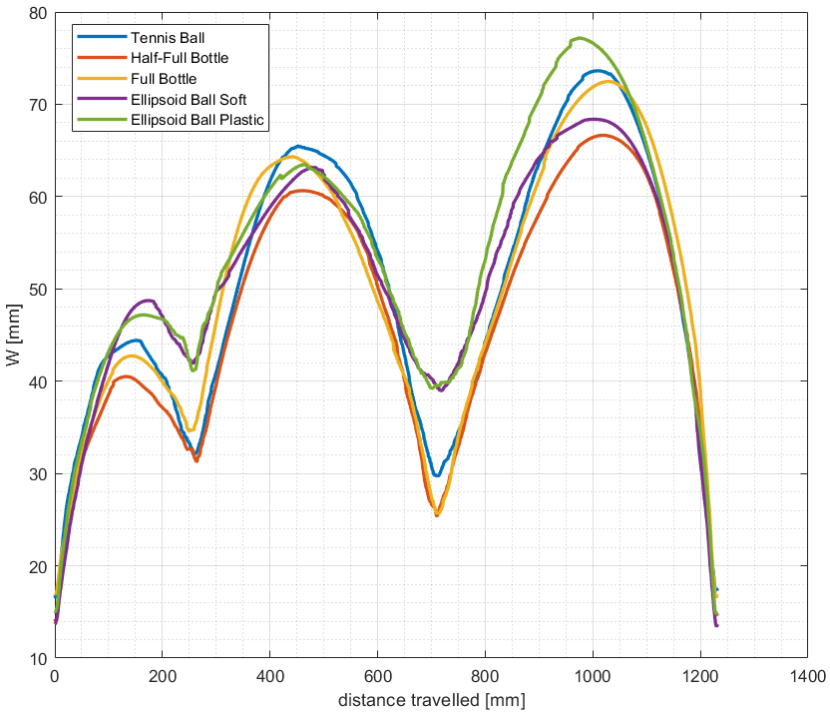

Figure 3.18 *$W_{obs}(s^*, \varphi)$ values averaged on 31 subjects during the object manipulation task*

The bell-shaped profiles of $W_{obs}(s^*, \varphi)$ are similar to the bell-shaped velocity profiles. The distance travelled in the reaching phase is almost the half of the one of the transport phase. A greater distance to be travelled allows the agents to be more flexible, freeing the motor system to go faster (Figure 3.16) and enabling more configurations at the reaching points (Figure 3.18).

3.3.3 Discussion

The presence of different external constraints during the execution of a given reaching motor task brought to statistically significant differences in the agent's motor difficulty. Differently from the previous case (influence of internal constraints on the ID_{obs}), this study extended the application of the stochastic Index of Difficulty to reaching motor tasks involving three-dimensional movements; therefore, the stochastic width $W_{obs}(s^*, \varphi)$ has been quantified through the methodology discussed in paragraph 3.1.2. The stochastic Index of Difficulty has been applied to a publicly available dataset (Herbst, Zelnik-Manor and Wolf, 2020b) of 31 healthy individuals performing multiple trials of a

three-dimensional object manipulation task consisting of reaching, grasping, moving and releasing objects characterized by different features. In the object manipulation task, the external constraints that have an influence on the agent's motor difficulty are due to the objects features (mass, stiffness, geometry, volume), since there are no other physical, environmental-relata constraints that limit movements that can be performed (e.g. environmental obstacles). Statistical results show that the mass and stiffness do not influence the agent's motor difficulty; on the contrary geometry and volume of objects, features summarized in the objects' grasp type, affect the agent's motor difficulty. These external constraints have an influence on the agent-environment interaction, affecting the agent's flexibility and its motor strategies (i.e., spatial configurations). Objects with different grasp types, have a relevant impact also in the different velocity profiles and velocity peaks, and the entity of the motor variability (expressed by W_{obs}) at points where accuracy is required. Results confirm that the manipulation of different objects affects the motor behaviour of agents, with a higher motor difficulty in manipulating objects characterized by a "large diameter" grip (bottle), compared to objects characterized by a "power sphere" grip (ellipsoid/tennis ball).

The strength in using the stochastic Index of Difficulty for the quantification of the agent's motor difficulty lies firstly in the type of movements involved. Observed movements of various nature or complexity can be analysed, rather than consider pre-defined distances to travel and targets to reach. In fact, since the current ID formulations (Table 1.1) do not consider movements executed, values obtained by applying them to a simple repetitive reaching task do not change considering different trials and different conditions (e.g., manipulation of different objects). Secondly, ID_{obs} can be applied in any application or experiment involving the motion of a body part (e.g., object manipulation, navigation, pick and place, manual sorting…): as long as reaching motor tasks require repetitive movements to be executed, the agent's motor difficulty can be evaluated. Furthermore, the stochastic width (W_{obs}), representative of the motor variability, contributes directly to the motor difficulty during the execution of a general repetitive motor task, instead of current ID formulations (Table 1.1), where variability is the spread of movements observed at the reaching target. In our case the motor variability is inherent in the ID_{obs}, since it contributes to the difficulty of movements performed: the stochastic Index of Difficulty evaluates the agent's motor difficulty, not the task difficulty. ID_{obs} tells us how flexible the agent during the execution of repetitive motor tasks is: higher the

motor alternatives that the agent can assume, greater the motor variability, and lower the agent's motor difficulty. The positive role of motor variability in decreasing the agent's motor difficulty is valid in repetitive motor tasks that allow the agent to explore the space and employ flexible motor strategies.

Results obtained can help future work, in which a complete factorial experiment will be designed, with which the effects of multiple objects' features (mass, volume, stiffness, geometry, main axis of symmetry), and their interaction, could be investigated through experiments consisting of a large dataset, where objects differ from one to more than one feature, and agents differ in motor abilities (e.g., age, experience). Unfortunately, this was not possible in the current paper because the dataset does not represent a complete factorial experimental design. However, the current dataset still gives us the useful information on what could be, among many, the main relevant factors in object manipulation tasks, hence the opportunity to formulate more refined hypothesis in the future about the effect of specific objects' features in the motor difficulty.

The proposed model of the agent's motor difficulty is representative of the stochasticity of repeated movements (i.e. average trajectory and their motor variability) executed by an agent as it moves and interacts with the environment (e.g., manipulating objects). The motor task is the mean by which the agent interacts with the surrounding environment. The agent's motor difficulty quantified by the stochastic Index of Difficulty is not a unique characteristic of the agent but is the characteristic of the combined agent-environment system. The relation between agent and environment pertains to the concept of affordance (Gibson, 1979a): it refers to the action possibilities of an agent in interacting with the environment, during which both abilities of the agent and features of the environment are considered (Chemero, 2003). The agent-environment interaction is expressed by the execution of motor activities, such as walking task, object manipulation task, etc…(Warren, 1984; Norman, 1988). A specific analysis and more rigorously explanation of the relationship between the agent's motor difficulty and the affordance is deepened and discussed in the next section, where the Stochastic Index of Difficulty is proposed to quantify its affordance and evaluate the agent's motor performance.

4. Stochastic Index of Difficulty-based affordance model

The proposed Stochastic Index of Difficulty allows to evaluate the motor difficulty experienced by an agent while performing repetitive motor tasks. The agent interacts with the environment through the execution of the required motor task, taking into account both agent (internal constraints) and environmental (external constraints) features. Nevertheless, the model can be employed to evaluate its motor performance, through a novel quantitative metrics related to the concept of affordance. To understand deeply how the affordance can be related to the stochastic ID, the following section is devoted to analyse the concept, starting from its original theorization to the various applications in industrial design and robotics research fields. The investigation about the origins of the affordance and its applications is useful to understand the potentiality of this concept in expressing the motor performance through the stochastic ID, and underline both strengths and gaps in the scientific literature.

4.1 Background on Affordance

The concept of affordance has been originally introduced by Gibson (Gibson, 1979a) to describe how living beings behave and perceive, i.e. interact, with the surroundings and the environment. How the living beings detect the world and the environment, is deeply affected by the actions that they can perform. In the ecological psychology perspective, the reality is perceived through the senses: it's the perceptual system of organisms that allows them to detect the action possibilities and interact with the surroundings. The study conducted by Gibson, relates the perception and behaviour of living beings to what the environment affords. The environment is perceived, not described through the world of physics (time, matter at the atomical level). As an example, an organism detects the changes of events, transition of processes, not purely the time. Through the detection of light (seeing), sounds (hearing), surfaces (touching), smell (smelling), the organism guides and controls its interaction (e.g., locomotion) in the environment. The characteristics of the environment that are perceived by the living beings can be related to terrain properties (inclination, material, irregularities), the presence of obstacles, barriers, objects that can afford grasping, carrying, lifting, and tools that can be used for

a given activity.

More in general, basing on the specific context, the living beings can have other synonymous such as animal, perceiver, actor, observer, subject, individual; for sakes of simplicity, they can refer to one simple definition, named 'agent' (Greeno, 1994; Burlamaqui and Dong, 2014): an agent is someone that interacts with the environment. The affordance is not entirely dependent on the agent, nor on the environment, it is the result of the interaction between the two. The affordance is neither objective, nor subjective, but is the result of the agent-environment interaction, and refers to action possibilities, that is, what the agent can do in a given environment (e.g., handle objects, walk, climb, etc…).

If a given interaction between the agent and the environment may occur, it means that it is affordable, on the contrary it is not. This is one of the characteristics of the affordance theory: it has a binary meaning. An action is affordable or not, there is no grey scale, no magnitude. An example is related to the stair climbing: Warren (Warren, 1984) found that if a stair riser is lower than the 88% of an individual's leg length, that subject is able to climb the stair, i.e., the stair affords climbing; on the contrary, it cannot be climbed, at least in a bipedal fashion. A given stair is defined 'climbable' or 'unclimbable' for a given agent through a biomechanical model, defined as the ratio between the riser height, and the leg length (Figure 4.1). In this way Warren defined a metrics to measure the affordance, differently from Gibson, where the affordance remained merely a concept.

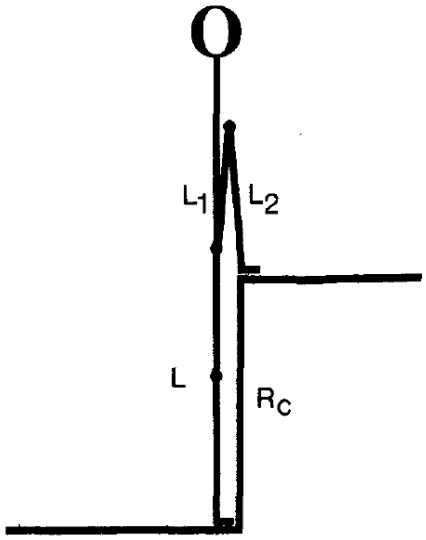

Figure 4.1 *Biomechanical model of the critical riser height Rc=L+L1-L2,with L1=f(L) and L2=f(L); the critical ratio Rc/L= 0.88 (Warren, 1984)*

The dimensionless critical ratio 0.88 can be applied for both short and tall climbers and remains invariant over different sized agents. By simply expressing the climbability through the critical ratio Rc/L, Warren succeeded in considering both the agent (L), and the environment (Rc), following the pillar concept that the affordance is a relational definition that links two counterparts: the agent and the environment. The Rc/L ratio has a consequence on motor behaviour: the human agent's judgment on whether a stair is climbable or not, is not defined by the stair height alone, but by its ratio to the agent's leg length. Experiments involving the concept of affordance like the one of Warren (Gibson *et al.*, 1987; Mark, 1987; Kinsella-Shaw, Shaw and Turvey, 1992; Chemero, 2000) aimed at describing how human agents perceive if an action is do-able or not, i.e. the action possibilities.

Conditions that enable the interaction depends on both agent and environmental characteristics. A surface can afford support or not for the locomotion: it depends on both features of the surface, and features of the agent. By considering a specific surface with given features, a young man/woman may be able to walk on it, while an older man/woman may not. Different environmental layouts define different behaviours for different agents. By considering a given agent, features of the environment contribute to define what it can or cannot do, i.e., the possibilities of actions, and their limits: an agent cannot walk through a wall (permanent obstacle), but the action is enabled in the presence of a doorway. The agent is also characterized by some features, that define its abilities for a given interaction with the environment: a wall can be climbable for an expert climber, but not for a novice one. Body-scaled measures, such as leg length, are an easily quantifiable measure of the agent's ability during a given interaction with the environment, but the direct relationship between ability and body-scaled measures does not always exist because ability may be independent of the agent's physical characteristics: two agents can interact with the environment differently even if they have the same anthropometric features. In fact, a given stair may be easily climbable by a subject, climbable with a greater difficulty by another, and non-climbable by a third subject, for different reasons. A biomechanical model, as the one of Warren, may be not sufficient to describe all the climber-stair scenarios, or more in general, the agent-environment fit. As highlighted by Chemero (Chemero, 2003), there are some agent's abilities while interacting with the environment that cannot be expressed only by body-scaled measures. (Cesari, Formenti and Olivato, 2003) reported that even in the classical

stair climbing experiment (as the Warren's experiments), people identified the affordability of the stair climbing, not basing on the relation between body dimensions and riser height, but as the relation between the stepping ability and riser height. Even if it was found that different agents (children, young adults, older adults) had the same optimal ratio of distance from step to riser height, they behaved differently; older adults showed a different flexibility than other participants, confirming that the stepping ability is the relevant factor in the interaction with the environment (stair climbing).

Multiple factors affect an agent's ability in performing a given action, such as biological features (age, sex), job, training, past experience, prior knowledge, etc… This conception of agent's ability was not considered in the original affordance definition provided by Gibson. In fact, the awareness of what an agent can do in an environment, i.e., actions that an agent is able to execute in an environment with given features, is detected by the agent without any mental calculation, being just directly perceived. The perception does not require any internal processing of the agent while interacting with the environment; in this sense, the agent is aware of the ability to execute certain actions through direct perception. By incorporating in the agent's ability to interact, other features in addition to direct perception, there is a deviation from the original Gibson's definition. This interpretation has been considered by following authors, since not only the direct perception must be considered to understand if an interaction is possible or not. In particular, this perspective has been considered when applying the affordance in the industrial design field and robotics.

4.1.1 The industrial design perspective

Since its original theorization, many authors deepened the analysis on affordance, suggesting other views and applications. Norman (Norman, 1988), in particular, considered the affordance in the industrial design. Under the Norman's point of view, the affordance depends on the past knowledge and experience of the observer and is not directly perceived. Norman states that the brain must process the information that comes from the surroundings, elaborate them in order to act properly: the 'pick-up information' step is not direct and automatic. Together with the perception, there is also the contribution due to the processing of the information (cognitive activity) (Fajen, 2007), and other factors that influence the behaviour of the agent, like prior experience and past

knowledge (Masoudi *et al.*, 2019).

In this context, affordance refers to the interaction between an object, and the agent, and considers qualities of the first, and abilities of the second. Furthermore, Norman makes a difference between the actual (real) and perceived affordance. The actual affordance is what the object has been created for: the affordance, in this sense, does not refer to a general interaction with an object, but to a specific interaction. The perceived affordance is the action possibilities that a subject perceives when interacting with the object. Therefore, given an object, it does not imply that the actual affordance is the same as the subject perceives (perceived affordance). The designer defines properties of a given object in order that its utility is perceived easily; unfortunately, even if an object is designed for a specific scope, its utility may be perceived differently, defining a greater or lower gap between the actual and perceived affordance. From the designer point of view, it is more important focusing on what actions the user perceives to be possible: the objective of the designer is to bring closer the perceived affordance to the actual one. The designers should focus on the capability of the agent to understand the utility of an object, instead of design the object first, and expect that the agent is able to understand it. While with Gibson's perspective the action possibilities were not linked to a specific purpose, in Norman not all the spectrum of action possibilities are considered, but only the ones that refer to the perceived usability/utility of an object. A mug could be thrown, moved, lifted (Gibson's action possibilities), but its main functionality is to drink from: therefore, the action possibilities related to the interaction with the mug, under Norman's point of view, refer to the actions that afford to drink from it. Being the mug, an object used in everyday life, in this case there is a perfect matching between the perceived and actual affordance.

4.1.2 The robotics perspective

The affordance has been re-interpreted and subjected to a new formalism in the field of robotics. In this context, rather than focusing on the direct perception as done by Gibson, authors deepened the relation between the affordance, the action and the learning: to interact with the environment, the robot must understand it, elaborate the information acquired by the sensorimotor system, in order to act properly. Therefore, these agents need to interpret the reality which cannot be understood solely through the direct

perception, i.e. extracting the relevant information from the environment without any modeling or interference. Cognitive processes such as learning, reasoning and inference must be executed, like in the Norman's perspective, to elaborate the information and finally act properly. Recent works in this field are focused on the affordance learning. One of the main aspect of affordance learning refers to the effects or consequences of a certain action in a given environment (Stoytchev, 2005). Among all, Steedman (Steedman, 2002) focused both on the pre-conditions allowing for actions to take place, and on the post-conditions generated by the actions (effects). Therefore, differently from the ecological psychology perspective, the affordance includes also the post-action, i.e., the effects due to the agent-environment interaction. Fitzpatrick and colleagues (Fitzpatrick *et al.*, 2003) considered the agent-environment interaction in the object manipulation, stating that a robot can learn manipulation affordances by just exploring the various interactions by acting on objects, observing the effects, and finally building relations; after repeated trials, the robot can understand the relation between a given action-object pair, and the effects due to their interaction. As the development processes proceed, exploratory activities become controlled and performed with a specific purpose. In the experiments performed, the robot learned about the 'rollability' affordance related to an object manipulation, by observing the effects in the environment after the interaction with it (Fitzpatrick *et al.*, 2003): a robot can learn the proper action to be executed by acting on the object and observing the effects on the environment. The affordance is acquired through the interaction of the robot with the environment.

The affordance learning can be greatly improved by the use of probabilistic models. Focusing on manipulation affordance, in some experiments a humanoid robot learned the liftability of objects through probabilistic relational models, where both object and action features contribute to the liftability estimation (Hart, Grupen and Jensen, 2005). Other authors faced the same theme by focusing on how robots can learn the 'graspability' (grasp affordance) related to an object, i.e. object-gripper configurations that bring to a successful grasp (Detry *et al.*, 2009). Considering a given object, the grasp affordance is initially constructed through the imitation of human demonstration, and grasp hypothesis densities (initial grasp densities) are built from visual cues. Then, through exploration, visual information about the effect of the object-gripper interaction are employed to build empirical grasp densities through the technique of the kernel density estimation (KDE): the robot improves its grasp knowledge by interacting with an object through multiple

grasp-and-drop actions, gaining more visual information through the grasping. These data are used to predict the likelihood of grasping success with specific object-gripper pose and evaluate what is the most probable object-gripper configuration that allows to grasp the object and lifting it up. Through the learning process, the grasp success rate improved by considering the empirical grasp densities (from experience), instead of the initial grasp densities (from imitation) (Detry *et al.*, 2010, 2011).

In this context, the execution of actions has a key role in the affordance learning of robots: through the sensorimotor experience and abilities, the robot understands what the most relevant information to pick-up from objects are, and consequently execute the action related to that object. In fact, the main purpose of applying the affordance to robots, is allowing them to effectively act on the environment, not to re-construct it with a detailed representation. Since this pick-up of visual information depends on both the agent and the environment, the robot needs to execute actions and capture the effect through its sensorimotor system: the affordance can be learnt through the interaction of the agent (robot) with the environment.

A robot can interact with the environment in multiple ways (i.e., perceived affordance), but only one, or few of them allow to act properly on an object, or in a situation (i.e. actual affordance): an object can me 'rollable', 'liftable', 'throwable'. Both prior knowledge and past experience developed with multiple agent-environment interactions help robots in identifying the proper actions to perform, related to a given situation. Some authors, like (Stark and Bowyer, 1991), tried to define the robot-object interaction not basing solely on geometrical features of the objects (mass, shape etc…), but also on the main functionality of the object: a hammer and a stone have different geometrical features, but both can be used to hit or strike. Lewis and colleagues (Lewis, Lee and Patla, 2005) applied the same reasoning in the locomotion affordance, showing that geometrical features of the environment are not enough to guide the foot placement of a robot. The robot visual system allows to avoid collisions, predict gait modulation, plan routes, pick-up geometrical and non-geometrical visual information from the surroundings. In the field of locomotion, the non-geometrical cues are necessary to understand if the locomotion is afforded or not: two identical geometric surfaces may both afford locomotion, but if one of them is covered by ice, this gives a 'slippery' feature to the surface resulting in lowering (or cancelling) the locomotion affordance, i.e., the possibility to walk on it.

The application of affordance in robotics, consists of three main phases: the first is related to the direct perception, i.e., pick the relevant information from the surroundings through the sensorimotor system. The second is related to the learning, i.e. build the relations between a given environmental situations and the consequence of a given action: by focusing on the object manipulation, the robot understands the interactive functionality of objects. Lastly, the control system of the robot uses the relations build to face the various situations. Through a continuous interaction between robot and environment, the robot could improve the quality of interactions.

Despite the widespread application of the concept of affordance in ecological psychology, product design, and robotics (e.g., grasp affordance, manipulation affordance, locomotion affordance), there is still a great lack in evaluating the affordance related to movements through a standardized quantitative metrics. Furthermore, no proposed metrics has a general validity aside from the field of application: each research field has its own formalization and evaluation. In the following paragraphs it is proposed firstly a novel formalization of the affordance, able to be applied in all the above-mentioned fields providing a high level of generalization, and secondly a model based on the stochastic Index of Difficulty, able to turn the affordance concept into a general quantitative metrics. Our model is based on comparing the motor behaviour of two agents: one is the 'reference' agent, able to optimally execute a given motor task, the second is the 'observed' agent. By comparing these two agents, a performance indicator expressing the 'level' of affordance is obtained. This way of reasoning is similar to the one suggested in (Ardón *et al.*, 2021) where about affordance metrics it is stated that: '…*an interesting approach would be to measure the similarity of the actions taken by the system with those a human would execute. For example, it could be interesting to measure the differences in the trajectories executed to achieve a task. Such differences could be measured in terms of distances in the point distributions of the trajectories*'. In our case, the dissimilarity of actions is expressed in probabilistic terms between the 'reference' one and the 'observed' one, where differences consider not only trajectories executed, but also the stochastic behaviours during a given interaction with the environment.

4.2 Modeling Affordance through the Stochastic Index of Difficulty

As previously described, the affordance expresses the interaction between an agent, and the environment. Multiple agent-environment interactions exist, by changing both the agent, and the environment, or either one. Nevertheless, in all the scenarios the interaction includes the movement of an agent's body part, even in the case of robotics. In fact, in robotics, the affordance learning is useful when the agent learns how to properly interact with the environment by actually acting with it multiple times and observing the effects. This characteristic is in line with our perspective about the affordance: the agent must interact physically (i.e., through movements) and purposefully with the environment, observing the consequences of its actions. The feature relative to the observation of the agent, and to the goal-specific interaction with the environment, have been commonly considered also in the product design (Norman's perspective), as well as in experiments performed in the ecological psychology field, such as in the stair climbing experiment of Warren (Warren, 1984).

The second feature considered in our affordance perspective is relative to the characteristics that define the agent. Being the affordance quantified after the observation of the agent-environment interaction, the agent cannot execute actions by just relying on its direct perception. An agent cannot use an object or a tool without knowing how it must be handled, and what is its main functionality; this information can be captured by interacting with it enough times in order to acquire sufficient knowledge about its features, utility, functionality etc…, and store this knowledge to be used for future interactions. Therefore, the prior experience and past knowledge characterize the agent and affect the agent-environment interaction, as in the Norman's perspective. Nevertheless, the peculiarities that identify an agent are not limited to these characteristics: biological (e.g., age, sex), anthropometric and physical measures must be considered, as well as skills, training level, innate features, intelligence etc… All these characteristics, define the ability of the agent in interacting with the environment. Different interactions require different agent's features: if a human agent is asked to solve a rubik's cube, the most important feature to consider may be the IQ: a human agent with a low IQ may be never capable to solve it, while a human agent with a high IQ will be

able to solve it in a short time. On an assembly line, a human agent (operator) with years of experience will execute an assembly task more efficiently, compared to a novice one. This is valid also in case of robotic agents, since the motor, control and sensory systems are influenced by the amount and variety of past interactions, morphology of the robot, its degrees of freedom, the perception and processing of visual information, actuators, etc…. Therefore, the agent's ability, summarized by the above-mentioned features, expresses its internal constraints.

In the same way, features of the environment are considered in our affordance perspective; these features are expressed by visual information of the environment such as the presence of obstacles, paths to walk, inclination of surfaces, mass, geometry, stiffness and shape of objects to manipulate, utility of tools etc…

Similar to Chemero (Chemero, 2003) who considered both abilities of the agent, and features of the environment, in the new affordance perspective, both internal and external constraints are considered.

Differently from its original definition, in the new affordance perspective the agent-environment interaction in not defined in a binary manner, but it has a scale, a magnitude that expresses how well the agent is behaving. In this way, by observing different agents interacting with the environment, it is possible to identify which one behaves better. Nevertheless, to consider the affordance in a continuous scale, it must be necessary to 'normalize' it, i.e., evaluate the affordance relative to an optimal agent, taking as a reference. If an optimal agent was not considered, it would not be possible to compare the interactions of multiple agents. Therefore, in the novel affordance perspective, two types of agents must be considered: the first one is the 'observed' agent, the second one is the optimal or 'reference' agent. The latter can be both observed and taken as a reference, or its optimal behaviour can be pre-defined, i.e. the optimal agent-environment interaction is pre-defined. Consequently, no 'actual' or 'perceived' terminology is used to briefly describe the type of affordance considered; in this context there is a 'relative' affordance, being the main goal to evaluate the observed agent-environment interaction relative to the optimal behaviour expressed by the 'reference' agent. The property of this novel perspective is equal to consider a fuzzy logic ('relative' affordance) instead of an ON/OFF/binary/Boolean logic (perceived or actual affordance). The 'fuzzy logic' affordance point of view is expressed quantitively into the use of probability, as the in robotics field, where the possibility of interacting properly with the environment is

evaluated by the use of probabilistic models.

As previously discussed, in any agent-environment interaction, the agent must execute movements (e.g., locomotion, navigation, grasping, manipulation…) and the motor behaviour of a specific body-part (called from now on end-effector) is observed. By bearing also in mind that the 'relative' affordance must be quantified in a continuous scale (sort of 'affordance level'), by means of probability, stochasticity of movements observed must be considered. The motor behaviour of the agent, with its path executed and motor variability, are the effects/consequences observed of the agent-environment interaction. All these features (observation, motor behaviour, motor variability) are inherent in the stochastic Index of Difficulty. In the following paragraph it is described quantitatively the technique to employ the stochastic ID to quantify the 'relative' affordance in a continuous scale.

4.2.1 The Stochastic Index of Difficulty-Affordance model: 2D Movements

As described in chapter two, the stochastic ID is capable of quantifying the motor difficulty experienced by an agent, while performing repetitive motor tasks. Results confirm that the model is sensitive to the variation of agents (variation of internal constraints), and to the variation of task/environmental features (variation of external constraints). To be able to quantify the affordance in a continuous scale (affordance level), two motor difficulties must be considered: the first related to the 'reference' agent, the second one to the 'observed' agent. Both motor difficulties are evaluated with some variations from the stochastic ID proposed in Equation 2.1. Both IDs are discussed in the following paragraphs.

4.2.1.1 The Reference Agent

The best agent-environment interaction can be summarized by the optimal motor behaviour of the agent. In robotics it can be related to the optimal object-gripper interactions, expressed by the placement configurations of the gripper (robot's end-effector) on the object in order to successfully execute the grasp; in the locomotion affordance, the optimal motor behaviour can refer to the minimization of the agent's cost function (e.g. minimum jerk) for a high-level motor coordination or, to the correct

placement of the foot (robot's end-effector), when considering a complex agent-environment interaction such as walking on a surface full of obstacles. This scenario can be also applied to human agents. When considering an assembly line manipulation task, the optimal motor behaviour can refer to the correct gathering of various components in order to obtain the final product; to assemble correctly all the various components the hand (human's end-effector) must place on each component in a specific manner.

In general, by considering a general motor task, the optimal motor behaviour can be summarized into the trajectory that allows the agent to successfully interact with the environment. In fact, in general motor task the agent executes movements, whose sequence defines the best path to follow.

Nevertheless, when considering repetitive motor tasks, even if the best path is defined, the motor behaviour of the reference agent cannot be expressed solely by the nominal trajectory: even the reference agent is not able to perfectly follow the nominal trajectory in each trial. As discussed in chapter two, the variability or stochasticity that stems from movements, should be addressed according to the specific theoretical and experimental context of interest. In this context, the motor variability, represents the equivalent motor solutions that allow to successfully execute the repetitive motor task (best agent-environment interaction). The focus is not on the sources that give rise to motor variability, but the effect that the stochastic motor behaviour has on the fulfilment of the repetitive motor task.

Therefore, the optimal motor behaviour of the reference agent in executing a repetitive motor task, is expressed by its nominal trajectory and motor variability. As discussed in chapter two, both elements are inherent in the stochastic Index of Difficulty (equation 3.1), characteristic of the combined agent-environment system. By considering the reference agent, nominal trajectory and motor variability can be, or both observed, or both defined a priori.

In the first case, the reference agent refers to the observed one that executes optimally the repetitive motor task. In this context the observed stochastic width expresses the maximum tolerance of movement variability allowing to successfully execute the repetitive motor task; its boundaries are defined and expressed through $W_{inf}(s)$ and $W_{sup}(s)$ (Figure 4.2). Since the reference agent is the best observed one, the average trajectory t_{avg} becomes the reference (nominal) trajectory t_{ref}, while the observed

stochastic width $W_{obs}(s, \varphi)$ becomes the reference stochastic width $W_{ref}(s, p)$ (p instead of φ defined in chapter 3.1 for sakes of clarity). Equation 3.3 is reintroduced with the new notation in equation 4.1:

$$\boldsymbol{W_{ref}(s, p) = 2 \cdot z(p) \cdot \sigma(q_k(s))} \quad (4.1)$$

As described in chapter two, z is the z-score of the standardized normal distribution, that depends on the probability level p (z = 1 for p = 0.6827; z = 2 for p = 0.9545; z = 2.066 for p = 0.9600; z = 3 for p = 0.9973), while $\sigma(q_k(s))$ is the standard deviation of the spatial configurations evaluated at curvilinear coordinate s.

This scenario is related to situations where the optimal agent-environment interaction can be defined only through experience, by considering multiple agents belonging to the same cluster (such as same age range, experience etc…) and choosing the one that executes optimally the repetitive motor task, taken therefore as a benchmark for a given agent cluster.

In the second case, both t_{ref} and $W_{ref}(s, p)$ (∀ curvilinear coordinate s) are defined a priori; being $W_{ref}(s, p)$ defined a priori, the reference stochastic width does not depend directly from the probability level p; in spite of this, it was decided not to change the notation of the reference stochastic width to consider a unique formulation for both scenarios; consequently, for both cases the reference stochastic width is expressed through $W_{ref}(s, p)$.

Spatial configurations reachable by the reference agent ∀ curvilinear coordinate s are assumed to be normally distributed since, as observed in the scientific literature, in repetitive motor tasks variability of agents' trial trajectories follow a gaussian distribution centred on their average along the entire path (Ghahramani and Wolpert, 1997; Messier and Kalaska, 1997; Van Beers, Haggard and Wolpert, 2004; Liu and Todorov, 2007; Guigon, Baraduc and Desmurget, 2008). The assumption that frequencies of spatial configurations reachable by the reference agent are normally distributed in the section orthogonal to t_{ref} at each curvilinear coordinate s, represents the best behaviour achievable, since the higher frequency is defined on $q_{ref}(s)$ (point ∈ t_{ref} at curvilinear coordinate s). Consequently, movements of the reference agent are assumed to follow a gaussian distribution centered on $q_{ref}(s)$, point of t_{ref} at the curvilinear coordinate s, with a given probability p (Figure 4.2). $f_{ref}(s, T)$ is the probability density function of

the distribution at curvilinear coordinate s.

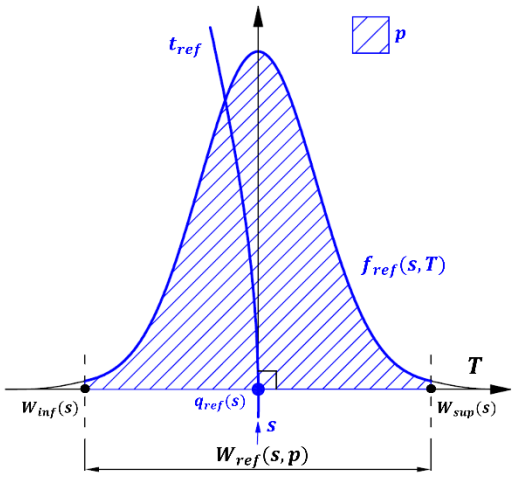

Figure 4.2 *Reference Agent's stochastic behaviour at curvilinear coordinate s*

Therefore, the stochastic Index of Difficulty able to evaluate the motor difficulty of the reference agent while executing repetitive motor tasks is defined as:

$$\boldsymbol{ID_{ref}} = \int_{\boldsymbol{t_{ref}}} \frac{\boldsymbol{ds}}{\boldsymbol{W_{ref}(s,p)}} \tag{4.2}$$

ID_{ref} expresses the optimal agent-environment interaction, represents the reference/optimal affordance. Nevertheless, to evaluate the quality of a specific observed agent-environment interaction relative to the optimal one, the related observed affordance must be evaluated. In the following the stochastic Index of Difficulty related to the observed agent is described.

4.2.1.2 The Observed Agent

Since the motor behaviour of the reference agent expressed by ID_{ref}, represents the optimal affordance, it can be employed as a standard for a given observed agent executing the same repetitive motor task. Therefore, the motor behaviour of the observed agent should be as close as possible to the one of the reference agent: higher the similarities between the two behaviours, better the agent-environment interaction. For a perfect matching between the two agents' behaviours, the motor difficulty experienced by the observed agent must be equal to ID_{ref}: in this case spatial configurations reachable by the observed agent along the entire path fit perfectly with the spatial configurations reachable by the reference one. The motor difficulty of the observed agent is evaluated

relative to the reference movements that should be performed while executing the motor task:

$$\boldsymbol{ID_{\cap}} = \int_{\boldsymbol{t_{avg}}} \frac{\boldsymbol{ds}}{\widetilde{\boldsymbol{W}}_{\cap}(\boldsymbol{s})} \tag{4.3}$$

t_{avg} is the average trajectory executed by the observed agent during the repetitive motor task, while the observed stochastic width $\widetilde{W}_{\cap}(s)$ is indicative of its local motor behaviour, defined in the section orthogonal to the reference trajectory t_{ref} at curvilinear coordinate s, as for the reference stochastic width $W_{ref}(s,p)$. $\widetilde{W}_{\cap}(s)$ is defined as:

$$\widetilde{\boldsymbol{W}}_{\cap}(\boldsymbol{s}) = \boldsymbol{W}_{\cap}(\boldsymbol{s}) \cdot \frac{\boldsymbol{p}_{\cap}(\boldsymbol{s})}{\boldsymbol{p}} \cdot \frac{\boldsymbol{\eta}_{\cap}(\boldsymbol{s})}{\boldsymbol{p}} \tag{4.4}$$

Where:

- $W_{\cap}(s)$ is the region where spatial configurations reachable by the observed agent are within $W_{ref}(s,p)$; $W_{\cap}(s) \in [0; W_{ref}(s,p)]$
- $p_{\cap}(s)$ quantifies the probability of the observed agent in reaching spatial configurations within $W_{ref}(s,p)$, evaluated from the PDF (Probability Density Function) of spatial configurations ($0 \leq p_{\cap}(s) \leq p$); $p_{\cap}(s)$ is normalized by p, so that the quantity $\frac{p_{\cap}(s)}{p} \in [0; 1]$
- $\eta_{\cap}(s)$ evaluates the minimum between the PDF (Probability Density Function) obtained from spatial configurations of the two agents ($0 \leq \eta_{\cap}(s) \leq p$); $\eta_{\cap}(s)$ is normalized by p, so that the quantity $\frac{\eta_{\cap}(s)}{p} \in [0; 1]$

Therefore, $\widetilde{W}_{\cap}(s) \in [0; W_{ref}(s,p)]$. From spatial configurations reached at s ($q_k(s)$), the corresponding probability density function $f_{obs}(s,T)$ can be evaluated (Figure 4.3). The three variables characterizing $\widetilde{W}_{\cap}(s)$ depend on $f_{obs}(s,T)$, and related features are described in the following.

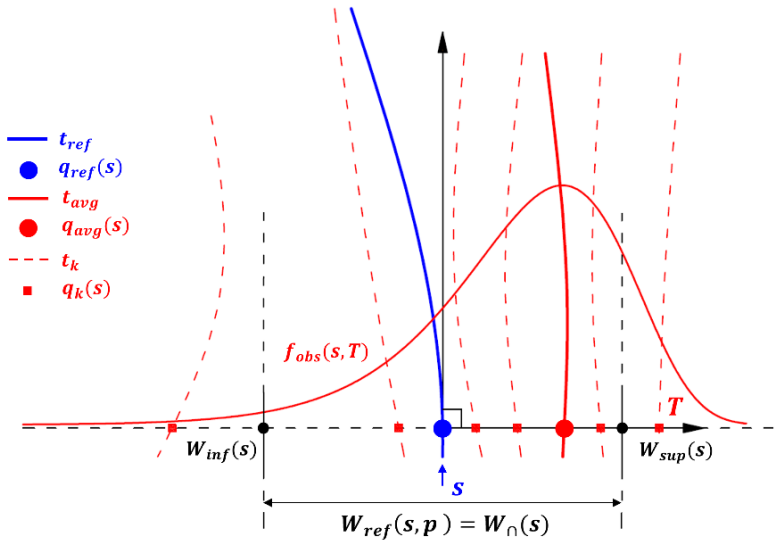

Figure 4.3 *Observed Agent's stochastic behaviour at curvilinear coordinate s*

$W_{\cap}(s)$ provides 'extensive' information about the spatial configurations reachable by the observed agent relative to the reference one. In Figure 4.3 it can be observed that $W_{\cap}(s) = W_{ref}(s,p)$, since $f_{obs}(s,T)$ has no upper or lower bounds that limit its extension. On the contrary, there can be cases where the observed agent is physically constrained, unable to reach all the spatial configurations within the reference stochastic width $W_{ref}(s,p)$ ($W_{\cap}(s) < W_{ref}(s,p)$): lower the value of $W_{\cap}(s)$, greater the distance from the optimal agent-environment interaction.

$p_{\cap}(s)$ quantifies the probability of the observed agent in reaching spatial configurations within $W_{ref}(s,p)$. $p_{\cap}(s)$ is evaluated from the probability density function $f_{obs}(s,T)$, between the boundaries of the reference stochastic width ($W_{inf}(s)$ and $W_{sup}(s)$):

$$\boldsymbol{p_{\cap}(s) = \int_{W_{inf}(s)}^{W_{sup}(s)} f_{obs}(s,T)\,dT} \tag{4.5}$$

Equation 4.5 is applied at each curvilinear coordinate s. When $p_{\cap}(s) = p$, all the spatial configurations reachable by the observed agent are within $W_{ref}(s,p)$. Differently from $W_{\cap}(s)$ that provides 'extensive' information, $p_{\cap}(s)$ provides 'quantitative' information. $p_{\cap}(s)$ expresses what is the likelihood of the observed agent in locating its end-effector within the reference stochastic width $W_{ref}(s,p)$ at curvilinear coordinate s.

Briefly speaking, the product between the 'extensive' and 'quantitative' variables $W_{\cap}(s) \cdot p_{\cap}(s)$ expresses the expected value of $W_{\cap}(s)$; by recalling the definition of the expected value of a random variable X:

$$\boldsymbol{E[X] = \sum_{i=1}^{n} p(x_i) * x_i} \tag{4.6}$$

Where $x_1, x_2, \dots, x_n$ are the possible outcomes (events) of the random variable X, and $p(x_1), p(x_2), \dots, p(x_n)$ the corresponding probabilities. By observing Figure 4.3, only two possible events ($W_\cap(s)$) are related to the states reachable by the observed agent at curvilinear coordinate s: the first when the agent's end-effector positions are within $W_{ref}(s,p)$ ($W_\cap(s)_1 = W_\cap(s) \neq 0$), with associated probability $p_\cap(s)$, and the second when the agent's end-effector positions are outside boundaries of $W_{ref}(s,p)$ ($W_\cap(s)_2 = 0$), with associated probability $1 - p_\cap(s)$. Therefore:

$$\begin{aligned} \boldsymbol{E[W_\cap(s)] = \sum_{i=1}^{2} p[W_\cap(s)_i] \cdot W_\cap(s)_i = W_\cap(s) \cdot p(s) + 0 \cdot \big(1 - p(s)\big)} \\ \boldsymbol{= W_\cap(s) \cdot p(s)} \end{aligned} \tag{4.7}$$

Nevertheless, the information inherent in $W_\cap(s)$ and $p_\cap(s)$, are not enough to characterize the stochastic behaviour of a given observed agent for two main reasons. Firstly, there is still an important missing feature describing the 'qualitative' information, related to the frequency distribution of spatial configurations. Secondly, it cannot be distinguishable the difference between two observed motor behaviours, by considering only $W_\cap(s)$ and $p_\cap(s)$. An example is depicted in Figure 4.4.

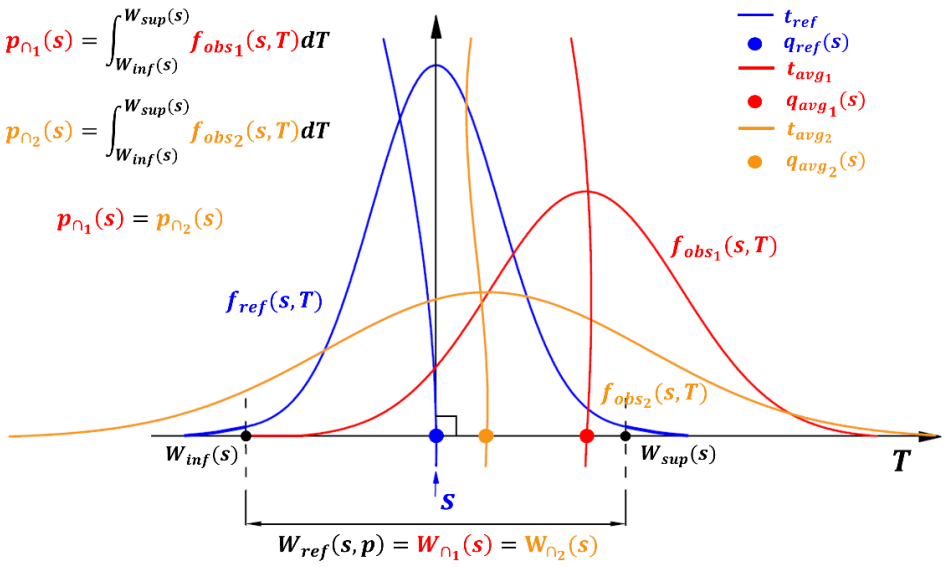

Figure 4.4 *Example of stochastic behaviours of two different observed agents (red and orange trends) in case of same $W_\cap(s)$ and $p_\cap(s)$, at curvilinear coordinate s. Blue trend is associated to the reference agent.*

The red and orange trends are related to two different observed agents, while the blue trend is related to the reference one. It is clearly observable that despite $p_{\cap_1}(s) = p_{\cap_2}(s)$ and $W_{\cap_1}(s) = W_{\cap_2}(s)$ the frequency distributions (red and orange) are different. Therefore, there is the necessity to consider the shape of the PDF when describing the stochastic behaviour: this is expressed by the variable $\eta_{\cap}(s)$, called 'overlapping index' (Pastore and Calcagnì, 2019). $\eta_{\cap}(s)$ allows to evaluate the similarity between two probability distribution functions (Equation 4.8):

$$\boldsymbol{\eta_{\cap}(s) = \int_{W_{inf}(s)}^{W_{sup}(s)} min\,[f_{ref}(s,T), f_{obs}(s,T)]dT} \tag{4.8}$$

$\eta_{\cap}(s)$ is evaluated by considering the minimum between the two PDF and by applying the integral between the boundaries of $W_{ref}(s,p)$. Graphically, $\eta_{\cap}(s)$ expresses the area in common between the two distributions (Figure 4.5): higher $\eta_{\cap}(s)$, greater the similarity between the two distributions.

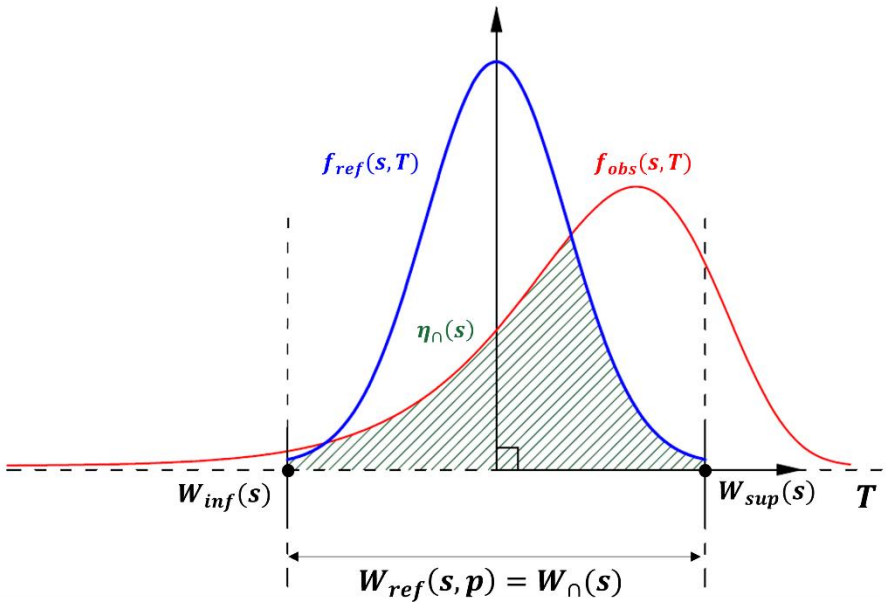

Figure 4.5 *Graphical representation of the overlapping index $\eta_{\cap}(s)$ at curvilinear coordinate s. The red trend is associated to the observed agent, the blue trend to the reference one.*

In Figure 4.6 different values of $\eta_{\cap}(s)$ are shown**,** assuming various PDFs related to the observed agent (Weibull distributions with scale parameter 'a' = 3, and different shape parameters 'b'), and comparing them with the PDF of the reference agent (Gaussian distribution, $p = 99\%$) at a given curvilinear coordinate s. It can be observed that $\eta_{\cap}(s)$

is sensitive to different distributions, and the highest value ($\eta_{\cap}(s) = 0.8619$) is obtained with the Weibull distribution (in magenta) closest to the reference one (Gaussian distribution).

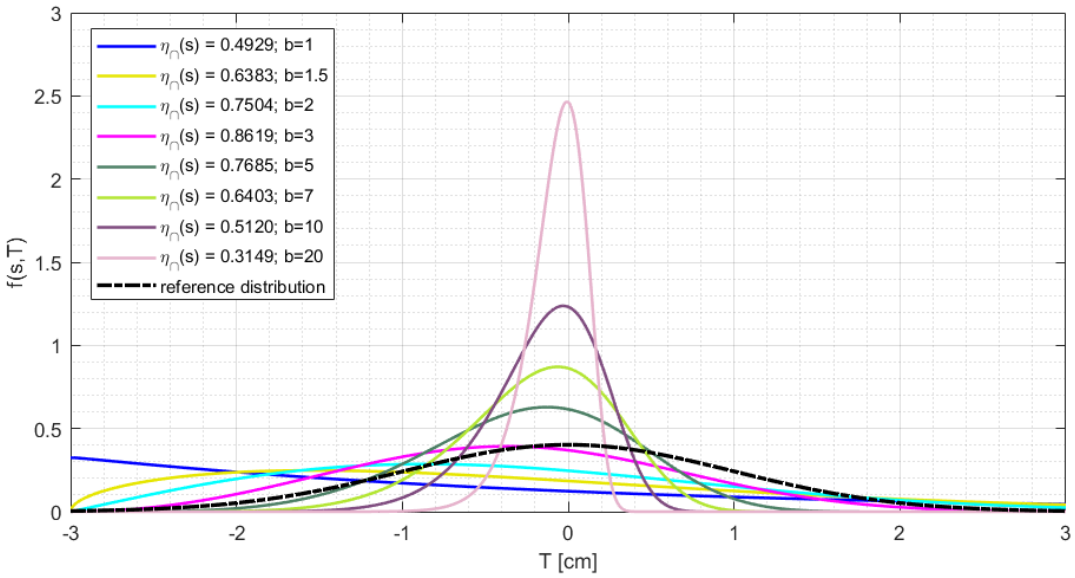

Figure 4.6 *Evaluation of $\eta_{\cap}(s)$ by comparing various Weibull distributions (scale parameter 3, b = shape parameter) with the reference one (Gaussian distribution)*

Therefore, the value of $\eta_{\cap}(s)$ changes basing on the specific shape of the PDF obtained from spatial configurations of the observed agent. Being evaluated between the boundaries of the reference stochastic width $W_{ref}(s,p)$, $\eta_{\cap}(s)$ is defined in the range $[0,p]$, as $p_{\cap}(s)$. Only in the case of perfect matching between the stochastic behaviours of the two agents (reference and observed), the entity of the overlapping index is equal to p; in this particular (hypothetical) scenario, the stochastic behaviour of the observed agent can be described only by the overlapping index since being $\eta_{\cap}(s) = p$, it means that $f_{ref}(s,T) = f_{obs}(s,T)$, $p_{\cap}(s) = p$, and $W_{\cap}(s) = W_{ref}(s,p)$. Nevertheless, in all the other cases, none of the three variables alone can describe the stochastic behaviour of the observed agent. An example is depicted in Figures 4.7 and 4.8. In both Figures the two PDFs $f_{ref}(s,T)$ and $f_{obs}(s,T)$ are compared: the first one is the reference Gaussian distribution (dashed black line), while the second one is the assumed observed distribution (Weibull distribution, coloured distributions) at curvilinear coordinate s. The observed distribution has been shifted along T in order to underline the different contributions of $W_{\cap}(s)$, $p_{\cap}(s)$ and $\eta_{\cap}(s)$, highlighting their mutual independence and needfulness. While Figure 4.7 considers the Weibull distribution with scale parameter 5

and shape parameter 8, Figure 4.8 considers the Weibull distribution with scale parameter 1 and shape parameter 2, in order to observe the sensitivity of $W_{\cap}(s)$, $p_{\cap}(s)$ and $\eta_{\cap}(s)$ with a minimal change of the observed PDF. In both figures the overlapping index $\eta_{\cap}(s)$ does not reach in any case its maximum value $(0.99 = p)$, since the two distributions (observed vs. reference) are not equal. Nevertheless, there are cases (mainly for $T \in [-2, 2]$) where $p_{\cap}(s)$ is extremely close to $0.99 = p$ since the majority of $f_{obs}(s, T)$ (Weibull distribution) is within the boundaries of the reference stochastic width $W_{ref}(s, 0.99) = 6$ [cm]: $W_{inf}(s) = -3\ [cm]$, $W_{sup}(s) = 3\ [cm]$.

In Figure 4.7 the maximum value of $W_{\cap}(s)$ $(W_{\cap}(s)_{max})$ is equal to $W_{ref}(s, 0.99) = 6\ [cm]$, since there are cases when the entire extension of $f_{obs}(s, T)$ exceeds $W_{ref}(s, 0.99)$, mainly for $T \in [1.3, 2]$; in Figure 4.8, instead $W_{\cap}(s)_{max}$ is always lower than 6 $[cm]$, since the entire extension of $f_{obs}(s, T)$ is within the boundaries defined by $W_{ref}(s, 0.99)$: the region where spatial configurations are reachable by the observed agent is lower than the limits defined by the reference stochastic width.

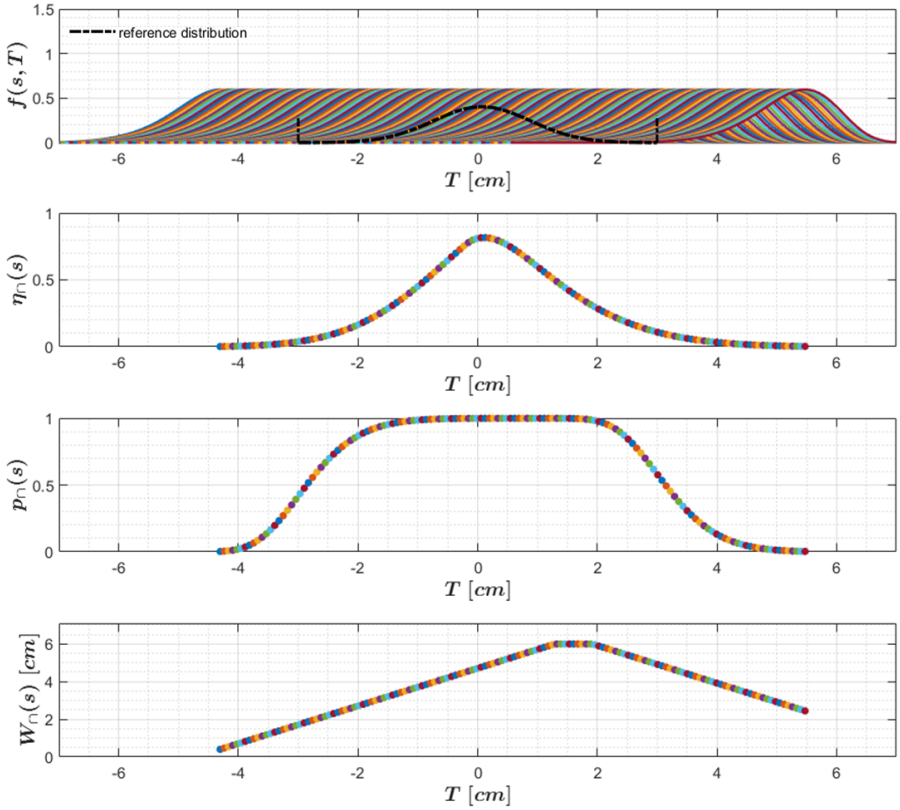

Figure 4.7 *Values of $W_{\cap}(s)$, $p_{\cap}(s)$ and $\eta_{\cap}(s)$ by comparing the reference distribution (Gaussian) with a Weibull distribution (scale parameter 5 and shape parameter 8) shifted along T at curvilinear coordinate s.*

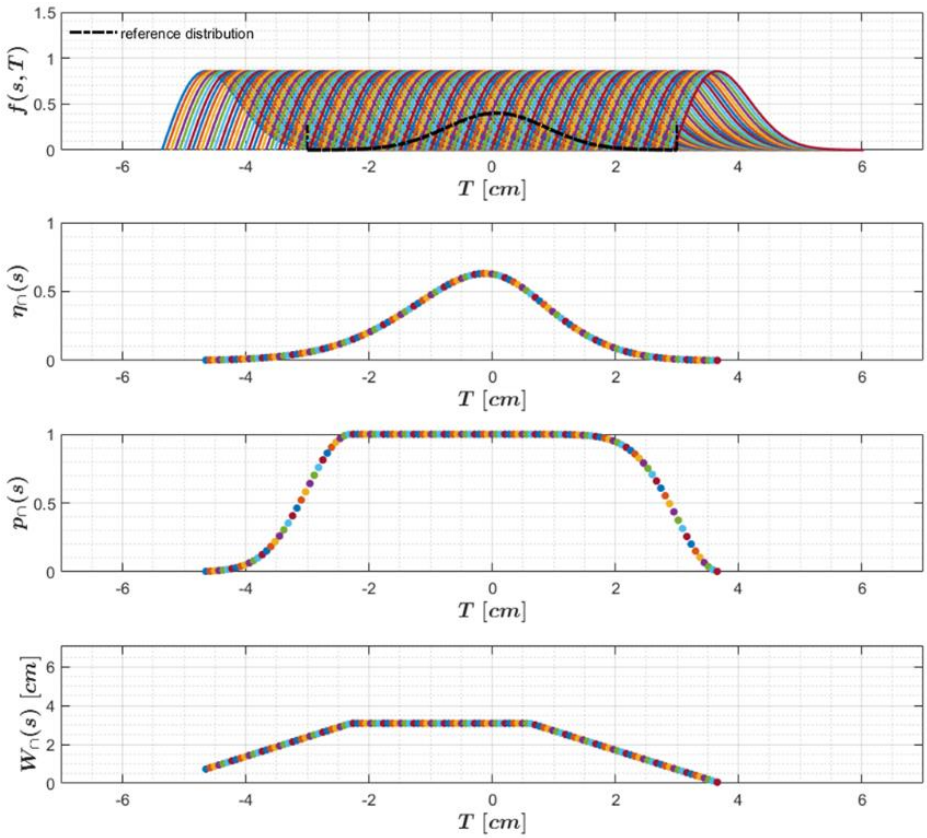

Figure 4.8 *Values of $W_\cap(s)$, $p_\cap(s)$ and $\eta_\cap(s)$ by comparing the reference distribution (Gaussian) with a Weibull distribution (scale parameter 1 and shape parameter 2) shifted along T at curvilinear coordinate s.*

In both Figures it can be observed that when the maximum frequency of $f_{obs}(s,T)$ (coloured distributions) is in the range $T \in [-2,2]$, $p_\cap(s)$ is almost constant, while $\eta_\cap(s)$ is very sensitive, varying its value nearly about the 70%. On the contrary, when the maximum frequency of $f_{obs}(s,T)$ is in the range $T < -2$ and $T > 2$, i.e. when approaching the tails of the reference Gaussian distribution, $\eta_\cap(s)$ is almost constant, while $p_\cap(s)$ varies from values close to p, to values close to 0. These simple observations show that there is the need of both $p_\cap(s)$ and $\eta_\cap(s)$, since some information captured from the first, are not captured by the other and vice versa.

Furthermore, even if in both Figures the same type of observed distributions are assumed (Weibull), with a little change in the scale and shape, an important difference in the trends of $W_\cap(s)$ and $\eta_\cap(s)$ can be observed. In the first case, as previously said, the maximum of $W_\cap(s)$ is not equal in the two Figures since it depends on the extension of $f_{obs}(s,T)$. In the second case, the maximum value of $\eta_\cap(s)$ is 0.81 in Figure 4.7, while 0.63 in Figure 4.8; this is caused by the shape of the two observed PDFs: in Figure 4.7 the $f_{obs}(s,T)$ is particularly close to the reference Gaussian distribution, while in Figure 4.8, $f_{obs}(s,T)$

has an important skeweness, bringing to a greater difference with $f_{ref}(s,T)$, and lower values of $\eta_{\cap}(s)$.

Therefore, the three variables $W_{\cap}(s)$, $p_{\cap}(s)$ and $\eta_{\cap}(s)$ that contribute to the evaluation of the observed stochastic width $\widetilde{W}_{\cap}(s)$ are all mutual independent, meaningful, and necessary to express locally the stochastic motor behaviour of the observed agent. As for $W_{ref}(s,p)$, $\widetilde{W}_{\cap}(s)$ still expresses the motor variability (of the observed agent) but modified through $W_{\cap}(s)$, $p_{\cap}(s)$ and $\eta_{\cap}(s)$ to capture the dissimilarity from the reference agent. The observed agent must not to be as flexible as possible, since the equivalent motor solutions that allow to successfully execute the repetitive motor task are defined by the reference agent. Not all the motor solutions of the observed agent can be useful for the execution of the task: an ever-increasing flexibility is not always beneficial (e.g., unnatural movements, presence of obstacles, too complex paths). Too much or too little variability is not useful for the execution of a given repetitive motor task. Therefore, the motor variability of the observed agent, inherent in the observed stochastic width $\widetilde{W}_{\cap}(s)$, must be as close as possible to the reference stochastic motor behaviour, expressed locally by $W_{ref}(s,p)$.

In order to obtain the overall motor behaviour of the observed agent relative to the reference one ($ID_{\cap}$), i.e., the observed agent-environment interaction (observed affordance), $\widetilde{W}_{\cap}(s)$ must be evaluated along the entire path (average trajectory) and integrated over t_{avg} (Equation 4.3).

In the present and previous paragraph, it has been described how the stochastic ID expressing the motor difficulty can be employed to evaluate the agent-environment interaction (both reference and observed). Nevertheless, to quantify the affordance of an observed agent relative to a reference one in a continuous scale, information inherent in ID_{ref} and $ID_{\cap}$ must be considered together in a unique model: in the following it is described how to obtain the affordance level.

4.2.1.3 The Affordance Level

The model allowing to evaluate the affordance level can be easily explained through Figure 4.9. Let's represent the motor behaviour of the reference agent with a blue set (Reference Behaviour, RB): RB expresses the optimal agent-environment interaction, considering the internal constraints of the reference agent (IC_{ref}) and external constraints

(EC); the motor behaviour is quantified through ID_{ref}. On the contrary, the motor behaviour of the observed agent is represented through a red set (Observed Behaviour, OB); in this case, when considering the result of the observed agent-environment interaction, not all the OB is considered (ID_{obs}), but the portion related to the RB, i.e., $ID_{\cap}$. Both the internal constraints of the observed agent (IC_{obs}) and external constraints (EC) are considered to evaluate $ID_{\cap}$. As previously discussed, not all the movements performed by the observed agent (OB) may be useful for the optimal execution of the repetitive motor task: the optimal execution is expressed by RB. Therefore, graphically, quantifying the affordance level (α) of the observed agent is equal to see how much the two sets overlap ($ID_{\cap}$): greater the overlapping, more the OB is close to RB ($ID_{\cap}$ closer to ID_{ref}), and higher is the affordance level α. To evaluate how close (or distant) is the behaviour of the observed agent to the reference one, the affordance level (α) is easily quantifiable by the ratio $ID_{ref} / ID_{\cap}$.

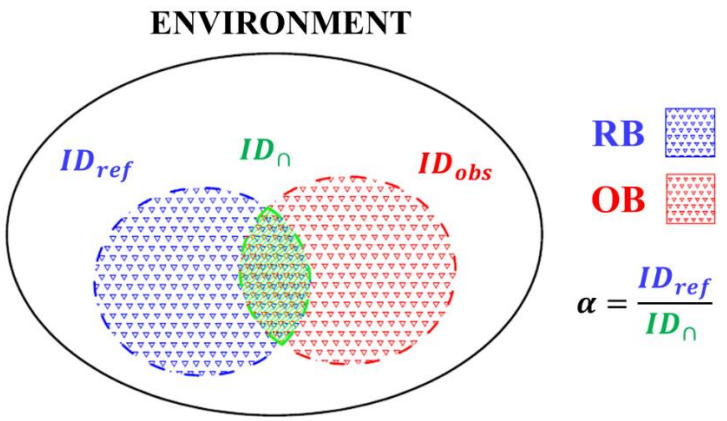

Figure 4.9 *Graphical representation of the Affordance Level (α); in blue the Reference Behaviour (RB), in red the Observed Behaviour (OB). If the two behaviours overlaps, $\alpha \neq 0$: greater the overlapping, closer $ID_{\cap}$ to ID_{ref}, higher the affordance level α*

$$\boldsymbol{\alpha = \frac{ID_{ref}}{ID_{\cap}} = \frac{\int_{t_{ref}} \frac{ds}{W_{ref}(s,p)}}{\int_{t_{avg}} \frac{ds}{\widetilde{W}_{\cap}(s)}}} \tag{4.9}$$

Where $\widetilde{W}_{\cap}(s) = W_{\cap}(s) \cdot \frac{p_{\cap}(s)}{p} \cdot \frac{\eta_{\cap}(s)}{p}$ is evaluated through equation 4.5, $\eta_{\cap}(s)$ through equation 4.8, and $W_{ref}(s,p)$ is evaluated through equation 4.1. The approach is similar to Warren (Warren, 1984) who defined a metrics to measure the affordance of climbing a stair (climbability) through the ratio between features of the environment Rc (riser's

height) and features of the agent L (Leg length). Nevertheless, the methodology of Warren can be applied only for climbing activities, considers only anthropometric features of the agent, and the measure is binary: only if a stair riser is lower than the 88% of an individual's leg length, that subject is able to climb the stair. On the contrary, our approach has a general validity since it is based on the observation of movements performed, and consequently takes into account the ability of the agent (and not merely anthropometric features).

Furthermore, our affordance is not defined entirely through an absolute approach (as for Warren), but how the observed agent interacts with the environment is studied in comparison with the reference behaviour, since not all the spatial configurations reachable by the observed one is useful for the optimal execution of the repetitive motor task.

Moreover, as previously discussed, our model is not described in a binary fashion, but the affordance level (α) is defined into a range: higher the value of α, better the observed agent-environment interaction. The methodology to calculate the magnitude of α is briefly schematized in Figure 4.10.

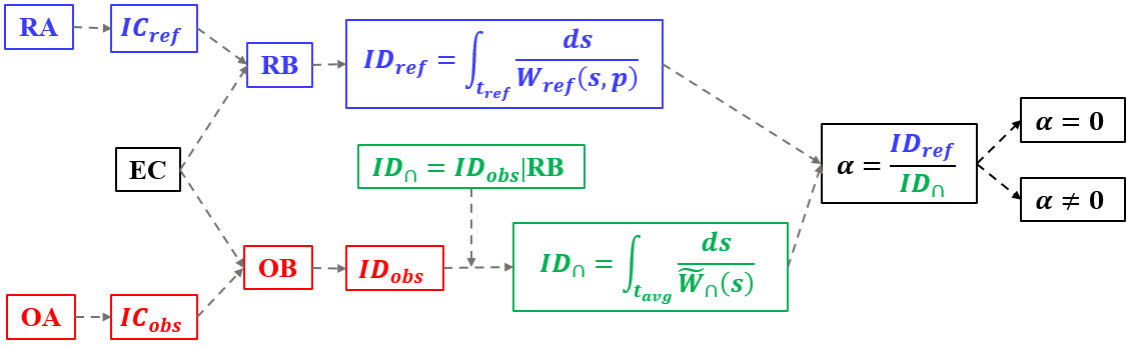

Legend
EC: External Constraints
RA: Reference Agent
OA: Observed Agent
IC_{ref}: Internal Constraints of RA
IC_{obs}: Internal Constraints of OA
RB: Reference Behaviour
OB: Observed Bhaviour
α: Affordance level $\in [0; 1]$

Figure 4.10 *Schematization for the quantification of the affordance level*

The graphical representation in Figure 4.9 has been schematized in Figure 4.10. It is important to underline that $ID_{\cap}$ is not defined directly from the OB, but a further step must be considered. If the merely observed motor behaviour is considered from the OB,

ID_{obs} is evaluated (defined in chapter 3.1). Nevertheless, ID_{obs} does not consider features related to the optimal movements that should be executed: this information is inherent in the RB. By considering the motor behaviour of the observed agent relative to the reference one, $ID_{\cap}$ is obtained.

As previously mentioned, the affordance level α has a range, defined $[0; 1]$. When there is no overlapping between RB and OB, the affordance level is close to 0. This happens practically when the average trajectory executed by the observed agent (t_{avg}) is far away from the reference trajectory t_{ref}, bringing to low values of the three variables $W_{\cap}(s)$, $p_{\cap}(s)$ and $\eta_{\cap}(s)$ at each curvilinear coordinate s. Consequently, the observed stochastic width $\widetilde{W}_{\cap}(s)$ is close to zero, $ID_{\cap} \to \infty$, and the affordance level tends to zero. On the contrary, when there is both the perfect matching between t_{avg} and t_{ref} (equal path executed), $W_{\cap}(s) = W_{ref}(s,p)$ and $p_{\cap}(s) = \eta_{\cap}(s) = p$ (equal stochastic behaviour), $\widetilde{W}_{\cap}(s) = W_{ref}(s,p) \cdot \frac{p^2}{p^2} = W_{ref}(s,p)$ at each curvilinear coordinate s. Therefore, by substituting these values in $ID_{\cap}$ of equation 4.9, the affordance level reaches the maximum value $\alpha = 1$.

In the following the model expressing the affordance level has been firstly tested through numerical simulations, and then validated through the same dataset considered for chapter 3.2.

4.2.2 Numerical Simulations

The affordance level has been tested through numerical simulations by defining firstly the behaviour of the reference agent through $W_{ref}(s,p)$, t_{ref} and $f_{ref}(s,T)$. The shape of the reference trajectory t_{ref} is shown in Figure 4.11. The extent of $W_{ref}(s,p)$ is set equal to 6 [cm] (with $p = 0.99$), and spatial configurations reachable by the reference agent are assumed to follow a Gaussian distribution (as described in chapter 4.2.1.1); both $f_{ref}(s,T)$ and $W_{ref}(s,p)$ are centred on t_{ref} and constant along s. The optimal reference agent-environment interaction is evaluated through ID_{ref} (equation 4.2).

The observed agent-environment interaction with respect to the reference agent is quantified through $ID_{\cap}$ (equation 4.3). t_{avg} and $f_{obs}(s,T)$ are defined a priori just for simulation purposes, while in other (real) cases t_{avg} is obtained from the multiple repetitive movements of the observed agent, and $f_{obs}(s,T)$ must be extracted from the

spatial configurations $q_k(s)$ (see Figure 4.3) reached by the observed agent at each curvilinear coordinate s. To test multiple scenarios, five different t_{avg} have been assumed: going from t_{avg_1} to t_{avg_5}, the difference with the reference trajectory t_{ref} increases (Figure 4.11). Therefore, the observed motor behaviour worsens from t_{avg_1} to t_{avg_5}, bringing to lower values of $W_\cap(s)$, $p_\cap(s)$ and $\eta_\cap(s)$ along the path.

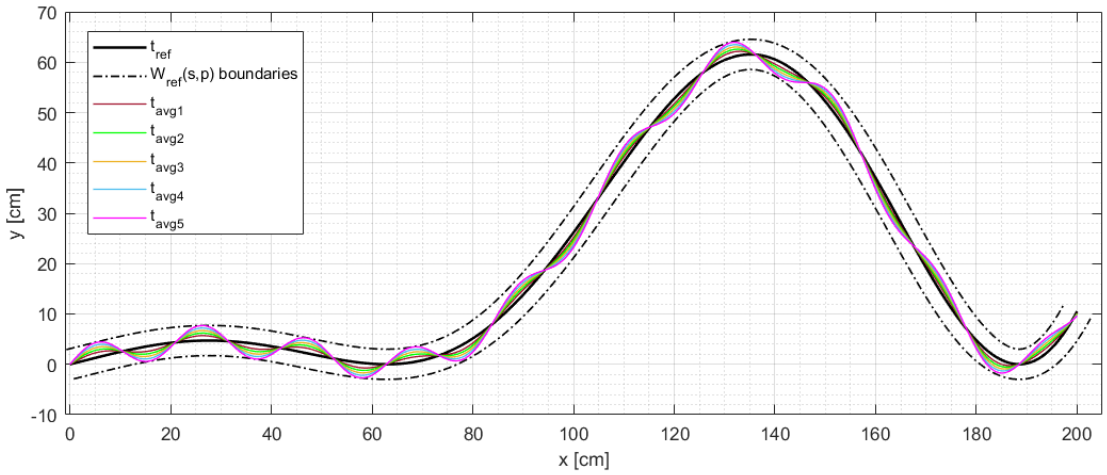

Figure 4.11 *Reference trajectory (t_{ref}), average (assumed) trajectories (t_{avg_i}), and reference stochastic width ($W_{ref}(s,p)$) employed for the numerical simulations*

Furthermore, for each of the five average trajectories, three $f_{obs}(s,T)$ have been assumed by varying the scale and shape parameters of the Weibull distribution. As done for the PDF of the reference agent, each $f_{obs}(s,T)$ is assumed to be the same along the curvilinear coordinate s, for every t_{avg}, but the position of each $f_{obs}(s,T)$, relative to the Gaussian distribution $f_{ref}(s,T)$ changes along the curvilinear coordinate s. In fact, each average trajectory t_{avg} has a variable distance from t_{ref} along s (Figure 4.11): therefore, the position of a given $f_{obs}(s,T)$, relative to $f_{ref}(s,T)$ changes accordingly. This is similar to consider the cases shown in Figures 4.7 and 4.8, but the shifting of a given $f_{obs}(s,T)$ is made along s, and not at a specific s. In Figure 4.12, it is depicted an example of the three $f_{obs}(s,T)$ employed, and the reference Gaussian distribution $f_{ref}(s,T)$.

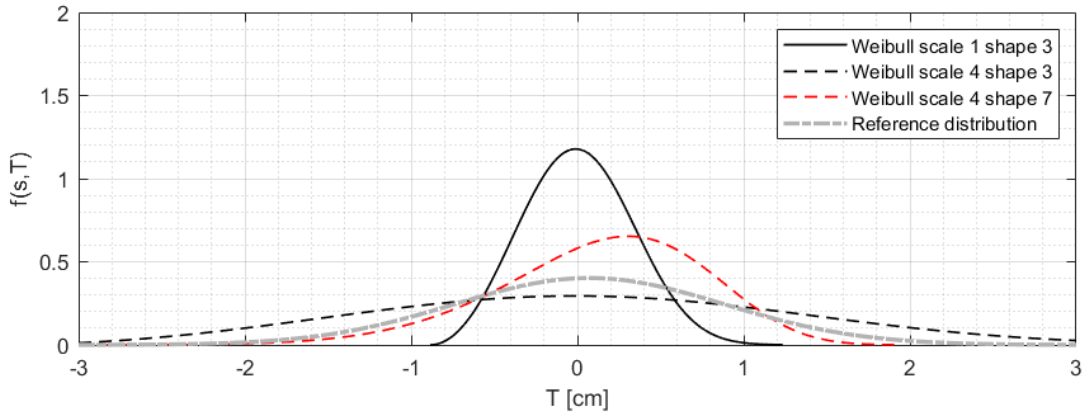

Figure 4.12 *The four $f_{obs}(s,T)$ employed for the numerical simulations. $T = 0$ coincides with the point $q_{ref}(s) \in t_{ref}$ at a given curvilinear coordinate s.*

After the quantification of ID_{ref} and $ID_{\cap}$, by considering every t_{avg}, each with a specific $f_{obs}(s,T)$, the corresponding affordance level is evaluated through equation 4.9. Results are depicted in Figure 4.13.

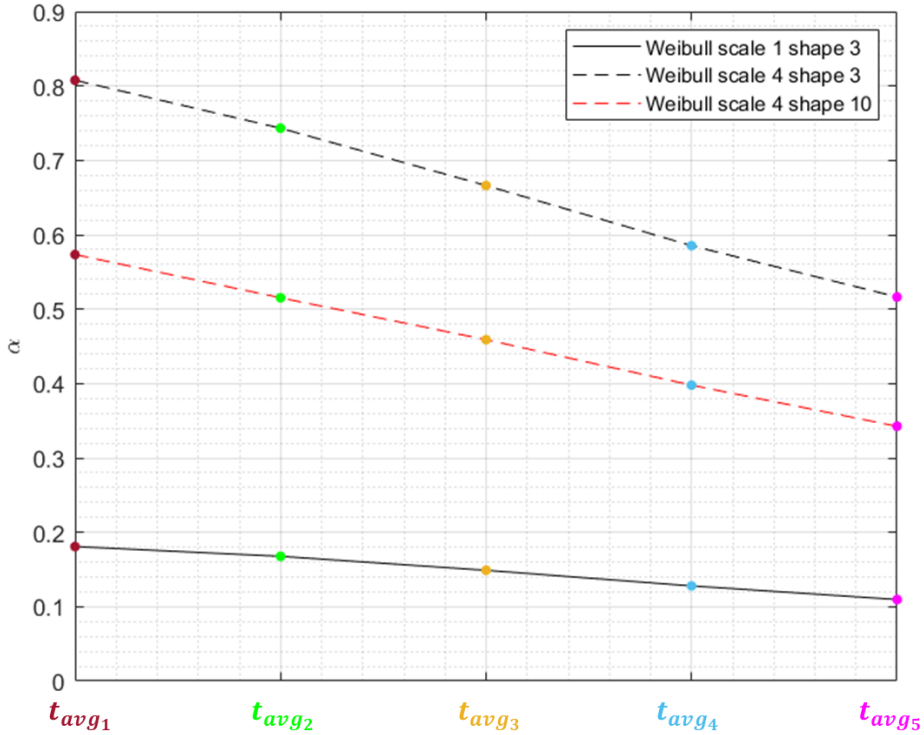

Figure 4.13 *Results of the numerical simulations. The affordance level α is quantified for each average trajectory t_{avg} and each $f_{obs}(s,T)$*

From Figure 4.13, for a given $f_{obs}(s,T)$ considered, it can be noticed that by increasing the differences between t_{ref} and the i^{th} average trajectory (from t_{avg_1} to t_{avg_5}), the affordance level α decreases. Furthermore the $f_{obs}(s,T)$ that allows to obtain the best results is the Weibull distribution with scale parameter 4 and shape parameter 3. This result can be easily explained by observing Figure 4.12: the black dashed $f_{obs}(s,T)$ is the

closest to the $f_{ref}(s,T)$ in terms of extension along T and frequency distribution; the red dashed $f_{obs}(s,T)$ presents a lower extension along T with an important skeweness, while the last $f_{obs}(s,T)$ presents a very limited extension along T.

Even with the assumptions made for the numerical simulations, it has been shown that α is able to capture differences in the motor behaviour between the two agents, and therefore quantify how close is the observed agent to the optimal agent-environment interaction. In the following, the affordance level has been tested on the walking dataset employed in chapter 3.2 to verify if the model is able to capture significant differences between agents by defining the 'Young' as the reference agent, while the 'Old' one as the observed one; features of ID_{ref} and $ID_{\cap}$ are obtained from observations of movements performed.

4.2.3 The Influence of Age

In the current paragraph, the α model is tested using the same dataset employed in chapter 3.2. The dataset regards differently healthy aged subjects executing a walking task on a treadmill at different speed conditions. The stride movement (see Figure 3.4) has been modelled as a generalized reaching motor task, where the ankle of the swing foot is considered as the subject's end-effector that during each stride of the gait cycle follows a repetitive trajectory.

In this context, the motor behaviour of each subject is obtained by averaging the second stride of each k^{th} walking trial ($k = 1, \dots, 11$). The differently healthy aged subjects have been divided into two groups: 'Young (21-37 years old, sample size = 20) and 'Old' (50-73 years old, sample size = 14). For a given speed condition, the average trajectories (t_l) of 'Young' ($l = 1, \dots, 20$) and 'Old' ($l = 1, \dots, 14$) subjects have been averaged to obtain the corresponding motor behaviour of each group (t_{avg}). The average motor behaviour of each subject and the average for each group are shown in Figure 4.14 for the 'Slow' and Figure 4.15 for 'Fast' speed condition. To test the model regarding the affordance level, it has been considered the 'Young' group has the reference agent, with the optimal agent-environment interaction, while the 'Old' group as the observed agent, with the observed-agent interaction. As described in chapter 4.2.1.1, this is the scenario where the reference agent is represented by an observed optimal behaviour ('Young' group), obtained in this context, as the average from the observation of multiple 'Young' subjects

(N=20). This assumption is consistent with results obtained in chapter 3.2, since it has been observed the older agents are characterized by a higher motor difficulty and lower flexibility.

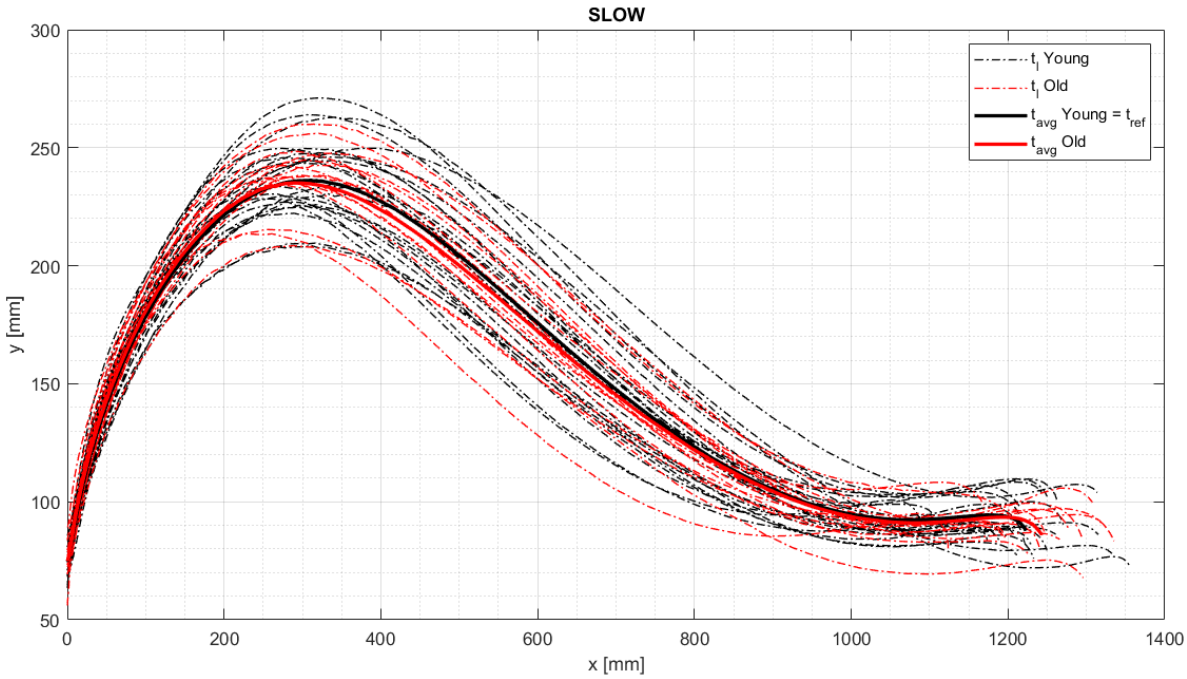

Figure 4.14 *The ankle's average trajectory of each subject (t_l) and the average (t_{avg}) for each group at slow speed condition*

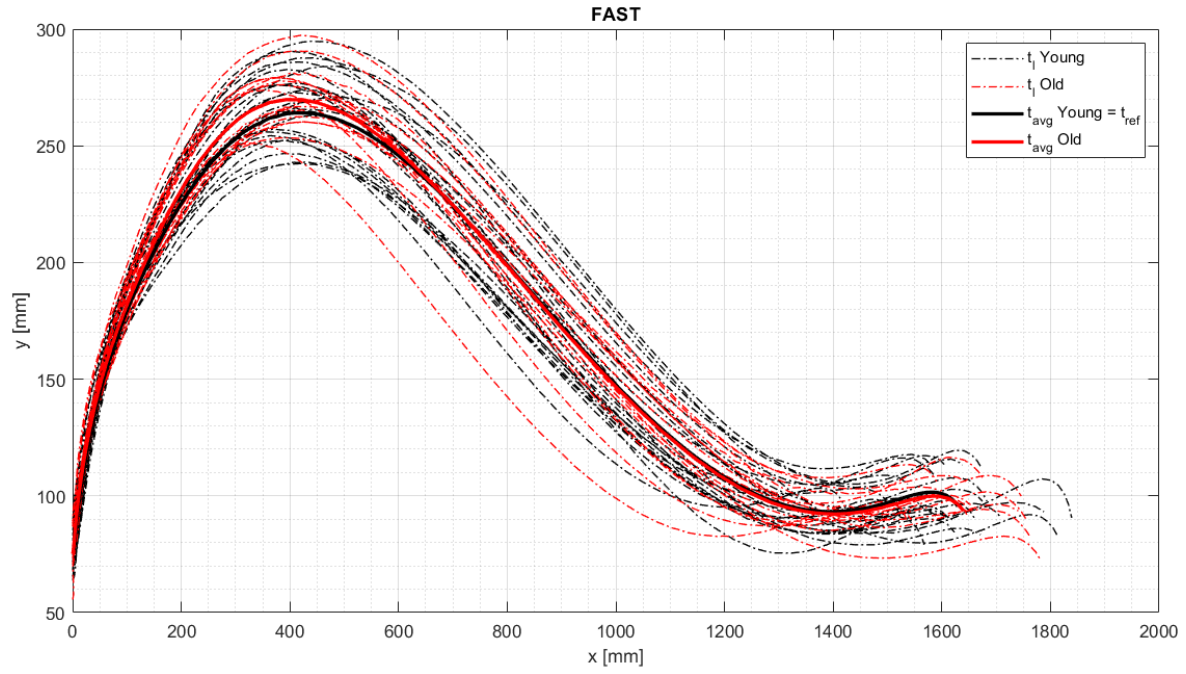

Figure 4.15 *The ankle's average trajectory of each subject (t_l) and the average (t_{avg}) for each group at fast speed condition*

Differently from the previous simulations performed, the motor behaviour of both agents (reference agent (Young) and observed agent (Old)) has been observed and not merely assumed. Therefore, at each curvilinear coordinate s, instead of assuming the stochastic behaviour of each agent, this information can be obtained from the analysis of movements performed. In particular the $f_{obs}(s,T)$ and $f_{ref}(s,T)$ can be obtained through the use of the Kernel Density Estimation (KDE) method.

4.2.3.1 Kernel Density Estimation

The Kernel Density Estimation (KDE) is a non-parametric method that allows to estimate the PDF of a random variable where the inference about the behaviour of a population is based on a finite data sample. The only assumption that must be made is that samples (x_l) must be independent. These samples belong to a distribution whose PDF (f) is unknown. The PDF can be obtained through the following equation:

$$\boldsymbol{f_h(x) = \frac{1}{N}\sum_{l=1}^{n} K_h(x - x_l)} \tag{4.10}$$

Where K_h is called 'kernel function' and h is its bandwidth. For each sample x_l, the kernel function is calculated. $f_h(x)$ is equal to the sum of all the kernel functions evaluated around data points x_l, normalized over the sample size N. Multiple kernel functions can be used (uniform, triangular, biweight, triweight, gaussian, etc…); depending on the specific kernel function employed, the resulting $f_h(x)$ changes. The expression of the gaussian kernel is the following:

$$\boldsymbol{K_h(x - x_l) = \frac{1}{h \cdot \sqrt{2\pi}} * e^{-\frac{1}{2}\left(\frac{x - x_l}{h}\right)^2}} \tag{4.11}$$

In Figure 4.16 an example of $f_h(x)$ obtained from a limited sample size ($N = 6$), by considering a gaussian kernel at each x_l.

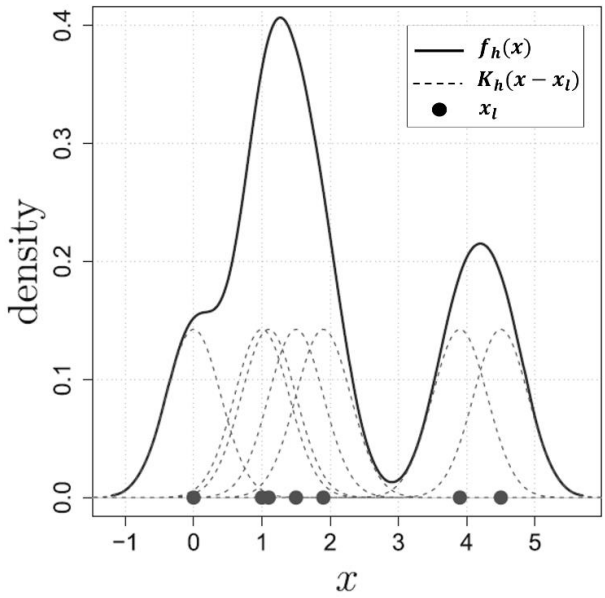

Figure 4.16 *Example of $f_h(x)$ obtained with the use of a gaussian kernel $K_h(x - x_l)$ ((Gramacki, 2018) pag. 30))*

Nevertheless, to obtain the $f_h(x)$ it must be defined the mean and the standard deviation of the gaussian kernel. The first is easily quantifiable and corresponds to the l^{th} observation x_l; the standard deviation, instead, is equal to the bandwidth h, and must be quantified.

The selection of the bandwidth influences deeply the resulting $f_h(x)$; an example is depicted in Figure 4.17. Therefore, the h must be chosen optimally in order to obtain an $f_h(x)$ as close as possible to the one that could have been obtained from the population. In literature there are multiple techniques to evaluate h, but one of the most widely used is called 'The Silverman's rule of thumb' (called also Gaussian approximation). This technique is based on the assumption that when the number of observations approaches infinite, the phenomenon can be described through a gaussian distribution. In short, through the use of this technique, the bandwidth h is evaluated by considering the sample size N, and the standard deviation evaluated over the N samples ($\hat{\sigma}$) (equation 4.12).

$$\boldsymbol{h = \left(\frac{4 \cdot \hat{\sigma}^5}{3 \cdot N}\right)^{\frac{1}{5}}} \tag{4.12}$$

More details about the KDE method are present in (Gramacki, 2018; Silverman, 2018).

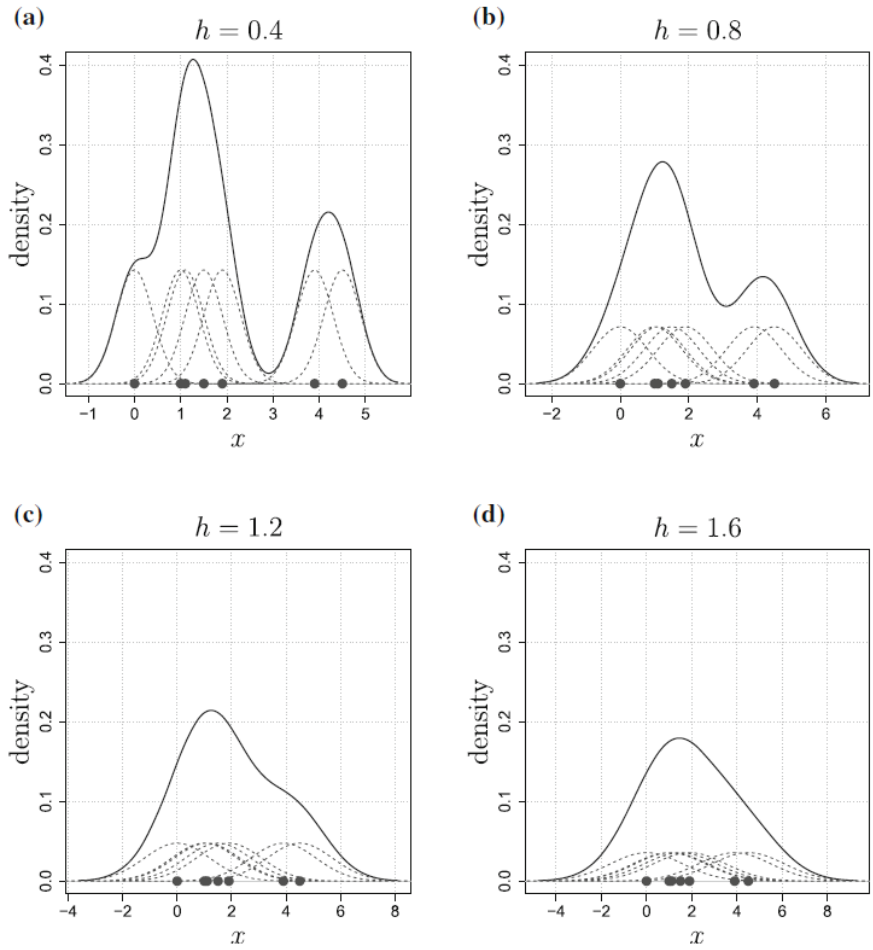

Figure 4.17 *Example of the $f_h(x)$ obtained with the use of a gaussian kernel, by varying the bandwidth h ((Gramacki, 2018), pag. 30)*

By considering the bidimensional case (bivariate kernel density estimation), equations and expressions necessary are summarized in Table 4.1. N is the sample size, while d is the number of dimensions considered (d=2, bivariate kernel density).

Table 4.1 *Equations and expressions for 2D KDE*

KDE $\boldsymbol{f_H(x) = \frac{1}{N}\sum_{l=1}^{N} K_H(x - x_l)}$	• $\boldsymbol{x = [x_1 \;\; x_2]^T}$ (2x1 matrix) • $\boldsymbol{x_l = [x_{l,1} \;\; x_{l,2}]^T}$ (2xN matrix) • $\boldsymbol{K_H(x - x_l)}$: bivariate kernel
Bandwidth $\boldsymbol{H}$	$\boldsymbol{H}$ is a symmetric and positive definite 2X2 matrix: $\begin{bmatrix} H_{11} & 0 \\ 0 & H_{22} \end{bmatrix}$
Silverman's rule of thumb	$\boldsymbol{\sqrt{H_{ii}} = \left(\frac{4}{d+2}\right)^{\frac{1}{d+4}} \cdot N^{-\frac{1}{d+4}} \cdot \hat{\sigma}_i}$

	• **d=2** for bivariate case • $\hat{\sigma}_i$ is the standard deviation of the ith variable evaluated over the sample size N
Bivariate gaussian kernel	$K_H(x - x_l) = \frac{1}{(2\pi)\sqrt{\lvert H \rvert}} * e^{-\frac{1}{2}(x-x_l)^T H^{-1}(x-x_l)}$

The 1D KDE has been applied in the walking dataset to obtain the PDF of the 'Young' group (reference agent, $f_{ref}(s,T)$), and the PDF of the 'Old' group (observed agent, $f_{obs}(s,T)$); results are in the following paragraph. The 2D KDE, instead, is considered in the ongoing research in order to extend the affordance level evaluation also in scenarios involving 3D movements: in case of 3D movements, the plane orthogonal to the reference trajectory at a given curvilinear coordinate s, intercepts the spatial configurations, whose extracted PDF is bivariate. Through this technique, rather than assuming a bivariate distribution of spatial configurations (as in Figure 3.2), the PDF is calculated on the real distribution of the spatial configurations. This topic is discussed more deeply in Chapter 5.

4.2.3.2 Results

The 1D KDE has been used in the walking dataset. This choice is reasonable and well supported since, as observed in the scientific literature, in repetitive motor tasks variability of agents' trial trajectories follow a gaussian distribution centred on their average along the entire path (Ghahramani and Wolpert, 1997; Messier and Kalaska, 1997; Van Beers, Haggard and Wolpert, 2004; Liu and Todorov, 2007; Guigon, Baraduc and Desmurget, 2008). In our case each observation (the previous x_l) is expressed by the point $q_l(s) \in t_l$, while $q_{avg}(s) \in t_{avg}$ at curvilinear coordinate s. In Figure 4.18 an example is depicted for 'Young' at slow speed condition; as previously discussed t_{avg} 'Young' is equal to t_{ref}, since it refers to the reference agent.

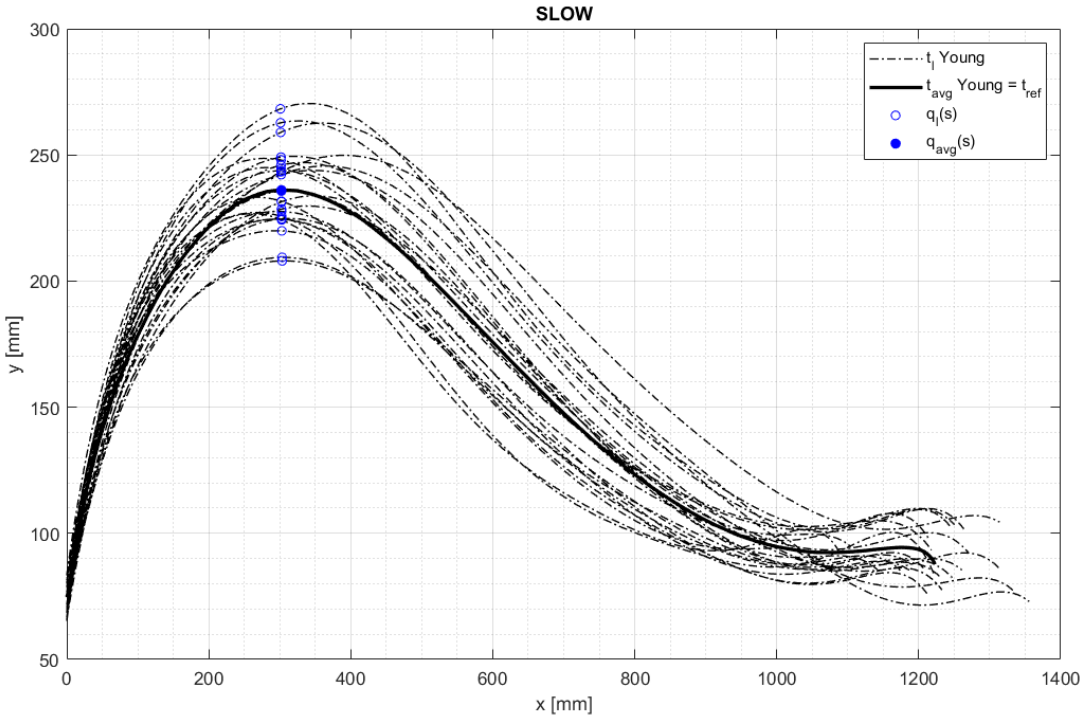

Figure 4.18 *The ankle's average trajectory of each subject (t_l) and the average (t_{avg}) for 'Young' at slow speed condition; $q_l(s)$ and $q_{avg}(s)$ are shown for a given s*

In order to not exclude cases when the $q_l(s)$ ($l = 1, \dots, 20$ for the 'Young' group, $l = 1, \dots, 14$ for the 'Old' group) are normally distributed, the Shapiro-Wilk test has been employed. As done for the evaluation of the stochastic width in chapter 3.1.1, the Shapiro-Wilk normality test (suggested for limited sample size) has been performed at each s by considering the distribution of the points $q_l(s)$ in the section orthogonal to t_{avg} (see Figure 4.18). If the Shapiro-Wilk test is not verified, the KDE is employed.

In Figure 4.19 the $f_{ref}(s, T)$ ('Young' agent) and $f_{obs}(s, T)$ ('Old' agent) at a given s at 'Slow' speed condition, have been estimated. It can be observed that $f_{obs}(s, T)$ is gaussian (Shapiro-Wilk test was verified), while $f_{ref}(s, T)$ has been obtained through the KDE method. Therefore, in this case, the stochastic behaviour of both agents is observed, and related features are obtained from the points $q_l(s)$ and $f(s, T)$.

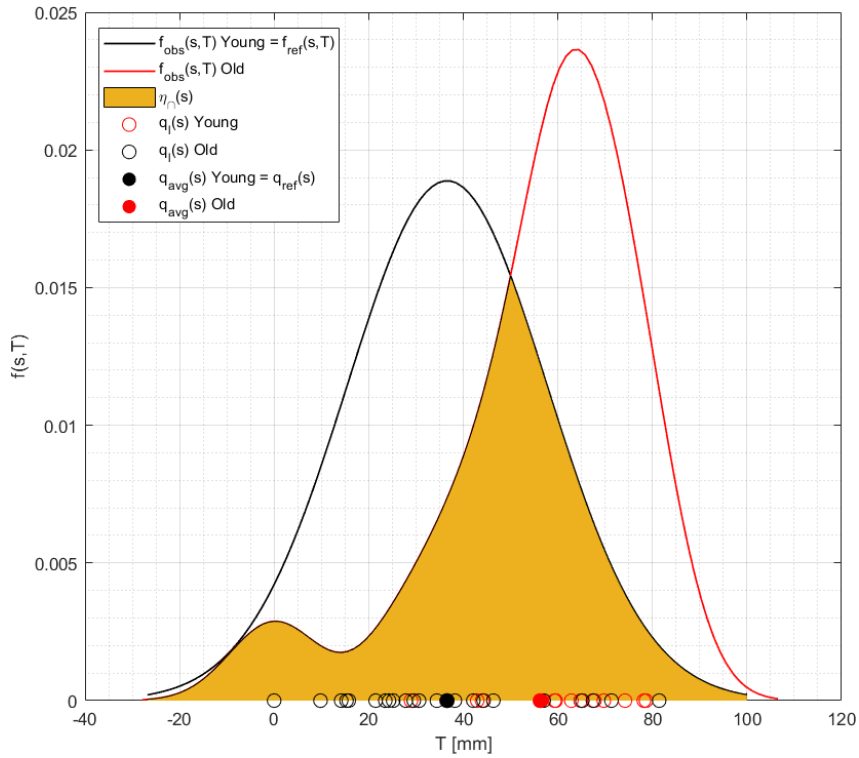

Figure 4.19 *$f_{ref}(s,T)$ ('Young' agent) and $f_{obs}(s,T)$ ('Old' agent) at a given curvilinear coordinate s and 'Slow' speed condition. Points $q_l(s)$, related average for both agents, and the entity of the overlapping index $\eta_\cap(s)$ are also depicted.*

To evaluate the affordance level α (equation 4.9), the motor difficulties of the observed ($ID_\cap$, equation 4.3) and reference (ID_{ref}, equation 4.2) agent have been quantified for both slow and fast speed conditions. In Table 4.1 results obtained.

Table 4.2 *Results of the affordance level applied to the walking dataset*

$\alpha_{slow} = \left(\frac{ID_{ref}}{ID_\cap}\right)_{slow} = \left(\frac{ID_{young}}{ID_{old}}\right)_{slow}$	0.6531
$\alpha_{fast} = \left(\frac{ID_{ref}}{ID_\cap}\right)_{fast} = \left(\frac{ID_{young}}{ID_{old}}\right)_{fast}$	0.5792

From Table 4.2 it can be noticed that in both speed conditions, the 'Old' agent-environment interaction is worse than the 'Young' agent environment interaction, and moreover, the worsening of the affordance is greater in the fast speed condition, compared to the slow one.

These preliminary results support the usefulness of the affordance level in capturing the different motor behaviours of agents, influenced in this context, by the different age of the agent.

4.2.4 The affordance level as similarity between two behaviours

In this paragraph the effectiveness of the affordance level as a tool to compare two motor behaviours is confirmed using an entropy measure that expresses the divergence between two distributions.

4.2.4.1 Entropy measures as divergence between distributions

In the scientific literature, the various entropy measures proposed in the last decades have been employed in multiple fields and for multiple purposes. One of these, called the Kullback-Leibler divergence (D_{KL}), allows to measure how a probability distribution is different from a second, the reference probability distribution. If $D_{KL} = 0$, the two distributions are equal. In Table 4.3, the expression of the Kullback-Leibler divergence is depicted.

Table 4.3 *Kullback-Leibler divergence*

$D_{KL}(P \parallel Q)$	$\sum_{z \in Z} \boldsymbol{P(z)} \cdot \mathbf{log_2} \frac{\boldsymbol{P(z)}}{\boldsymbol{Q(z)}}$	(a)
$D_{KL}(Q \parallel P)$	$\sum_{z \in Z} \boldsymbol{Q(z)} \cdot \mathbf{log_2} \frac{\boldsymbol{Q(z)}}{\boldsymbol{P(z)}}$	(b)

$z = x$ in the unidimensional case, while $z = [x, y]$ in the bidimensional case. Z is the probability space related to z.

Nevertheless, two main problems characterize this measure: the first is that D_{KL} is not upper-bounded; the second is related to the non-symmetry of D_{KL}: depending on what is defined as reference probability, the result changes; therefore, focusing on Table 4.3, (a)≠(b), i.e. $D_{KL}(P \parallel Q) \neq D_{KL}(Q \parallel P)$. These two problems are solved by considering another entropy measure, called the Jensen-Shannon divergence (JSD). JSD is upper-bounded, symmetric and is based on D_{KL}. The JSD is expressed in equation 4.13.

$$\boldsymbol{JSD(P \parallel Q) = \frac{1}{2}\left(D_{KL}(P \parallel M)\right) + \frac{1}{2}\left(D_{KL}(Q \parallel M)\right)} \quad (4.13)$$

Being symmetric $JSD(P \parallel Q) = JSD(Q \parallel P)$, while $M = \frac{(P+Q)}{2}$. Being $JSD \in [0; \log_b 2]$, by considering b=2, JSD is expressed in bit unit, $\in [0; 1]$.

4.2.4.2 *Affordance level vs. JSD*

Let's consider the affordance level at a given curvilinear coordinate s^*. Equation 4.9 becomes:

$$\boldsymbol{\alpha(s^*) = \frac{W_{\cap}(s^*)}{W_{ref}(s^*)} \cdot \frac{p_{\cap}(s^*)}{p} \cdot \frac{\eta_{\cap}(s^*)}{p}} \tag{4.14}$$

$p_{\cap}(s^*)$ is evaluated through equation 4.5, while $\eta_{\cap}(s^*)$ evaluated through equation 4.8. As JSD, $\alpha(s^*) \in [0; 1]$: when $\alpha(s^*) = 1$, there is the perfect matching between the reference and observed behaviour, corresponding to the case of $JSD = 0$ $[bit]$, i.e. the two distributions are identical. On the contrary when $JSD = 1$ $[bit]$, i.e. $\alpha(s^*) = 0$, there is the maximum divergence between the two behaviours. While $\alpha(s^*)$ expresses the similarity, JSD expresses the dissimilarity. These trends have been confirmed through numerical simulations both in univariate and bivariate cases. In Figure 4.20 is considered the univariate case with the gaussian distribution as the reference, the Weibull distribution (scale parameter 4 and shape parameter 7) shifted along T at curvilinear coordinate s^* as observed distribution.

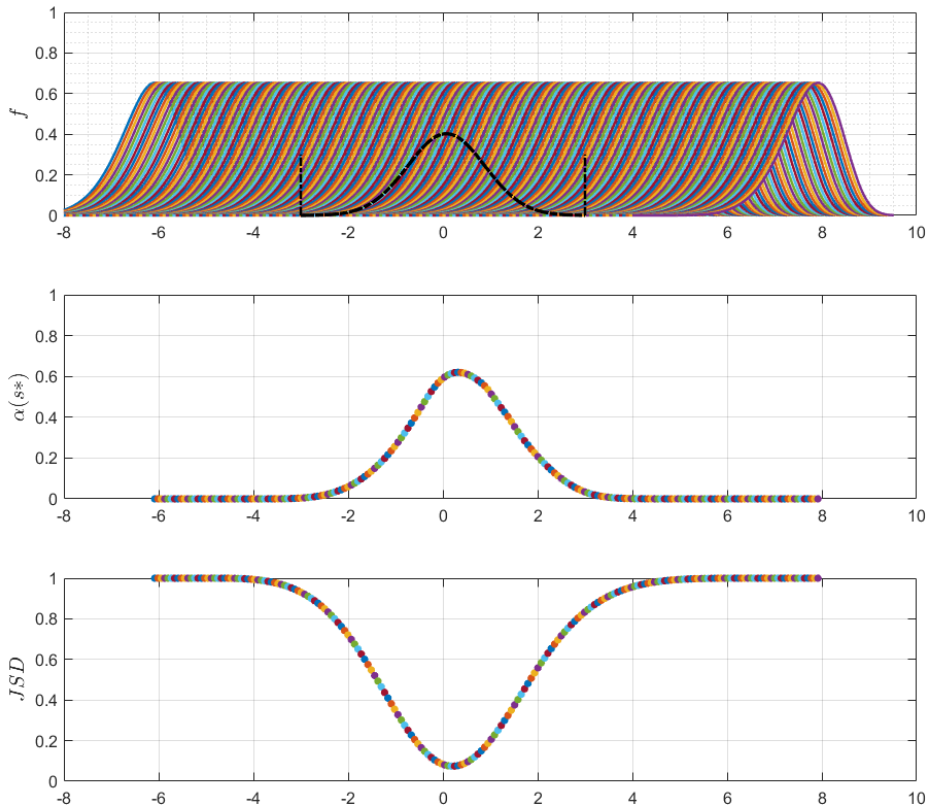

Figure 4.20 *Numerical results of $\alpha(s^*)$ vs. JSD in the univariate case, by considering Weibull distribution (scale parameter 4 and shape parameter 7) as the observed one, gaussian distribution as the reference one.*

From Figure 4.20 it can be observed that the two trends of $\alpha(s^*)$ and JSD are opposite: the maximum of $\alpha(s^*)$ corresponds to the minimum of JSD.

Same trends can be observed in the bivariate case. In this scenario, a randomized number of points have been generated in the (x,y) plane, representative of the plane intercepted at the curvilinear coordinate s^*, orthogonal to a given reference trajectory (equivalent to $P(s)$ in Figure 3.2). These points (green in Figure 4.21) represent the behaviour of the reference agent, i.e., the spatial configurations achieved at a given curvilinear coordinate s^*. For sakes of simplicity, and only for simulation purposes, the behaviour of the observed agent is expressed by the same points, translated and rotated in order to obtain a different behaviour (red in Figure 4.21). By applying the 2D KDE (Table 4.1), the PDFs of the two agents are obtained (Figure 4.22).

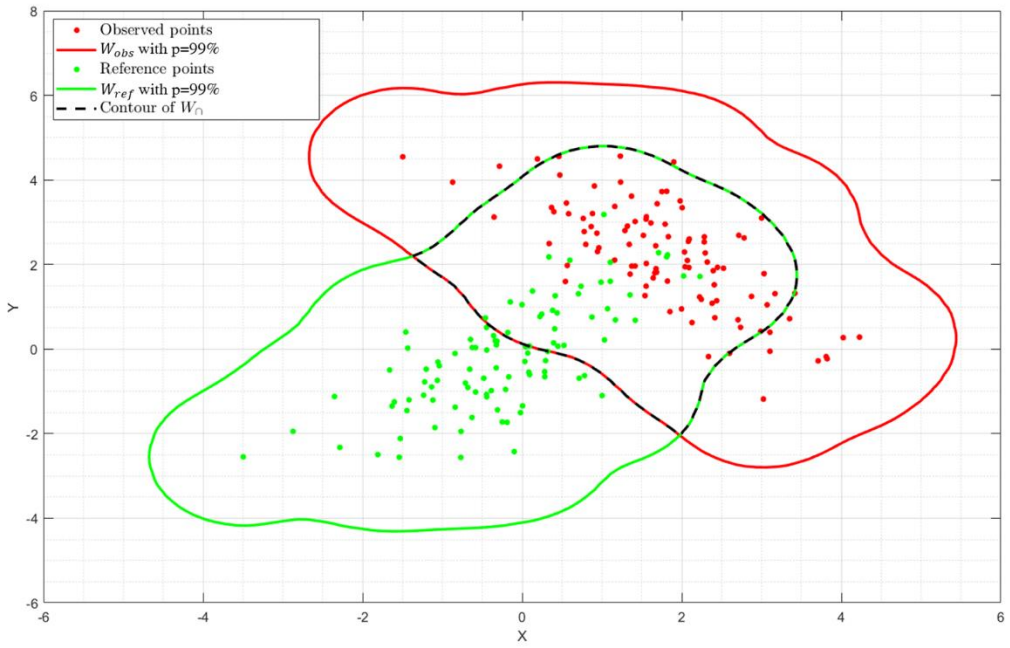

Figure 4.21 *Example of spatial configurations achieved by the reference and observed agent*

In this case W_{ref} ($W_{ref}(s^*, p)$) refers to the area that includes the 99% of the spatial configurations of the reference agent; W_{obs} instead ($W_{obs}(s^*, p)$) refers to the area that includes the 99% of the spatial configurations of the observed agent. The intersection between W_{ref} and W_{obs} gives rise to $W_\cap$.

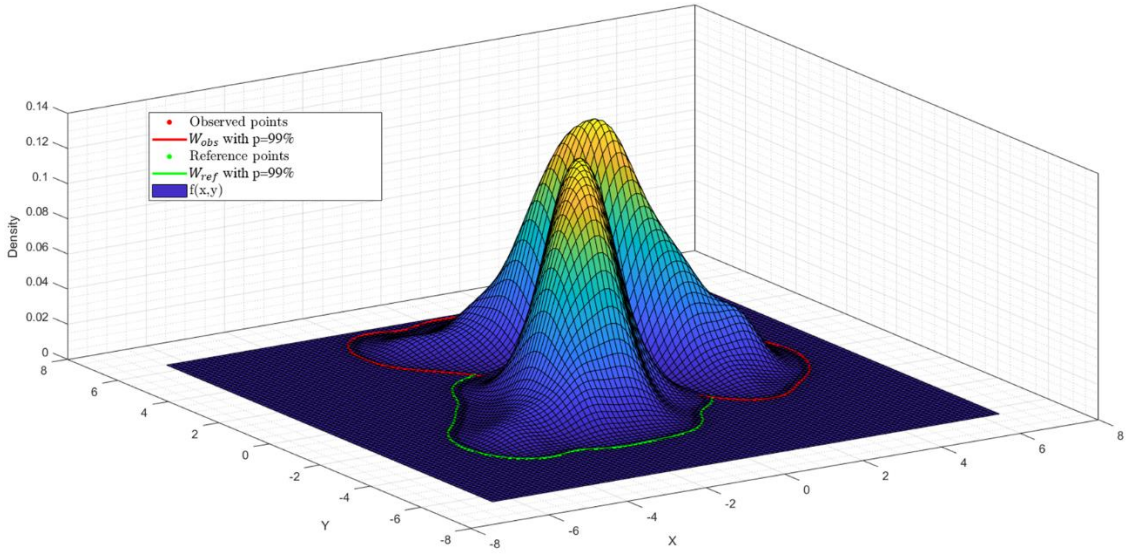

Figure 4.22 *PDFs obtained by applying 2D KDE on the spatial configurations (points in Figure 4.21) of the reference and observed agent*

In order to confirm the opposite trends of $\alpha(s^*)$ and JSD, multiple simulations have been performed by translating points referring to the observed agent in the (x,y) plane. Results are in Figure 4.23. By increasing the distance between the reference-observed behaviours, the dissimilarity between the two distributions increases: the JSD values increase and tend to one (maximum divergence), while the $\alpha(s^*)$ values decrease and tend to zero.

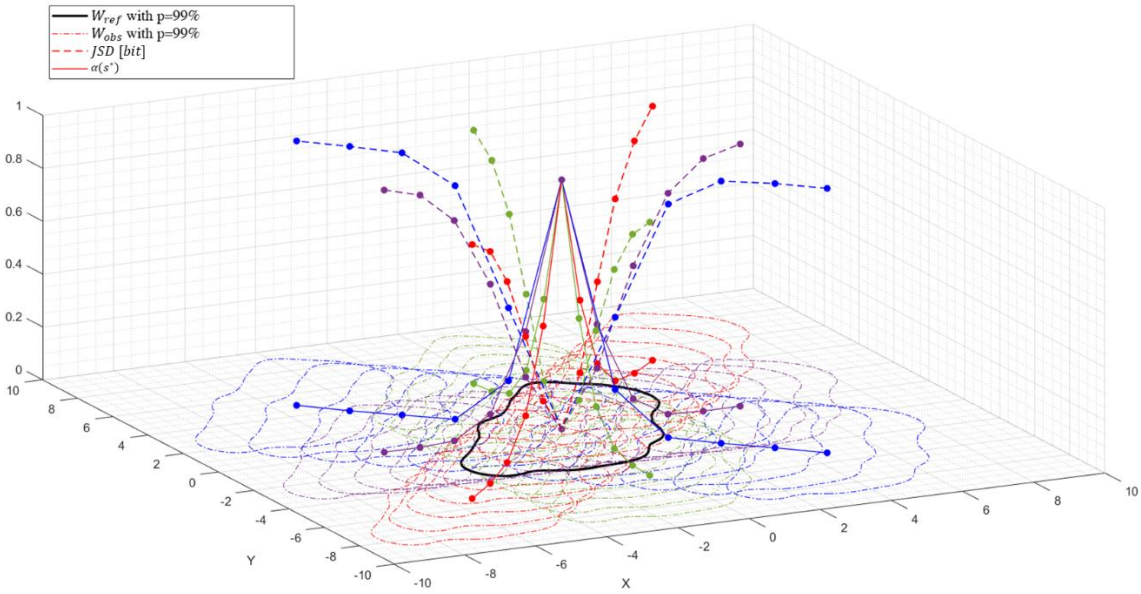

Figure 4.23 *Numerical results of $\alpha(s^*)$ vs. JSD in the bivariate case*

The opposite relation between $\alpha(s^*)$ and JSD confirms that the affordance level, as theorized and formalized in the present work through W, $p_{\cap}$ and $\eta_{\cap}$, expresses the similarity between two motor behaviours.

4.2.5 Discussion

In the present chapter, a novel metrics to quantify the affordance has been proposed. Originally, the concept of affordance descried how agents interact with the environment. Depending on the perspective, the affordance can be directly perceived (Gibson, 1979b), a mental processing may be needed (chapter 4.1.1), or the elaboration of the information acquired by the sensorimotor system must be executed (chapter 4.1.2) in order to evaluate what are the actions that can be executed in interacting with the environment. The affordance expresses the agent-environment interaction: it must consider both the agent capabilities and features of the surroundings. Anthropometric features (as in (Warren, 1984)) are not enough to describe the agent, but its abilities (internal constraints) must be considered; moreover both geometrical and non-geometrical features of the environment (external constraints) must be considered to characterize the surroundings.

A common aspect related to the various perspectives is that the interaction of the agent with the environment is characterized by movements executed through a specific end-effector (e.g., fingers, hand, foot…); in Norman's (Norman, 1988) movements are performed to grasp/manipulate products, while in robotics they refer also to locomotion and exploration. Therefore, the motor behaviour represents the result of the agent-environment interaction, taking into account the average path executed, as well as the stochasticity of movements performed: these features are inherent in the stochastic Index of Difficulty (stochastic ID). Nevertheless, not all the movements expressing the result of the agent-environment interaction are necessary or useful for the execution of the repetitive motor task; therefore, the affordance level has been defined as the ratio between two stochastic IDs: the first related to the optimal agent-environment interaction (reference agent), while the second related to the observed interaction (observed agent). In this way the affordance level can be employed as a useful tool to predict how good is a motor behaviour compared to an optimal one. Moreover, the proposed quantitative metrics is defined in a range (dropping the original binary approach), considers the motor behaviours (including stochasticity of movements), and can be applied in any context involving the repetitive movements of an agent's end effector.

Preliminary results obtained by considering numerical simulations and applying the affordance level to the walking dataset, confirmed that:

1) The affordance level is sensitive to the different motor behaviours, i.e., average path and stochasticity of movements
2) The three variables $W_{\cap}(s)$, $p_{\cap}(s)$ and $\eta_{\cap}(s)$ are mutually independent and necessary to describe the observed stochastic width $\widetilde{W}_{\cap}(s)$
3) The affordance level is capable of quantifying how close is the observed agent-environment interaction to an optimal one
4) The affordance level is sensitive to the different internal constraints of agents (different age in this context)

Furthermore, in paragraph 4.2.4, the reasonings made for the definition of the affordance level (parameters that express $\widetilde{W}_{\cap}(s)$) have been confirmed to represent the difference between two motor behaviours, by comparing the affordance level (at a given curvilinear coordinate s^*) to the Jensen-Shannon divergence (JSD). Results confirmed that both in the univariate and bivariate case, the affordance level is capable of quantifying how close is the observed agent-environment interaction to an optimal one, i.e., how much is the dissimilarity between two motor behaviours, that can be expressed as the divergence between two distributions.

Nevertheless, the proposed quantitative metrics in evaluating the affordance level must be strengthened and improved in order to extend its use in multiple areas. The very next studies will be firstly focused on extending the proposed methodology described in chapter 4.2.1 in case of repetitive motor tasks involving 3D movements; therefore, all the reasonings involving the stochastic widths (reference and observed) must be extended, and motor variability will be two-dimensional, as seen in chapter 3.1.2. Therefore, next phases will be devoted to sharpening the proposed methodology in order to be available and easily implemented in both industrial and laboratory environments (controlled environment). The multiple applications of the proposed quantitative metrics, as well as the utility of the previous models showed in the present dissertation will be described in the next chapter.

5. Applications

In the present dissertation, new motor performance models able to evaluate the capacity of an agent in performing repetitive motor tasks have been discussed. Results show the power in considering the Fitts' law's Index of Difficulty (ID) as a tool to evaluate the motor performance of an agent in executing repetitive motor tasks involving the use of smart devices (i.e., tablet and interactive pen), or just observing movements of the agent's end effector (i.e, feet or hand). Nevertheless, the application of the proposed models is not limited to scenarios considered, and their feasibility is of general validity. In the following, applications for each proposed model are discussed.

5.1 The 'Speed-ID-Accuracy' model

In the first scenario, the continuous formulation of the Fitts' ID has been employed to improve the so called 'Speed-Accuracy' trade-off model: higher the velocity in reaching a target displaced at distance 'A' from a starting point, higher the uncertainty of placement at the target. Our 'Speed-ID-Accuracy' model improves the prediction in quantifying the SD of positions reached at the target when movements to execute are constrained along the entire path, with both nominal trajectory and spatial constraints defined a priori. These geometrical features, summarized in the continuous formulation of the Fitts' ID (ID_t), affect the accuracy in target reaching, confirming that the ID_t, representing the geometrical task difficulty, can be employed as a valuable tool to enhance the prediction in quantifying spatial information, such as the SD in acquiring a given target. Through the 'Speed-ID-Accuracy' model, the accuracy of agents in reaching a given target is considered as dependent not only on the average speed of execution, but also on the task difficulty calculated through the assigned geometry of the task. By extending the 'Speed-Accuracy' model to the 'Speed-ID-Accuracy' model, the range and variety of applications increase. In specific contexts, a proper model can be usefully defined to assess whether the accuracy required in accomplishing a reaching motor task of a given geometrical complexity (ID_t), can be ensured with a given speed of execution, and a given time window. As an example, in manual assembly activities, the reaching areas can be designed by defining the completion time and task geometrical features in order to predict the movements' accuracy of the agent. In the medical field, such as dentistry or surgery, the accuracy of movements at the endpoint (e.g., on the patient) is

of critical importance. The surgeon must execute specific movements in order to successfully execute the surgical on dental operation. By defining the allowable range of motion such as nominal trajectory and path tolerance (through ID_t), and the average speed of movement, it can be predicted the accuracy in placing the specific tool on the patient's teeth or other body parts.

Despite the novel applications of the geometrical ID, the proposed model does not consider the ergonomics of movements performed, and the motor behaviour of agents in performing repetitive motor tasks. The application of the ID_t, is focused only on the performance required by the task, in terms of accuracy and time of execution, without worrying about how movements are performed. Therefore, the ID_t has been extended to consider the motor behaviour of agents through the stochastic Index of Difficulty.

5.2 The stochastic Index of Difficulty

In order to consider the motor behaviour while performing repetitive motor tasks, the ID_t has been re-evaluated in order to express the motor difficulty of agents, not the task difficulty associated to geometrical task features. When observing the merely execution of a repetitive motor task (e.g., walking task, manipulation task), without any reference behaviour, the motor difficulty experienced by an agent can be evaluated through ID_{obs}. The utility of ID_{obs} are multiple, and related applications are discussed in the following. One of the main concepts regarding ID_{obs}, is that flexibility of movements enables agents to perform the same repetitive motor task with multiple motor alternatives, resulting in a lower motor difficulty.

Let's consider an agent that must interact with the environment by walking repeatedly firstly on an even surface, fully walkable and free of obstacles, and secondly on a surface characterized by slippery zones (no walkable zones), and obstacles. In the first scenario, the agent can interact with the environment by walking, freely changing the frequency, length and speed of the stride; the agent can exploit alternative motor solutions, resulting in a higher flexibility of movements and a lower motor difficulty. On the contrary, in the second scenario, the agent is not allowed to freely choose where to place the feet, due to features of the environment; therefore, the agent is more constrained in movements to execute, being unable to exploit the motor redundancy, resulting in a higher motor difficulty. Let's consider instead the scenario where two different agents execute repetitive motor tasks in highly dynamic environments: in this case, agents must be ready to adapt their motor choices in case of unpredictable events like the presence of sudden obstacles. An agent that in non-perturbed conditions is capable of choosing between a greater number of motor alternatives, will be able to react better to unpredictable events since he/she can reach spatial configurations that another agent, characterized by a lower motor flexibility, may not be able to reach. The different extent of motor flexibility expressed by the motor variability, is inherent in the stochastic Index of Difficulty ID_{obs}. ID_{obs} can be also employed in the rehabilitation field in case of agents affected by motor disfunctions, motor diseases, or chronic pain, characterized by a limited flexibility or limited range of motion in executing everyday motor activities. The stochastic Index of Difficulty can be a valuable tool to monitor motor flexibility improvements during rehabilitation program: a higher motor variability of movements performed, brings to

lowering the stochastic ID. Furthermore, it has been observed that when agents are able to employ multiple motor alternatives to execute a given movement (higher motor flexibility), the presence of a greater motor variability brings agents to be less susceptible to musculoskeletal disorders (Kilbom, 1994; Madeleine, Mathiassen and Arendt-Nielsen, 2008)

The stochastic ID is the result of the agent-environment interaction, and therefore is affected by both internal (agent features) and external constraints (environmental features). The agent-environment interaction pertains to the concept of affordance, allowing to employ the stochastic ID as a tool to quantify the quality of an observed agent-environment interaction relative to an optimal one, i.e., the affordance level.

5.3 The affordance level

While the geometrical ID (ID_t) considers only pre-defined task features to assess the motor performance (i.e., accuracy in the target reaching), the stochastic Index of Difficulty (ID_{obs}) considers only the observed behaviour of an agent for the evaluation of the motor performance (i.e., higher flexibility, lower motor difficulty). While the first focused only on pre-defined features of the task, the second focused only on observed features of the agent. Both features, instead, are considered in the affordance level: the optimal execution of a repetitive motor task is associated to the 'reference' agent and evaluated through ID_{ref}, while the observed motor behaviour is associated to the 'observed' agent and evaluated through $ID_{\cap}$. Higher the difference between the two motor behaviours, lower the affordance level. In this context, the motor performance does not consider only the successfully achieving of the task goal, but also how movements are performed. The optimal execution of the repetitive motor task (i.e., reference agent's motor behaviour) considers both the efficiency in satisfying the task goal, and the efficiency of the motor behaviour, intended as ergonomic and allowable movements.

Under the ergonomic perspective, repetitive motor tasks are considered correctly executed if motor variability is allowed; despite it may affect negatively the task goal efficiency and error rate (Domkin *et al.*, 2005), is beneficial from an ergonomic point of view since it allows muscle tissues to recover faster from preceding exposures (Bongers, Kremer and Laak, 2002). In particular, focusing on a repetitive physical activity involving the repetitive motion of the trunk, the postural variability as well as the performance variability (i.e., task goal inefficiency) tend to decay with time (Cohen and Sternad, 2009); this phenomenon is not beneficial from an ergonomic point of view, since a postural variability reduction can bring to a greater physiological fatigue of muscle tissues, increasing the exposure of WMSD over time (Mathiassen, 2006). On the contrary, a more flexible motor strategy expressed by an increase of the postural variability, tends to delay the back muscle fatigue during lifting (Côté *et al.*, 2008; Fuller, Fung and Côté, 2011). More in general, repetitive motor tasks are observed during MMH (Manual Material Handling): these physical activities involve not only the lifting, but the general manipulation of materials. MMH can be performed in industrial environments/factories as well as outdoor, such as in the case of door-to-door waste collection system or construction work. Through a door-to-door system, all domestic fractions are collected

from the street by an operator whose activities require the lifting/lowering, pushing/pulling of bins, boxes and bags. The operator is subjected to physical fatigue and may perform repetitive movements inappropriately, bringing to physical diseases and WMSD over the time. Same physical features are characterized in construction work, where operators are subjected to frequent and repetitive exposures to lifting, bending, handling, and prolonged static postures (Wang *et al.*, 2017).

In all the mentioned scenarios, the affordance level can be employed as a synthetic measure/index that evaluates if movements of the observed operator are performed correctly. Surely to quantify the affordance level, the optimal motor behaviour of the reference operator must be defined: it can be delineated by providing to an operator instructions or practical examples on how movements should be properly carried out. After that ergonomic experts confirm that movements performed have been correctly executed, the related recorded motion data can be employed as reference for the following motor behaviours.

The affordance level model can be applied also in repetitive motor tasks that require a motor training. An example is related to the use of wearable devices such as exoskeletons; despite their use is becoming more and more effective, train operators to use exoskeletons is challenging due to the multiple designs of these wearable tools; furthermore, the employment of exoskeletons can be also harmful when its use is not compliant with its design, i.e. outside the safety ranges of torques and motions. Therefore, there is the necessity to properly train the motor skills of operators with easiness, while guaranteeing safety conditions. To facilitate and accelerate the motor skill training of operators, some authors proposed to employ VR and haptic feedback devices to support the training phase in the use of exoskeletons (Bhatti *et al.*, 2009); in particular Ye et al. (Ye *et al.*, 2022) employed this technology to transfer the motor behaviour of an experienced exoskeleton user to a novice one: the visual information given by VR is augmented through the use of haptic feedback devices that provide the novice user the sensory information experienced by an expert exoskeleton user. The combination between VR and haptic system allows a low time and resource consuming training, since it can be employed not only on-site, but in multiple environments, such as laboratories. The exoskeleton is not needed for the initial training of the novice user, but only the real experience of the expert user, transferred through the training system, is required.

The same technology (VR + haptic device) has been employed for industrial manipulation

tasks (Gopher, 2012), where the feedback related to the object contact in VR is given by a force trigger of the haptic device (Hayward *et al.*, 2004).

In both examples where VR + haptic device technology has been employed, improvements related to the motor training of operators can be easily monitored through the affordance level. In this case the refence agent can refer to an operator considered as an expert user (e.g., in the use of exoskeleton) or experienced operator (e.g., in case of manipulation task). As in the previous case, the motion data of the reference motor behaviour must be recorded and collected for future use.

The affordance level can be further employed to monitor the motor training of an agent whose experience must be transferred to another type of agent (e.g., from human to robot operator). In this case one of the easiest implementable techniques for the motor training is the kinesthetic teaching. When the experience of an operator must be transferred to a robot (e.g., robotic arm for the pick and place), the kinesthetic teaching allows to program robots for repetitive industrial tasks, simply by demonstration of the operator, requiring a small amount of time in terms of iterations and robot programming (Dimeas *et al.*, 2019). The robot learns movements to be performed just through the motor guidance of the operator. In this case the affordance level can be employed to detect the motor behaviour differences between the operator's movements (i.e., reference agent) and the robot's movements (i.e., observed agent), and monitor its motion changing during the training process.

A further application of the affordance level is related to the design of the workplace configuration for manual assembly tasks. In case of motor activities that are performed repeatedly and involve the grasping, moving, aligning, attaching of two or more parts together, the distance of components to manipulate, their number and position in the workplace, contribute to the complexity of movements to be performed. All these features describe the environment where the operator must work, and therefore are related to the 'external' features. Reaching targets, as well as positions of the components to manipulate can be designed in order to maximize the motor performance of an operator in terms of task goal achievement. By selecting the workplace design that allows to obtain the maximum task efficiency, movements of the corresponding operator can be employed as a reference. By evaluating the affordance level of various operators (relative to the reference one), a proper operator can be chosen. Therefore, the affordance level can be employed as a metric to solve resource allocation problems.

The current research is focused on the evaluation of the affordance level in case of manual sorting activities; this research is aimed at studying how the different affordance levels, obtained by comparing movements performed by the optimal (reference) operator with an observed operator, have a different impact on the performance of sorting, on the errors of commission/omission made, on the time needed to sort a certain amount of fraction in a given time window, or if the affordance level is influenced by the operator fatigue phenomenon. A brief discussion on the formalization of this topic is made in the following.

5.3.1 Manual sorting

The ongoing research is focused on the evaluation of the affordance level in case of manual sorting executed by an operator on a conveyor belt. The manual sorting is a common repetitive motor task executed in current industrial environments; the sorting can be executed for a given waste fraction, or just to exclude items that are considered scraps (e.g., rotten fruit, defective component etc…). The affordance level can be employed to evaluate the dissimilarity between an optimal operator-environment interaction, i.e., reference operator that has a perfect sorting performance (i.e., no omission/commission errors), and the observed operator-environment interaction. Let's focus on Figure 5.1

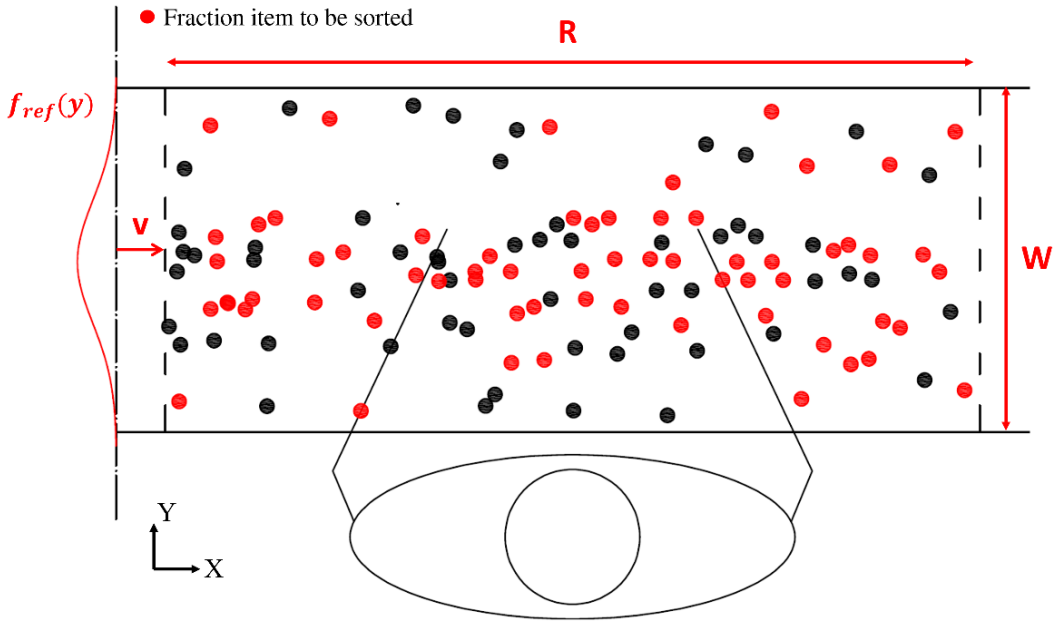

Figure 5.1 *Example of a workstation for manual sorting*

R expresses the extension of the reachable zone along x, while W expresses the extension of the reachable zone along y (i.e., the width of the conveyor belt). In this case it is assumed that the reachable zone of the operator has dimension R*W. v is the velocity (constant) of the conveyor belt. Let's assume that the PDF along y ($f_{ref}(y)$) of the fraction to be sorted is gaussian, with a greater amount of the fraction to be sorted on the centre of the conveyor belt (centre line of W). Along x, and for a given y, the PDF is constant, i.e., does not change with time. It can be easily considered that the perfect operator-environment interaction is obtained when an agent sorts all the quantity related to a specific fraction in the reachable zone; this quantity can be easily evaluated through (Q*R)/v, where Q is amount of fraction to be sorted in given time window, information provided for the specific application. In order to obtain the optimal performance, the positions reached by the operator on the conveyor belt to pick up and sort the fraction, should be as close as possible to the PDF of the fraction to be sorted ($f_{ref}(x(y), y)$). Therefore, greater the dissimilarity between the PDF of the points reached by the operator on the conveyor belt, and the predefined PDF of the fraction to be sorted, lower the affordance level (greater the Jensen-Shannon divergence). To test this hypothesis, three scenarios are considered.

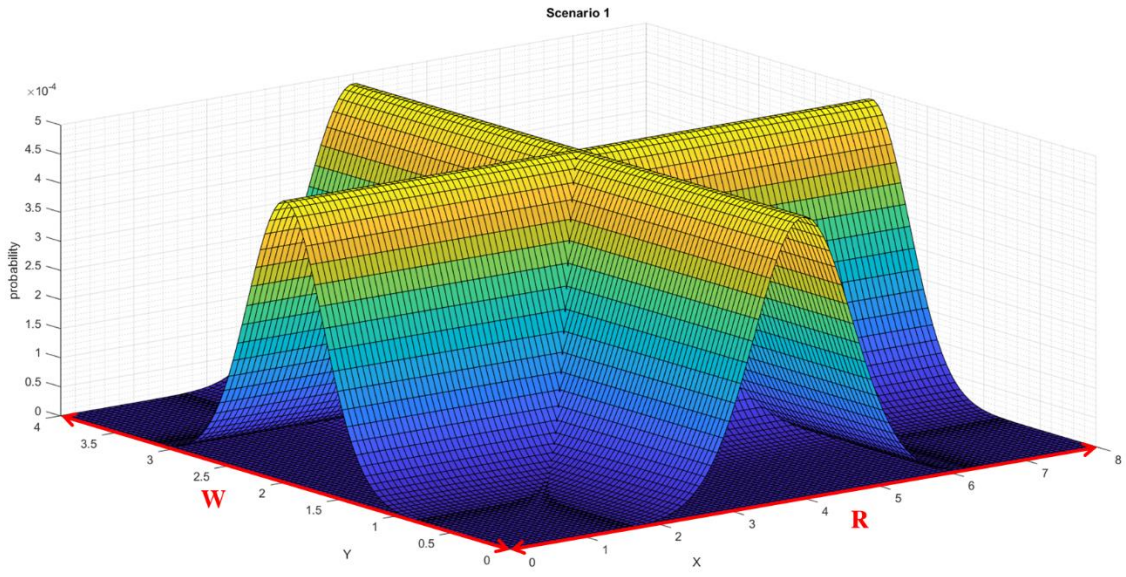

5.2a

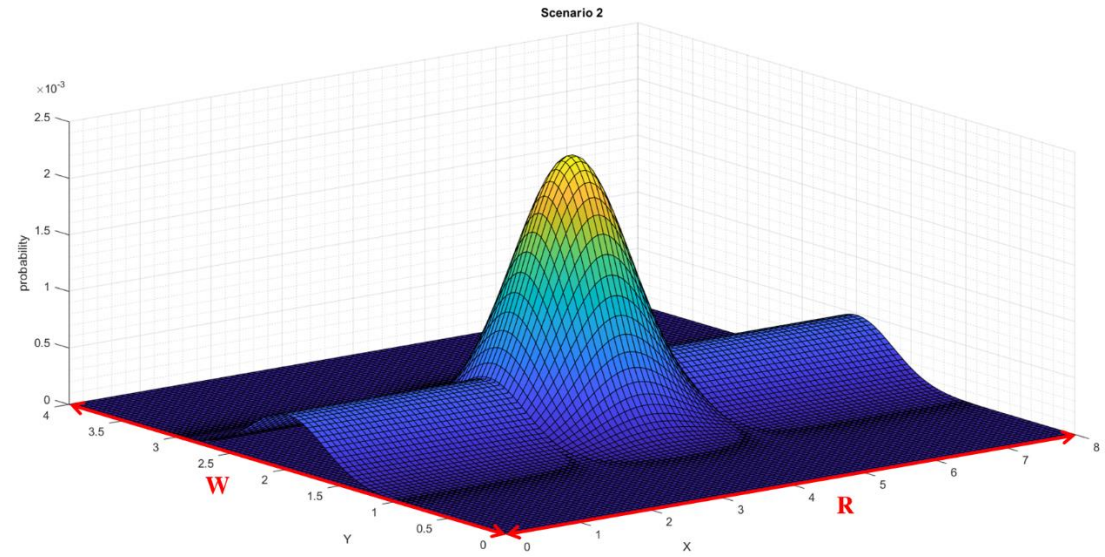

5.2b

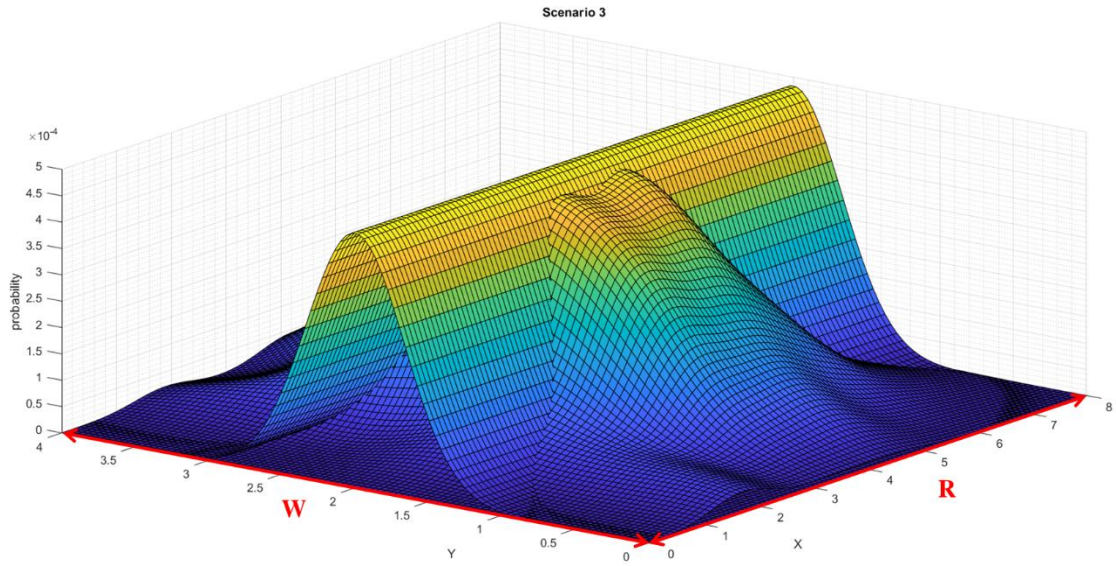

5.2c

Figure 5.2 *The three scenarios considered for the manual sorting example; R has length 8 [dm](along x), while W has width 4 [dm] (along y).* f_{ref} *is gaussian along x, and constant along x (for a given y)*

By focusing on the three scenarios, some comments can be made. In scenario 1, it is assumed that the PDF obtained from observed movements has the maximum frequency along y, for x=4, with a gaussian behaviour; in scenario 2, it is assumed that the PDF obtained from observed movements has a bivariate gaussian distribution, with maximum frequency in (4,4); in scenario 3, instead, the PDF is almost bivariate gaussian, more smoothed that the previous case. It can be easily concluded by comparing the f_{ref} and the assumed f_{obs} that the major dissimilarity is observed in scenario 1, while scenario 3 is the best one among the others. These observations are supported by results obtained in

applying equations 4.13 (JSD) and 4.14 ($\alpha(s^*)$) (Table 5.1); in this case s^* identifies the conveyor's belt reachable zone.

Table 5.1 *Results in evaluating the Affordance level and JSD for the three scenarios of the manual sorting*

	Scenario 1	**Scenario 2**	**Scenario 3**
$\boldsymbol{\alpha(s^*)}$	0.2635	0.3689	0.4905
JSD	0.6350	0.4167	0.2047

By considering multiple operators in series on the conveyor belt (one operator for each workstation), picking movements executed by the first operator, will change the $f_{ref}(x(y), y)$, and therefore, the second operator will perform picking movements based on a different distribution of fractions to be sorted on the conveyor belt $f_{ref}(x(y), y)_2$. Same thing happens for the following operators placed on the same conveyor belt. In this case, a study can be carried out to understand if the different movements performed by each operator (influenced by movements executed by the previous operators), have an impact on the sorting performance.

This example shows that the concept of affordance level, can be applied not only by considering the entire repetitive movements executed, i.e., the entire trajectory as in the walking example (paragraph 4.2.3); the affordance level can be evaluated also when it is focused only on placements/spatial configurations reached on a physical plane (as the manual sorting example), as long as repetitive movements are performed.

Q and v represent the external constraints of the system considered: varying these parameters, the motor behaviour of the observed operator changes, and so does the affordance level and JSD.

In the very next future, the analysis on the variation of movements performed by the observed operator (i.e., affordance level), due to the change of external constraints, or due to movements performed by previous operators, will be devoted to understanding if these variations affect the performance, type of movements executed (ergonomics point of view), errors made, execution time, or if these variations are affected by the operator fatigue phenomenon.

5.4 Experiment apparatus

In order to quantify the affordance level as well as the stochastic Index of Difficulty (ID_{obs}), the motor behaviour of agents must be evaluated. Therefore, movements performed must me adequately captured by a suitable experiment apparatus. MOtion CAPture (MOCAP) systems allow to monitor the evolution of body motion over time and digitalize movements of different body parts by providing their position and orientation. Three types of MOCAP are commonly used. The inertial MOCAP employs inertial sensors (IMUs, Inertial Measurement Units) equipped with accelerometers and gyroscopes attached to specific body parts. Through the inertial sensors and the use of specific algorithms, the position and orientation of body parts are reconstructed. This system does not require any cameras or visual recording of motion data. The marker-based optical MOCAP requires, instead, the use of multiple cameras that simultaneously record the environment where the operator works and capture movements performed. To record movements, passive markers that are attached to specific body parts of the operator, reflect the infrared light of cameras. One of the main disadvantages of these two methods rely on the necessity for operators to wear suits where passive markers or inertial sensors are mounted.

On the contrary, marker-less optimal MOCAP does not need any suits or devices (markers, inertial sensors) to be worn. This technology relies on the use of depth camera technology to digitalize human movements. With depth cameras, each pixel captured contains information about the distance of the moving body by perceiving depth through light differences with respect to the background static scene. Specific vision algorithms process the images captured by depth cameras and reconstruct the body motions. The main advantage of marker-less MOCAP relies on its reliability and flexibility: it can be employed in multiple environments (laboratory/outdoor/factory) as long as it is properly enlightened. Furthermore, as seen in (Elhayek *et al.*, 2015), this technology needs only few cameras (2-3) also in outdoor environments, instead of 8-10 cameras required for marker-based MOCAP.

Therefore, multiple MOCAP systems allow to capture movements performed, each with its own features. However, marker-less MOCAP system seems to be the most promising technology to be employed to monitor body movements due to its adaptability in multiple work environments: it can be employed outdoor to monitor operators performing door-

to-door waste collection, or in case of manual activities required for the construction work; in controlled environments (laboratories) the marker-less MOCAP system can be employed to capture motion data during the training of robotic arms, as well as during rehabilitations programs (stochastic Index of Difficulty), or can be employed in industrial environments, such as for manual assembly tasks.

6. Conclusion

In the present dissertation, it is investigated the role of motor behaviour, performed or required, for the execution of repetitive motor tasks. The motor behaviour is quantified through the continuous formulation of the information-based Index of Difficulty measure, and directly employed in the models proposed. Basing on the specific context, the proposed models are able to quantify the pre-defined geometrical difficulty, the observed motor difficulty, or the affordance of agents during the execution of repetitive motor tasks. The main novelty of evaluating the motor performance by considering the proposed ID relies on focusing on the overall movements, instead to specific points of the repetitive motor task. The motor performance can be intended differently, basing on the specific scenario considered: it can express the accuracy in reaching a target ('Speed-ID-Accuracy'), the motor flexibility (ID_{obs}), or the affordance level. In all the cases considered, it has been observed that the motor performance is affected by movements (pre-defined or executed). Nevertheless, the applicability of the proposed models is not limited to the scenarios considered. The model able to quantify the affordance level is one of the most promising one, due to its wide range of applicability in multiple contexts, as the one of manual sorting. To the best of our knowledge, this is the first study that propose a quantitative metrics to evaluate the affordance by considering the motor behavior. This may provide a valuable base to develop a benchmark on the execution of repetitive motor tasks; unacceptable/acceptable/optimal affordance levels can be defined as motor performance indicators in the execution of typical movements (e.g., everyday motor activities), as well as in specific industrial, laboratory or outdoor applications that require the execution of repetitive motor tasks.

7. Bibliography

Accot, J. and Zhai, S. (1997) 'Beyond Fitts' law: Models for trajectory-based HCI tasks', in *Conference on Human Factors in Computing Systems - Proceedings*.

Accot, J. and Zhai, S. (2003) 'Refining Fitts' law models for bivariate pointing', in *Conference on Human Factors in Computing Systems - Proceedings*.

Ardón, P. *et al.* (2021) 'Building Affordance Relations for Robotic Agents - A Review', in *Proceedings of the International Joint Conference on Artificial Intelligence (IJCAI)*, pp. 4302–4311.

Atkeson, C. G. and Hollerbach, J. M. (1985) 'Kinematic features of untreated vertical arm movements', *Journal of Neuroscience*, 5(9), pp. 2318–2330.

Van Beers, R. J., Haggard, P. and Wolpert, D. M. (2004) 'The Role of Execution Noise in Movement Variability', *Journal of Neurophysiology*, 91(2), pp. 1050–1063.

Bernstein, N. (1967) *The Co-ordination and Regulation of Movements*. Pergamon Press.

Bhatti, A. *et al.* (2009) 'Haptically enable interactive virtual assembly training system development and evaluation', in *SIMTECT 2009. Proceedings of the 2009 International Design Engineering Technical Conferences & Computers and Computers and Information in Engineering Conference*, pp. 1–6.

Bloem, B. *et al.* (2002) 'Triggering of balance corrections and compensatory strategies in a patient with total leg proprioceptive loss', *Experimental Brain Research*, 142(1), pp. 91–107.

Bongers, P. M., Kremer, A. M. and Laak, J. Ter (2002) 'Are psychosocial factors, risk factors for symptoms and signs of the shoulder, elbow, or hand/wrist?: A review of the epidemiological literature', *American Journal of Industrial Medicine*, 41(5), pp. 315–342.

Burlamaqui, L. and Dong, A. (2014) 'The Use and Misuse of the Concept of Affordance', in *Proceedings of the 6th International Conference on Design Computing and Cognition '14 (DCC'14)*.

Cashaback, J. G. A., McGregor, H. R. and Gribble, P. L. (2015) 'The human motor system alters its reaching movement plan for task-irrelevant, positional forces', *Journal of Neurophysiology*, 113(7), pp. 2137–2149.

Cesari, P., Formenti, F. and Olivato, P. (2003) 'A common perceptual parameter for stair climbing for children, young and old adults', *Human Movement Science*, 22(1), pp. 111–124.

Cha, Y. and Myung, R. (2010) 'Extended Fitts' law in Three-Dimensional Pointing Tasks', in *Proceedings of the Human Factors and Ergonomics Society Annual Meeting*, pp. 972–976.

Chemero, A. (2000) 'What Events Are', *Ecological Psychology*, 12, pp. 37–42.

Chemero, A. (2003) 'An Outline of a Theory of Affordances', *Ecological Psychology*, 15(2), pp. 181–195.

Clouston, S. A. P. *et al.* (2013) 'The dynamic relationship between physical function and cognition in longitudinal aging cohorts', *Epidemiologic Reviews*, 35, pp. 33–50.

Cohen, R. G. and Sternad, D. (2009) 'Variability in motor learning: Relocating, channeling and reducing noise', *Experimental Brain Research*, 193(1), pp. 69–83.

Cooper, R. (2016) 'Occupational activity across adult life and its association with grip strength', *Occupational and Environmental Medicine*, 73, pp. 425–426.

Côté, J. N. *et al.* (2008) 'Effects of fatigue on intermuscular coordination during repetitive hammering', *Motor Control*, 12(2), pp. 79–92.

Crossman, E. R. F. W. and Goodeve, P. J. (1983) 'Feedback control of hand-movement and Fitts' Law', *The Quarterly Journal of Experimental Psychology Section A*, 35, pp. 251–278.

Daffertshofer, A. *et al.* (2004) 'PCA in studying coordination and variability: A tutorial', *Clinical Biomechanics*, 19, pp. 415–428.

Dalenogare, L. S. *et al.* (2018) 'The expected contribution of Industry 4.0 technologies for industrial performance', *International Journal of Production Economics*, 204, pp. 383–394.

Detry, R. *et al.* (2009) 'Learning object-specific grasp affordance densities', in *2009 IEEE 8th International Conference on Development and Learning, ICDL 2009*.

Detry, R. *et al.* (2010) 'Learning continuous grasp affordances by sensorimotor exploration', in Sigaud, O. and Peters, J. (eds) *Studies in Computational Intelligence*.

Detry, R. *et al.* (2011) 'Learning Grasp Affordance Densities', *Paladyn, Journal of Behavioral Robotics*, 2(1), pp. 1–17.

Digiesi, S., Lucchese, A. and Mummolo, C. (2020) 'A "speed-difficulty-accuracy" model following a general trajectory motor task with spatial constraints: An information-based model', *Applied Sciences (Switzerland)*, 10(21), p. 7516.

Dimeas, F. *et al.* (2019) 'Towards Progressive Automation of Repetitive Tasks Through Physical Human-Robot Interaction', in *Springer Proceedings in Advanced Robotics*.

Dingwell, J. B., John, J. and Cusumano, J. P. (2010) 'Do humans optimally exploit redundancy to control step variability in walking?', *PLoS Computational Biology*, 6(7), p. e1000856.

Domkin, D. *et al.* (2005) 'Joint angle variability in 3D bimanual pointing: Uncontrolled manifold analysis', *Experimental Brain Research*, 163, pp. 44–57.

Elhayek, A. *et al.* (2015) 'Efficient ConvNet-based marker-less motion capture in general scenes with a low number of cameras', in *Proceedings of the IEEE Computer Society Conference on Computer Vision and Pattern Recognition*.

Elliott, D. *et al.* (2010) 'Goal-Directed Aiming: Two Components but Multiple Processes', *Psychological Bulletin*, 136(6), pp. 1023–1044.

Fajen, B. R. (2007) 'Affordance-based control of visually guided action', *Ecological Psychology*, 19(4), pp. 383–410.

Feix, T. *et al.* (2016) 'The GRASP Taxonomy of Human Grasp Types', *IEEE Transactions on Human-Machine Systems*, 46(1), pp. 66–77.

Feix, T., Bullock, I. M. and Dollar, A. M. (2014) 'Analysis of human grasping behavior: Object characteristics and grasp type', *IEEE Transactions on Haptics*, 7(3).

Fettermann, D. C. *et al.* (2018) 'How does Industry 4.0 contribute to operations management?', *Journal of Industrial and Production Engineering*, 35(4), pp. 255–268.

Fitts, P. M. (1954) 'The information capacity of the human motor system in controlling the amplitude of movement', *Journal of Experimental Psychology*, 47(6), pp. 381–391.

Fitts, P. M. and Peterson, J. R. (1964) 'Information capacity of discrete motor responses', *Journal of Experimental Psychology*, 67(2), pp. 103–112.

Fitzpatrick, P. *et al.* (2003) 'Learning about objects through action - Initial steps towards

artificial cognition', in *Proceedings - IEEE International Conference on Robotics and Automation*, pp. 3140–3145.

Fried, L. P. *et al.* (2001) 'Frailty in older adults: Evidence for a phenotype', *Journals of Gerontology - Series A Biological Sciences and Medical Sciences*, pp. M146–M157.

Fukuchi, C. A., Fukuchi, R. K. and Duarte, M. (2018) 'A public dataset of overground and treadmill walking kinematics and kinetics in healthy individuals', *PeerJ*, 6, p. e4640.

Fuller, J. R., Fung, J. and Côté, J. N. (2011) 'Time-dependent adaptations to posture and movement characteristics during the development of repetitive reaching induced fatigue', *Experimental Brain Research*, 211(1), pp. 133–143.

Gale, C. R., Cooper, C. and Sayer, A. A. (2015) 'Prevalence of frailty and disability: findings from the English Longitudinal Study of Ageing', *Age and Ageing*, 44, pp. 162–165.

Gehlsen, G. M. and Whaley, M. H. (1990) 'Falls in the elderly: Part II, balance, strength, and flexibility', *Archives of Physical Medicine and Rehabilitation*, 71(10), pp. 739–741.

Ghahramani, Z. and Wolpert, D. M. (1997) 'Modular decomposition in visuomotor learning', *Nature*, 386, pp. 392–395.

Gibson, E. J. *et al.* (1987) 'Detection of the Traversability of Surfaces by Crawling and Walking Infants', *Journal of Experimental Psychology: Human Perception and Performance*, 13, pp. 533–544.

Gibson, J. J. (1979a) *The Ecological Approach to Visual Perception*. Edited by H. Mifflin. Boston, MA.

Gibson, J. J. (1979b) 'The theory of affordances', in *The ecological approach to visual perception*. Hillsdale, NJ.: Lawrence Erlbaum Associates.

Gielen, C. C. A. M., van Bolhuis, B. M. and Theeuwen, M. (1995) 'On the control of biologically and kinematically redundant manipulators', *Human Movement Science*.

Gopher, D. (2012) 'Skill training in Multimodal virtual environments', *Work*, 41(1), pp. 2284–2287.

Gordon, J., Ghilardi, M. F. and Ghez, C. (1994) 'Accuracy of planar reaching movements - I. Independence of direction and extent variability', *Experimental Brain Research*, 99, pp. 97–111.

Gramacki, A. (2018) *Nonparametric Kernel Density Estimation and Its Computational Aspects*. Springer Nature.

Greeno, J. G. (1994) 'Gibson's Affordances', *Psychological Review*, 101(2), pp. 336–342.

Grossman, T. and Balakrishnan, R. (2004) 'Pointing at trivariate targets in 3D environments', in *Conference on Human Factors in Computing Systems - Proceedings*, pp. 447–454.

Grossman, T. and Balakrishnan, R. (2005) 'A probabilistic approach to modeling two-dimensional pointing', *ACM Transactions on Computer-Human Interaction*.

Guiard, Y., Beaudouin-Lafon, M. and Mottet, D. (1999) 'Navigation as multiscale pointing: Extending Fitts' model to very high precision tasks', in *Conference on Human Factors in Computing Systems - Proceedings*, pp. 450–457.

Guigon, E., Baraduc, P. and Desmurget, M. (2008) 'Optimality, stochasticity, and variability in motor behavior', *Journal of Computational Neuroscience*, 24(1), pp. 57–68.

Habidin, N. F. *et al.* (2018) 'Total productive maintenance, kaizen event, and performance', *International Journal of Quality and Reliability Management*, 35(9), pp. 1853–1867.

Hancock, P. A. *et al.* (2013) 'Human-automation interaction research: Past, present, and future', *Ergonomics in Design*, 21, pp. 9–14.

Hansen, S., Elliott, D. and Khan, M. A. (2008) 'Quantifying the variability of three-dimensional aiming movements using ellipsoids', *Motor Control*, 12, pp. 241–251.

Hart, S., Grupen, R. and Jensen, D. (2005) 'A relational representation for procedural task knowledge', in *Proceedings of the National Conference on Artificial Intelligence*, pp. 1280–1285.

Hayward, V. *et al.* (2004) 'Haptic interfaces and devices', *Sensor Review*, 24(1), pp. 16–29.

Herbst, Y., Zelnik-Manor, L. and Wolf, A. (2020a) 'Analysis of subject specific grasping patterns', *PLoS ONE*, 15(7), p. e0234969.

Herbst, Y., Zelnik-Manor, L. and Wolf, A. (2020b) 'BRML Grasp Dataset [Internet], OSF repository'. Available at: https://osf.io/xj6dw/.

Herzfeld, D. J. and Shadmehr, R. (2014) 'Motor variability is not noise, but grist for the learning mill', *Nature Neuroscience*, 17(2), pp. 149–150.

Hoffmann, E. R. (1991) 'A comparison of hand and foot movement times', *Ergonomics*, 34, pp. 397–406.

Hogg, D. N. *et al.* (1995) 'Development of a situation awareness measure to evaluate advanced alarm systems in nuclear power plant control rooms', *Ergonomics*, 38(11), pp. 2394–2413.

Hooi, L. W. and Leong, T. Y. (2017) 'Total productive maintenance and manufacturing performance improvement', *Journal of Quality in Maintenance Engineering*, 23(1), pp. 2–21.

Hornof, A. J. (2001) 'Visual Search and Mouse-Pointing in Labeled versus Unlabeled Two-Dimensional Visual Hierarchies', *ACM Transactions on Computer-Human Interaction*, 8(3), pp. 171–197.

Hourcade, J. P. and Berkel, T. R. (2008) 'Simple pen interaction performance of young and older adults using handheld computers', *Interacting with Computers*, 20, pp. 166–183.

Hsieh, M. H. *et al.* (2012) 'A decision support system for identifying abnormal operating procedures in a nuclear power plant', *Nuclear Engineering and Design*, 249, pp. 413–418.

Hsu, C. L. *et al.* (2012) 'Examining the relationship between specific cognitive processes and falls risk in older adults: A systematic review', *Osteoporosis International*, 23, pp. 2409–2424.

Jeannerod, M. (1984) 'The timing of natural prehension movements', *Journal of Motor Behavior*, 16(3), pp. 235–254.

Johnson, R. A. and Wichern, D. W. (2015) *Applied Multivariate Statistical Analysis*. 6th edn. Edited by Pearson India.

Jolliffe, I. T. (2002) *Principal Component Analysis*. 2nd edn. Edited by Springer Nature.

Kaur, M. *et al.* (2015) 'Justification of synergistic implementation of TQM-TPM paradigms using analytical hierarchy process', *International Journal of Process Management and Benchmarking*, 5(1), pp. 1–18.

Kerr, B. A. and Langolf, G. D. (1977) 'Speed of Aiming Movements', *Quarterly Journal of Experimental Psychology*, 29, pp. 475–481.

Kilbom, Å. (1994) ‘Repetitive work of the upper extremity: Part II - The scientific basis (knowledge base) for the guide’, *International Journal of Industrial Ergonomics*, 14, pp. 59–86.

Kinsella-Shaw, J. M., Shaw, B. and Turvey, M. T. (1992) ‘Perceiving “Walk-on-able” Slopes’, *Ecological Psychology*, 4, pp. 223–239.

Lai, Z. H. *et al.* (2020) ‘Smart augmented reality instructional system for mechanical assembly towards worker-centered intelligent manufacturing’, *Journal of Manufacturing Systems*, 55, pp. 69–81.

Lasi, H. *et al.* (2014) ‘Industry 4.0’, *Business and Information Systems Engineering*, 6(4), pp. 239–242.

Latash, M. L., Scholz, J. P. and Schöner, G. (2002) ‘Motor control strategies revealed in the structure of motor variability’, *Exercise and Sport Sciences Reviews*, 30(1), pp. 26–31.

Latash, M. L., Scholz, J. P. and Schöner, G. (2007) ‘Toward a new theory of motor synergies’, *Motor Control*, 11(2), p. 276.

Lewis, M. A., Lee, H. K. and Patla, A. (2005) ‘Foot placement selection using non-geometric visual properties’, *International Journal of Robotics Research*, 24(7), pp. 553–561.

Liu, D. and Todorov, E. (2007) ‘Evidence for the flexible sensorimotor strategies predicted by optimal feedback control’, *Journal of Neuroscience*, 27(35), pp. 9354–9368.

Lucchese, A. *et al.* (2021) ‘An Agent-Specific Stochastic Model of Generalized Reaching Task Difficulty’, *Applied Sciences*, 11(10).

Lucchese, A., Digiesi, S. and Mummolo, C. (2022) ‘Analytical-Stochastic Model of Motor Difficulty for Three-Dimensional Manipulation Tasks’, *PLoS ONE*, 17(10), p. e0276308.

Machuca, M. D. B. and Stuerzlinger, W. (2019) ‘The effect of stereo display deficiencies on virtual hand pointing’, in *Conference on Human Factors in Computing Systems - Proceedings*.

MacKenzie, I. S. (1992) ‘Fitts’ Law as a Research and Design Tool in Human-Computer Interaction’, *Human–Computer Interaction*, 7(1), pp. 91–139.

MacKenzie, I. S. and Buxton, W. (1992) ‘Extending Fitts’ law to two-dimensional tasks’, in *Conference on Human Factors in Computing Systems - Proceedings*, pp. 219–226.

MacKenzie, I. S. and Oniszczak, A. (1998) ‘Comparison of three selection techniques for touchpads’, in *Conference on Human Factors in Computing Systems - Proceedings*, pp. 336–343.

Mackenzie, S. and Jusoh, S. (2000) ‘An evaluation of two input devices for remote pointing’, in *Eighth IFIP Working Conference on Engineering for Human–Computer Interaction-EHCI*, pp. 235–249.

Madeleine, P., Mathiassen, S. E. and Arendt-Nielsen, L. (2008) ‘Changes in the degree of motor variability associated with experimental and chronic neck-shoulder pain during a standardised repetitive arm movement’, *Experimental Brain Research*, 185, pp. 689–698.

Mark, L. S. (1987) ‘Eyeheight-Scaled Information About Affordances: A Study of Sitting and Stair Climbing’, *Journal of Experimental Psychology: Human Perception and Performance*, 13, pp. 361–370.

Masoudi, N. *et al.* (2019) ‘A review of affordances and affordance-based design to address usability’, in *Proceedings of the International Conference on Engineering Design, ICED*.

Mathiassen, S. E. (2006) ‘Diversity and variation in biomechanical exposure: What is it, and

why would we like to know?', *Applied Ergonomics*, 37(4), pp. 419–427.

Messier, J. and Kalaska, J. F. (1997) 'Differential effect of task conditions on errors of direction and extent of reaching movements', *Experimental Brain Research*, 115(3), pp. 469–478.

Meyer, D. E. *et al.* (1988) 'Optimality in human motor performance: Ideal control of rapid aimed movements.', *Psychological Review*, 95(3), pp. 340–370.

Millanvoye, M. (1998) *Ageing of the organism before sixty years of age.* Edited by J. Marquie, D. Paumes Cau-Bareille, and S. Volkoff. London: Taylor & Francis.

Morasso, P. (1981) 'Spatial control of arm movements', *Experimental Brain Research*, 42, pp. 223–227.

Morley, J. E. *et al.* (2013) 'Frailty consensus: A call to action', *Journal of the American Medical Directors Association*, 14, pp. 392–397.

Mosyurchak, A. *et al.* (2017) 'Prognosis of behaviour of machine tool spindles, their diagnostics and maintenance', *MM Science Journal*, pp. 2100–2014.

Mourtzis, D., Xanthi, F. and Zogopoulos, V. (2019) 'An adaptive framework for augmented reality instructions considering workforce skill', *Procedia CIRP*, 81, pp. 363–368.

Müller, H. and Sternad, D. (2009) 'Motor learning: Changes in the structure of variability in a redundant task', in *Progress in Motor Control*. Springer Science, pp. 439–456.

Mummolo, C., Mangialardi, L. and Kim, J. H. (2013) 'Quantifying dynamic characteristics of human walking for comprehensive gait cycle', *Journal of Biomechanical Engineering*, 135(9), p. 091006.

Munir, S. *et al.* (2013) 'Cyber physical system challenges for human-in-the-loop control', *8th International Workshop on Feedback Computing*, 4, pp. 1–4.

Murata, A. and Fukunaga, D. (2018) 'Extended Fitts' model of pointing time in eye-gaze input system - Incorporating effects of target shape and movement direction into modeling', *Applied Ergonomics*, 68, pp. 54–60.

Murata, A. and Iwase, H. (2001) 'Extending fitts' law to a three-dimensional pointing task', *Human Movement Science*, 20(6), pp. 791–805.

National Research Council, Health and safety needs of older workers (2004). Washington, D.C: The National Academies Press.

Nonaka, H. *et al.* (2002) 'Age-related changes in the interactive mobility of the hip and knee joints: A geometrical analysis', *Gait and Posture*, 15(3), pp. 236–243.

Norman, D. (1988) *The Psychology of Everyday Things*. New York: Basic Books.

Oh, J. Y. and Stuerzlinger, W. (2002) 'Laser pointers as collaborative pointing devices', in *Proceedings - Graphics Interface*, pp. 141–149.

Osborne, M. and Mavers, S. (2019) 'Integrating augmented reality in training and industrial applications', in *Proceedings - 2019 8th International Conference of Educational Innovation through Technology, EITT 2019*, pp. 142–146.

Park, J., Kim, Y. and Jung, W. (2016) 'A framework to estimate HEPs from the full-scope simulators of NPPs: Unsafe act definition, identification and quantification', in *Korea At. Energy Res. Inst.* Daejeon, South Korea.

Pastore, M. and Calcagnì, A. (2019) 'Measuring distribution similarities between samples: A

distribution-free overlapping index', *Frontiers in Psychology*, 10.

Pereira, A. C. and Romero, F. (2017) 'A review of the meanings and the implications of the Industry 4.0 concept', *Procedia Manufacturing*, 13, pp. 1206–1214.

Peruzzini, M. and Pellicciari, M. (2017) 'A framework to design a human-centred adaptive manufacturing system for aging workers', *Advanced Engineering Informatics*, 33, pp. 330–349.

Pirker, W. and Katzenschlager, R. (2017) 'Gait disorders in adults and the elderly: A clinical guide', *Wiener Klinische Wochenschrift*, pp. 1–15.

Poupyrev, I., Okabe, M. and Maruyama, S. (2004) 'Haptic feedback for pen computing: Directions and strategies', in *Conference on Human Factors in Computing Systems - Proceedings*, pp. 1309–1312.

Preatoni, E. *et al.* (2013) 'Movement variability and skills monitoring in sports', *Sports Biomechanics*, 12(2), pp. 69–92.

Ranganathan, R., Lee, M. H. and Newell, K. M. (2020) 'Repetition Without Repetition: Challenges in Understanding Behavioral Flexibility in Motor Skill', *Frontiers in Psychology*, 11.

Robertson, E. M. and Miall, R. C. (1997) 'Multi-joint limbs permit a flexible response to unpredictable events', *Experimental Brain Research*, 117, pp. 148–152.

Rødseth, H., Schjølberg, P. and Marhaug, A. (2017) 'Deep digital maintenance', *Advances in Manufacturing*, 5(4), pp. 299–310.

Romero, D. *et al.* (2015) 'Towards a human-centred reference architecture for next generation balanced automation systems: Human-automation symbiosis', *IFIP Advances in Information and Communication Technology*, 460, pp. 556–566.

Romero, D. *et al.* (2016) 'Towards an operator 4.0 typology: A human-centric perspective on the fourth industrial revolution technologies', *CIE 2016: 46th International Conferences on Computers and Industrial Engineering*, 11, pp. 1–11.

Ronsky, J. L., Nigg, B. M. and Fisher, V. (1995) 'Correlation between physical activity and the gait characteristics and ankle joint flexibility of the elderly', *Clinical Biomechanics*, 10(1), pp. 41–49.

Schmidt, R. *et al.* (2015) 'Industry 4.0 - Potentials for creating smart products: Empirical research results', *Lecture Notes in Business Information Processing*, 12, pp. 16–27.

Schmidt, R. A. and et al (1979) 'Motor-output variability: A theory for the accuracy of rapid motor acts', *Psychological Review*, 86(5), pp. 415–451.

Scholz, J. P. and Schöner, G. (1999) 'The uncontrolled manifold concept: Identifying control variables for a functional task', *Experimental Brain Research*.

Schwatka, N. V., Butler, L. M. and Rosecrance, J. R. (2012) 'An aging workforce and injury in the construction industry', *Epidemiologic Reviews*, 34, pp. 156–167.

Shannon, C. E. (1948) 'A Mathematical Theory of Communication', *Bell System Technical Journal*, 27(3), pp. 379–423.

Sheridan, T. B. and Ferrell, W. R. (1963) 'Remote Manipulative Control with Transmission Delay', *IEEE Transactions on Human Factors in Electronics*, 4, pp. 25–29.

Silverman, B. W. (2018) *Density estimation: For statistics and data analysis*, *Density Estimation: For Statistics and Data Analysis*. Taylor & Francis Group.

Silvestri, L. *et al.* (2020) 'Maintenance transformation through Industry 4.0 technologies: A systematic literature review', *Computers in Industry*, 123, p. 103335.

Singh, H. V. P. and Mahmoud, Q. H. (2017) 'EYE-on-HMI: A Framework for monitoring human machine interfaces in control rooms', in *Canadian Conference on Electrical and Computer Engineering*, pp. 1–5.

Singh, P. *et al.* (2016) 'Exploration of joint redundancy but not task space variability facilitates supervised motor learning', *Proceedings of the National Academy of Sciences of the United States of America*, 113(50), pp. 14414–14419.

Smeets, J. B. J. (1994) 'Bi-articular muscles and the accuracy of motor control', *Human Movement Science*, 13, pp. 587–600.

Spirduso, W. W. (1995) *Physical dimensions of aging*. Champaign, IL.

Stark, L. and Bowyer, K. (1991) 'Achieving Generalized Object Recognition through Reasoning about Association of Function to Structure', *IEEE Transactions on Pattern Analysis and Machine Intelligence*, 13(10), pp. 1097–1104.

Steedman, M. (2002) 'Plans, affordances, and combinatory grammar', *Linguistics and Philosophy*, 25.

Steel, C. (2019) 'The potential of Augmented Reality to amplify learning and achieve high performance in the flow of work', in *ASCILITE 2019 - Conference Proceedings - 36th International Conference of Innovation, Practice and Research in the Use of Educational Technologies in Tertiary Education: Personalised Learning. Diverse Goals. One Heart.*, pp. 563–568.

Stergiou, N., Harbourne, R. T. and Cavanaugh, J. T. (2006) 'Optimal movement variability: A new theoretical perspective for neurologic physical therapy', *Journal of Neurologic Physical Therapy*, 30, pp. 120–129.

Stoytchev, A. (2005) 'Toward Learning the Binding Affordances of Objects: A Behavior-Grounded Approach', in *AAAI Symposium on Developmental Robotics*.

Sun, S. *et al.* (2020) 'Healthy operator 4.0: A human cyber–physical system architecture for smart workplaces', *Sensors (Switzerland)*, 20(7), pp. 2011–2020.

Tambouratzis, T. *et al.* (2019) 'Applying the Computational Intelligence Paradigm to Nuclear Power Plant Operation', *International Journal of Energy Optimization and Engineering*, 9(1), pp. 27–109.

Todorov, E. and Jordan, M. I. (2002) 'Optimal feedback control as a theory of motor coordination', *Nature Neuroscience*, 5, pp. 1226–1235.

UNFPA (2012) 'Envelhecimento no Século XXI: Celebração e Desafio', *Fundo de População das Nações Unidas (UNFPA)*, p. 12.

Vicente, K. J. *et al.* (1996) 'Evaluation of a rankine cycle display for nuclear power plant monitoring and diagnosis', *Human Factors*, 38(3), pp. 506–521.

Walker-Bone, K. *et al.* (2016) 'Heavy manual work throughout the working lifetime and muscle strength among men at retirement age', *Occupational and Environmental Medicine*, 73, pp. 284–286.

Wang, X. *et al.* (2017) 'Work-related musculoskeletal disorders among construction workers in the United States from 1992 to 2014', *Occupational and Environmental Medicine*, 74(5), pp. 374–380.

Warren, W. H. (1984) ‘Perceiving affordances: Visual guidance of stair climbing’, *Journal of Experimental Psychology: Human Perception and Performance*, 10(5), pp. 683–703.

Woodworth, R. S. (1899) ‘Accuracy of voluntary movement.’, *The Psychological Review: Monograph Supplements*, 3.

Wu, H. G. *et al.* (2014) ‘Temporal structure of motor variability is dynamically regulated and predicts motor learning ability’, *Nature Neuroscience*.

Wu, X. *et al.* (2016) ‘Validation of “alarm bar” alternative interface for digital control panel design: A preliminary experimental study’, *International Journal of Industrial Ergonomics*, 51, pp. 43–51.

Xu, L. Da, Xu, E. L. and Li, L. (2018) ‘Industry 4.0: State of the art and future trends’, *International Journal of Production Research*, 56(8), pp. 2941–2962.

Ye, Y. *et al.* (2022) ‘Sensation transfer for immersive exoskeleton motor training: Implications of haptics and viewpoints’, *Automation in Construction*, 141, p. 104411.

Zelaznik, H. N. *et al.* (1988) ‘Role of Temporal and Spatial Precision in Determining the Nature of the Speed-Accuracy Trade-Off in Aimed-Hand Movements’, *Journal of Experimental Psychology: Human Perception and Performance*, 14(2), pp. 221–230.

Zhai, S., Accot, J. and Woltjer, R. (2004) ‘Human action laws in electronic virtual worlds: An empirical study of path steering performance in VR’, *Presence: Teleoperators and Virtual Environments*, 13(2), pp. 113–127.

Zhang, J., Lockhart, T. E. and Soangra, R. (2014) ‘Classifying lower extremity muscle fatigue during walking using machine learning and inertial sensors’, *Annals of Biomedical Engineering*, 42, pp. 600–612.

Zhang, X., Zha, H. and Feng, W. (2012) ‘Extending Fitts’ law to account for the effects of movement direction on 2D pointing’, in *Conference on Human Factors in Computing Systems - Proceedings*.

Zheng, T. *et al.* (2021) ‘The applications of Industry 4.0 technologies in manufacturing context: a systematic literature review’, *International Journal of Production Research*, pp. 1922–1954.

Zolotová, I. *et al.* (2020) ‘Smart and cognitive solutions for Operator 4.0: Laboratory H-CPPS case studies’, *Computers and Industrial Engineering*, 139, p. 105471.